Investigation of the “foreign body response” and its pharmacological regulation in chronic intracerebral cannula implantation in rats

---

Aus dem Institut für Hirnforschung, Abteilung Neuropharmakologie,
Zentrum für Kognitionswissenschaften

DISSERTATION

zur Erlangung des akademischen Grades eines Doktors der Naturwissenschaften (Dr. rer. nat.)

Vorgelegt dem Fachbereich 2 (Biologie/Chemie) der Universität Bremen

von

LINDA HAYN

im November 2015

Universität Bremen

Dissertation:

1. Gutachter: Prof. Dr. Michael Koch

2. Gutachter: Prof. Dr. Ursula Dicke

Dissertationskolloquium:

Zeit: 14.12.2015, 13:00 Uhr

Ort: Raum 2030, Cognium, Universität Bremen

Statutory declaration

Herewith, I declare that the submitted dissertation entitled "*Investigation of the 'foreign body response' and its pharmacological regulation in chronic intracerebral cannula implantation in rats"* has been written independently by me and only comprises my original work. I did not use any external support except for the quoted literature and the sources mentioned in the dissertation. I clearly marked and separately listed all of the literature and sources which I employed when producing this academic work. Moreover, I declare that the three submitted copies are identical.

_____

(Linda Hayn)

Bremen, November 2015

List of publications

(*****) indicates publications included in this thesis. Articles have been published or submitted to international neuroscientific journals.

Articles

*** Hayn L**, Koch M (2015) Suppression of excitotoxicity and foreign body response by memantine in chronic cannula implantation into the rat brain. Brain Res Bull 117: 54-68.

*** Hayn L**, Deppermann L, Koch M (2015) Suppression of the foreign body response and neuroprotection by apyrase and minocycline in chronic cannula implantation. Behav Brain Res (under review).

Brosda J, **Hayn L**, Klein C, Koch M, Meyer C, Schallhorn R, Wegener N (2011) Pharmacological and parametrical investigation of prepulse inhibition of startle and prepulse elicited reactions in Wistar rats. Pharmacol Biochem Behav 99: 22-28.

Schulz S, Gundelach J, **Hayn L**, Koch M, Svärd HK (2014) Acute Co-Administration of the Cannabinoid Receptor Agonist WIN 55-212,2 does not Influence 3,4-Methylenedioxymetamphetamine (MDMA)-Induced Effects on Effort-Based Decision Making, Locomotion, Food Intake and Body Temperature. Biochem Pharmacol 3: 127.

Feja M, **Hayn L**, Koch M (2014) Nucleus accumbens core and shell inactivation differentially affects impulsive behaviours in rats. Prog Neuropsychopharmacol Biol Psychiatry 54: 31-42.

Talks

* 29. Jahrestagung der Gesellschaft für Neuropsychologie (GNP); Oldenburg; Symposium 4: Neuropharmacology. **Hayn, L (2014)** Reducing the “foreign body response” of chronic implants by acute intracranial treatments in rats.

* ZKW-Advisory Board Meeting; Universität Bremen 2014. Slot 4: **Hayn, L (2014)** Reducing the “foreign body response” of chronic implants by acute intracranial treatments in rats.

Contents

1 Zusammenfassung

In den letzten Jahrzehnten wurde ein immenser Fortschritt im Bereich von Gehirn-Computer-Schnittstellen (brain-computer interfaces; BCIs) erzielt, welche ein neues Werkzeug zur Wiederherstellung der Mobilität von Patienten darstellen, die unter einer Lähmung oder einer Amputation leiden. Zu diesem Zweck können die besten Signale zur Kontrolle von BCIs durch intrakortikal implantierte Elektroden empfangen werden, welche die größte Fehlerfreiheit, Bewegungsgenauigkeit und Geschwindigkeit aufweisen. Obwohl bereits Neuroprothesen entwickelt werden konnten, die in den ersten Humanstudien ihre Funktionalität sogar Jahre nach einer Verletzung des zentralen Nervensystems demonstrierten, stellt die Biokompatibilität von chronischen Implantaten weiterhin ein Problem dar. Es ist von enormem Wert und Interesse, die Gewebsreaktion auf diese chronischen Gehirnimplantate, wie Elektrodenarrays, besser zu verstehen und zu kontrollieren, um sicher stellen zu können, dass die chronische Elektrodenimplantation in klinischer Anwendung sicher und vorteilhaft genug ist, das Risiko des operativen Eingriffs in Kauf zu nehmen.

Die Gewebsreaktion auf ein chronisch verweilendes Gehirnimplantat wird auch als „Fremdkörperreaktion“ bezeichnet und beinhaltet eine Glianarbenbildung, die von fortschreitender Neurodegeneration begleitet wird. Beides trägt zu eine inkonsistenten Leistungsfähigkeit der ableitenden Elektroden bei und führt zu einem Signalverlust der abgeleiteten elektrischen Potentiale. Die Fremdkörperreaktion kann in eine akute Phase, die durch das mechanische Trauma der Implantation hervorgerufen wird, und in eine chronische Phase, aufgrund der anhaltenden inflammatorischen Prozesse an der Schnittstelle, unterteilt werden. Die akute Immunreaktion ist ein über ein bis drei Wochen andauernder Prozess, der durch den Zelltod von Neuronen und Gliazellen, sowie durch die Verletzung von Blutgefäßen gekennzeichnet ist. Dies wiederum führt zur Gewebsinfiltration durch Makrophagen und zu einer Aktivierung der Mikrogliazellen und Astrozyten. Die chronische Reaktion ist durch sogenannte „frustrierte Phagozytose“ der Makrophagen und Mikrogliazellen sowie durch anhaltende Entzündungsprozesse an der Oberfläche des Implantats gekennzeichnet. Diese wird von reaktiven Astrozyten begleitet, die eine dichte Verkapselungsschicht um das Implantat formen, um das gesunde Hirngewebe von den anhaltenden Entzündungsprozessen zu isolieren.

Der motorische Kortex, der als wesentliches Implantationsziel für BCIs angesehen wird, ist Teil des Frontallappens und an der Planung, Kontrolle und Ausführung von willkürlichen Bewegungen beteiligt. Da die Fähigkeit zu gezielter Greifbewegung (*skilled reaching*) nach Futter bei Ratte und Mensch ähnlich ist - wahrscheinlich aufgrund eines gemeinsamen Ursprungs in frühen Tetrapoden - hat sich die Prüfung der gezielten Greifbewegung zu einem Modellsystem entwickelt, um die Funktionalität des motorischen Kortex zu untersuchen. Innerhalb des primären motorischen Kortex bei Ratten (M1) kann die Repräsentation der Zugreifbewegung (*grasp*) dem rostralen Vorderbein-Areal (*rostral forelimb area*; RFA), und die Annäherungsbewegung (*reach*) dem kaudalen Vorderbein-Areal (*caudal forelimb area*; CFA) zugeordnet werden.

Aufgrund der Sensibilität der gezielten Greifbewegung gegenüber kortikaler motorischer Störungen, wurde in dieser Arbeit davon ausgegangen, dass das Ausmaß der Glianarbenbildung und des neuronalen Zelltods durch die chronische Fremdkörper-implantation in das CFA auch auf Verhaltensebene messbar ist. Im Anschluss an eine reversible Inaktivierungsstudie durch den $GABA_A$-Agonisten Muscimol, um die akuten Defizite in der gezielten Greifbewegung und die genaue Funktion des CFA bei Ratten bestimmen zu können, wurde die Kanülenimplantation von lokaler Substanzapplikation begleitet, um der Fremdkörperreaktion entgegenzuwirken. Unterschiede in der Fremdkörperreaktion wurden anhand der Verhaltensperformanz der Ratten in einer Aufgabe zur gezielten Greifbewegung (*skilled reaching task*), sowie einer Aufgabe zum gewandten Laufen auf einer Sprossenleiter (*skilled walking task*) und im Offenfeld (*open field*) bestimmt. Darüber hinaus wurde die Verteilung der Neurone und Gliazellen in der Umgebung des Implantats untersucht. Die Studien dienten als Grundlagenuntersuchung und ahmen die Implantation eines Elektrodenarrays anhand der Implantation einer Stahlkanüle in M1 nach. Das Ziel der Arbeit war es, die Fremdkörperreaktion zu reduzieren, indem bei den frühen Ereignissen nach der Kanülenimplantation angesetzt wurde, um somit die induzierten Kaskaden von fortschreitendem Zelltod und Gliazellaktivierung zu hemmen.

1.1 Studie 1 (in *Brain Research Bulletin*, 2015)

In *"Suppression of excitotoxicity and foreign body response by memantine in chronic cannula implantation into the rat brain"* wurde beabsichtigt, die exzitotoxische Kaskade des Glutamat-induzierten Zelltods zu reduzieren, die in der akuten Phase nach

Fremdkörperimplantation aufgrund der Gewebsverletzung induziert wird. Die Ansammlung von Glutamat im Extrazellularraum führt zu einer Überstimulierung von Glutamatrezeptoren, wobei der N-Methyl-D-Aspartat (NMDA)-Rezeptor eine zentrale Rolle beim exzitotoxischen Zelltod übernimmt. Extrasynaptisch lokalisierte NMDA-Rezeptoren, die eine NR2B-Untereinheit enthalten (NR2BRs), haben einen entgegengesetzten Effekt zu den synaptisch lokalisierten NMDA-Rezeptoren, die eine NR2A-Untereinheit enthalten (NR2ARs). Eine übermäßige Aktivierung des ersten Typs führt zu einer Hemmung von speziellen Überlebenssignalwegen und exzitotoxischem Zelltod von apoptotischer oder nekrotischer Natur. Diesen Zelltod-fördernden Effekten kann durch den nicht-kompetitiven Antagonisten Memantin, der eine geringe Affinität zum Rezeptor hat, bevorzugt offene Kanäle blockiert, und darüber hinaus eine Präferenz für die extrasynaptisch lokalisierten NR2BRs aufweist, entgegengewirkt werden.

Beide Memantin-Dosierungen (20 µg/µl; 50 µg/µl), die lokal während der Kanülenimplantation in das CFA verabreicht wurden, erhöhten im Vergleich zu den Kontrolltieren die Anzahl überlebender Neurone in der Nähe des Implantats zwei sowie sechs Wochen nach Implantation beachtlich. Dieser beträchtliche Neuronenanstieg ging mit einer leichten Abnahme an reaktiven Astrozyten in Implantatnähe einher, die nach sechs Wochen deutlicher war, ohne jedoch eine Änderung der Mikroglia-/Makrophagenanzahl zu bewirken. Die Verhaltensperformanz war generell am stärksten bei der gezielten Greifbewegung beeinträchtigt, mittelmäßig beim gewandten Laufen, und ohne offensichtliche Beeinträchtigung im Offenfeld. Die Memantingabe führte zu einer schnellen Wiederherstellung der Verhaltensperformanz, die lediglich in den ersten zwei Wochen leicht absank.

Schlussfolgernd legen diese Daten nahe, dass es ein wirkungsvoller Ansatz ist, bei den ganz frühen Ereignissen nach der Implantation einzugreifen und die Kaskaden sekundären Zelltods durch die glutamaterge Exzitotoxizität zu inhibieren, um die neuronalen Netzwerke in Implantatnähe zu erhalten.

1.2 Studie 2 (eingereicht bei *Behavioural Brain Research*, 2015)

"Suppression of the foreign body response and neuroprotection by apyrase and minocycline in chronic cannula implantation" zielte darauf ab, das Ausmaß der anhaltenden Gliazellaktivierung und den sich selbst erhaltenden Zyklus von Mikroglia-induziertem Zelltod

durch das ATP/ADP-hydrolysierende Enzym Apyrase sowie durch das Breitbandantibiotikum Minocyclin zu reduzieren. Da ATP und sein Metabolit ADP beide in der akuten Phase nach einer Hirnverletzung freigesetzt werden und ausschlaggebend an der Vermittlung der Mikroglia-Migration zur Einstichstelle sowie an der astrozytären Kommunikation beteiligt sind, wurde angenommen, dass Apyrase die Gliazellaktivierung sowie den Mikroglia-induzierten sekundären Zelltod unterdrückt. Minocyclin kombiniert aufgrund seines breiten Spektrums an anti-inflammatorischen und anti-apoptotischen Eigenschaften die Ansätze beider Strategien. Daher wurde angenommen, dass es die Kaskade fortschreitenden Zelltods hemmt, die durch das initiale Trauma sowie durch die übermäßige Mikrogliazellaktivierung ausgelöst wird, die ebenfalls zu dem sich selbst erhaltenden Zelltod-Zyklus beiträgt.

Trotz der eher vorübergehenden Verminderung von Mikrogliazellen in Implantatnähe nach Apyrasegabe (0,3 U/µl), hatte die Neuronenpopulation schnell wieder den Ausgangswert erreicht, was jedoch nicht automatisch zu einer äquivalenten Wiederherstellung der Verhaltensperformanz führte. Das Breitbandantibiotikum Minocyclin (20 µg/µl) mit seinen anti-inflammatorischen und anti-apoptotischen Eigenschaften führte zu einem Anstieg der Neuronenpopulation in Implantatnähe nach zwei sowie sechs Wochen, der äquivalent zur gesteigerten Verhaltensperformanz war und von einer Verminderung der Mikroglia-Anzahl sowie einer vorübergehenden Minderung der Astrozytendichte begleitet wurde.

Abschließend lässt sich sagen, dass eine Verminderung der Mikroglia-Aktivierung und des sich selbst erhaltenden Mikroglia-induzierten Zelltod-Zyklus die geringste Wirkung in Bezug auf die Erhaltung der Integrität neuronaler Netzwerke zeigt, wie aus den Verhaltensdaten zu erkennen ist, wohingegen die durch Minocyclin kombinierten Ansätze eine umfassende Verbesserung hervorrufen.

1.3 Fazit

Zusammengefasst legen die vorliegenden Studien nahe, dass es ein wirkungsvoller Ansatz ist, bei den ganz frühen Ereignissen nach der Implantation einzugreifen und die Kaskaden sekundären Zelltods durch die glutamaterge Exzitotoxizität zu inhibieren, um die neuronalen Netzwerke in Implantatnähe zu erhalten. Obwohl die Inhibition der Mikroglia-Antwort und die damit verbundene Reduktion von pro-inflammatorischen und neurotoxischen Molekülen zu einem Anstieg der neuronalen Überlebensrate in Implantatsnähe führt, schafft es dieser

Ansatz, der auf diese zeitlich später eintretende Kaskade abzielt, nicht, die neuronalen Netzwerke im selben Ausmaß zu erhalten. Die Langzeitergebnisse der Studien betrachtend, wird die Glianarbenbildung eher weniger durch die lokale Verabreichung von Substanzen während der Implantation beeinflusst, sondern scheint stattdessen primär ein Resultat der chronischen Präsenz des Fremdkörpers zu sein.

2 Abstract

Over the past decades, immense progress has been made in the field of brain-computer interfaces (BCIs), which provide a new mean to restore mobility in patients suffering from paralysis or amputations. For this purpose, best signals for BCI control can be recorded by intracortically implanted electrodes, providing best precision, accuracy and speed. Although neuroprosthetics have been developed and demonstrated functionality in some first human trials even years after an injury to the central nervous system (CNS), several hurdles have yet to be overcome, since the biocompatibility of these chronic brain implants still remains a major problem. It is of enormous value and interest to better understand and control the tissue response to chronically implanted devices into the brain, such as an electrode array, to ensure that chronic electrode implantation in clinical application is safe and beneficial enough to take the risk of the surgical intervention.

The tissue response to a chronically indwelling implant in the brain is also referred to as “foreign body response” and involves the formation of a glial scar that is accompanied by progressive neurodegeneration. Both contributes to inconsistent performance of recording electrodes and results in a loss of recorded electrical potentials. The foreign body response can be subdivided into an acute phase that is caused by the mechanical trauma of insertion, and a chronic phase due to enduring inflammatory processes at the interface. The acute immune response is a one-to-three week enduring process that is characterised by neuronal and glial cell injury and the damage of blood vessels, which infiltrates macrophages and activates microglial cells and astrocytes. The chronic response is characterised by so called “frustrated phagocytosis” of the macrophages and microglial cells, and persistent inflammation at the implant surface, accompanied by reactive astrocytes forming a dense encapsulating layer to separate the healthy tissue from the enduring inflammation.

The motor cortex, which is considered the main target for BCIs, is part of the frontal lobe and is involved in planning, control and execution of voluntary movements. Since skilled reaching for food is similar in rats and humans, most probably due to a common origin in early tetrapods, the skilled reaching task has evolved into a model system to analyse the functionality of the motor cortex. Within the primary motor cortex of rats (M1), grasping representation can be assigned to the rostral forelimb area (RFA), while reaching representation is primarily found in the caudal forelimb area (CFA).

Due to the sensitivity of the skilled reaching task to motor cortical disturbances, the impact of glial scar formation and neuronal cell death following the chronic implantation of a foreign body into the CFA was suggested in this work to be also measurable on the behavioural level. In this regard, a reversible inactivation study by means of the $GABA_A$ agonist muscimol was initially conducted in order to examine the acute deficits in the skilled reaching task and the precise function of the CFA in Lister Hooded rats. Subsequently, cannula implantation was accompanied by local substance administration, in order to antagonise the foreign body response. Differences in the foreign body response were evaluated by means of rats' behavioural performance in a skilled reaching task as well as in a skilled walking task (rung ladder) and in the open field. Moreover, the distribution of neurons and glial cells in the vicinity of the implant was immunohistologically assessed. The studies served as a proof-of-principle investigation mimicking the implantation of a device such as an electrode array into M1 by means of a steel cannula. The aim of the thesis was to reduce the foreign body response by interfering with the very early events after cannula implantation and to thereby inhibit the induced cascades of enduring cell death and glial cell activation.

2.1 Study 1 (in *Brain Research Bulletin*, 2015)

In *"Suppression of excitotoxicity and foreign body response by memantine in chronic cannula implantation into the rat brain"*, the excitotoxic cascade of glutamate-induced cell death that is induced in the acute phase after foreign body implantation due to the tissue injury was intended to be reduced. The accumulation of glutamate in the extracellular space overstimulates glutamate receptors with N-methyl-D-aspartate (NMDA) receptors playing a pivotal role in excitotoxic cell death. Extrasynaptically located NR2B subunit containing NMDA receptors (NR2BRs) have opposing actions to synaptically located NR2A subunit containing NMDA receptors (NR2ARs), with excessive activation of the first type resulting in the inhibition of pro-survival pathways and excitotoxic cell death of apoptotic or necrotic nature. These cell death promoting effects can be counteracted by the uncompetitive, low-affinity, open-channel blocker memantine, with a preference for extrasynaptically located NR2BRs over synaptically located NR2ARs.

Both doses of memantine (20 µg/µl; 50 µg/µl) that were locally applied during cannula implantation into the CFA, considerably increased the number of surviving neurons

in the vicinity of the implant compared to controls two as well as six weeks after the implantation. This remarkable increase in neurons was accompanied by a slight decrease in reactive astrocytes in implant vicinity that was more pronounced at six weeks and no change in the number of microglial cells/infiltrated macrophages. Behavioural performance was generally most impaired in the skilled reaching task, with moderate impairments in the skilled walking task in the first week and no obvious impairments in the open field. Memantine administration resulted in a quick recovery of the behavioural performance that was only slightly decreased in the first two weeks.

In conclusion, these data suggest that interfering with the very initial events after device implantation targeting the cascades of secondary cell death due to glutamate excitotoxicity seems to be an efficient approach to maintain neuronal networks in the vicinity of an implant.

2.2 Study 2 (submitted in *Behavioural Brain Research*, 2015)

In *"Suppression of the foreign body response and neuroprotection by apyrase and minocycline in chronic cannula implantation"*, the extent of persistent glial cell activation and the self-perpetuating cycle of microglial-induced secondary cell death was aimed to be reduced by means of the ATP/ADP-hydrolysing enzyme apyrase and the broad spectrum antibiotic minocycline. Since ATP and its metabolite ADP are both released in the acute phase after brain injury, and are key in mediating the microglial response towards the site of injury and also in astrocyte communication, apyrase was assumed to reduce the amount of glial cell activation as well as the microglial-induced secondary cell death. Minocycline combined the approaches of both strategies due to its broad range of anti-inflammatory and anti-apoptotic properties and was assumed to inhibit the cascades of enduring cell death induced by the initial trauma as well as the excessive microglial cell activation that further contributes to the self-perpetuating cycle of cell death.

Despite a rather temporary decrease of microglial cells in the vicinity of the implant after apyrase treatment (0.3 U/µl), neuronal populations had quickly recovered close to baseline levels, which however did not automatically result in an equivalent recovery of behavioural performance. The broad-spectrum antibiotic minocycline (20 µg/µl), with anti-inflammatory and anti-apoptotic properties, caused an increase of the neuronal population in the vicinity of the implant at two as well as six weeks that was equivalent to the increased

behavioural performance, accompanied by a decreased number of microglial cells and a temporary decrease in astrocyte density.

In conclusion, aiming to reduce microglial activation and thereby the self-perpetuating cycle of microglial-induced cell death, was least effective in terms of maintaining the integrity of neuronal networks as derived from the behavioural performance. Nevertheless, the combined approaches of minocycline demonstrated overall improvements.

2.3 Conclusion

Taken together, the present results suggest that interfering with the very initial events after device implantation targeting the cascades of secondary cell death due to glutamate excitotoxicity seems to be an efficient approach to maintain neuronal networks in the vicinity of an implant. Although reducing the microglial response and thereby the degree of pro-inflammatory and neurotoxic molecules increases the neuronal survival in the vicinity of an implant, targeting these delayed cascades does not maintain neuronal networks to the same extent. Moreover, regarding the long-term results, glial scar formation is apparently rather less influenced by the acute administration of substances during cannula implantation, but instead seems to be primarily a consequence of the chronic presence of the foreign body.

3 General introduction

Over the past decades, growing interest emerged on the chronic implantation of electrodes into the brain to restore mobility in patients that suffer from paralysis, amputations or from a motor system or affective disorder (Lebedev and Nicolelis, 2006;Kringelbach et al., 2007;Hochberg et al., 2012;Jackson, 2012). Research on brain-computer interfaces (BCIs) has rapidly evolved accompanied by an ongoing debate about the acquisition of electrophysiological signals from the brain by means of non-invasive or invasive BCIs (Wolpaw et al., 2000). Signals recorded by electrodes are processed and translated into commands that reflect the users' intent. Non-invasive BCIs derive the users' intent from scalp-recorded electroencephalographic (EEG) activity, evaluated via sensorimotor cortex rhythms, slow cortical potentials and P300 evoked potentials. Invasive BCIs record electrical activity of the brain via intracranially implanted electrodes either from subdural or epidural electrocorticographic (ECoG) activity or from single unit-based systems implanted into the brain parenchyma. ECoG signals are derived from sensorimotor rhythms similar to EEG signals but are much more robust and carry highly specific and anatomically focal information about cortical processing. Best signals for BCI control are however achieved by intracortically implanted electrodes that record neuronal action potentials or local field potentials with multi-electrode single unit recordings providing best precision, accuracy and speed. Depending on the patients' insult or disease and actual needs, different device outputs are required ranging from simple communication via cursor control, over the control of a motorised wheel chair, to very fine control of a prosthetic limb **(Fig. 3.1)** (Wolpaw et al., 2002;Leuthardt et al., 2006;Mak and Wolpaw, 2009). For fine-tuned, real-time control of artificial devices or of the own limbs it is moreover essential to receive sensory feedback, which is why long-term solutions include not only electrode recordings from motor cortices, but also microstimulation of somatosensory cortices by means of brain-computer-brain interfaces (Nicolelis and Lebedev, 2009).

3.1 Applications of chronic brain implants

3.1.1 Human diseases

BCIs provide a new means to restore mobility and independence in patients suffering from amputations or paralysis due to spinal cord injury, brainstem stroke, amyotrophic lateral

sclerosis, cerebral palsy or other disorders that involve the loss of movement control (Mak and Wolpaw, 2009). Patients with long-standing tetraplegia have already been successfully implanted with neural interface systems and were able to control complex devices such as a robotic arm by recording neural signals from the primary motor cortex (M1). Even years after an injury of the central nervous system (CNS), the application of BCIs has been demonstrated to be feasible, indicating that M1-neuronal ensemble activity remains functionally engaged despite subcortical damage of descending motor pathways (Hochberg et al., 2006;Chadwick et al., 2011;Hochberg et al., 2012).

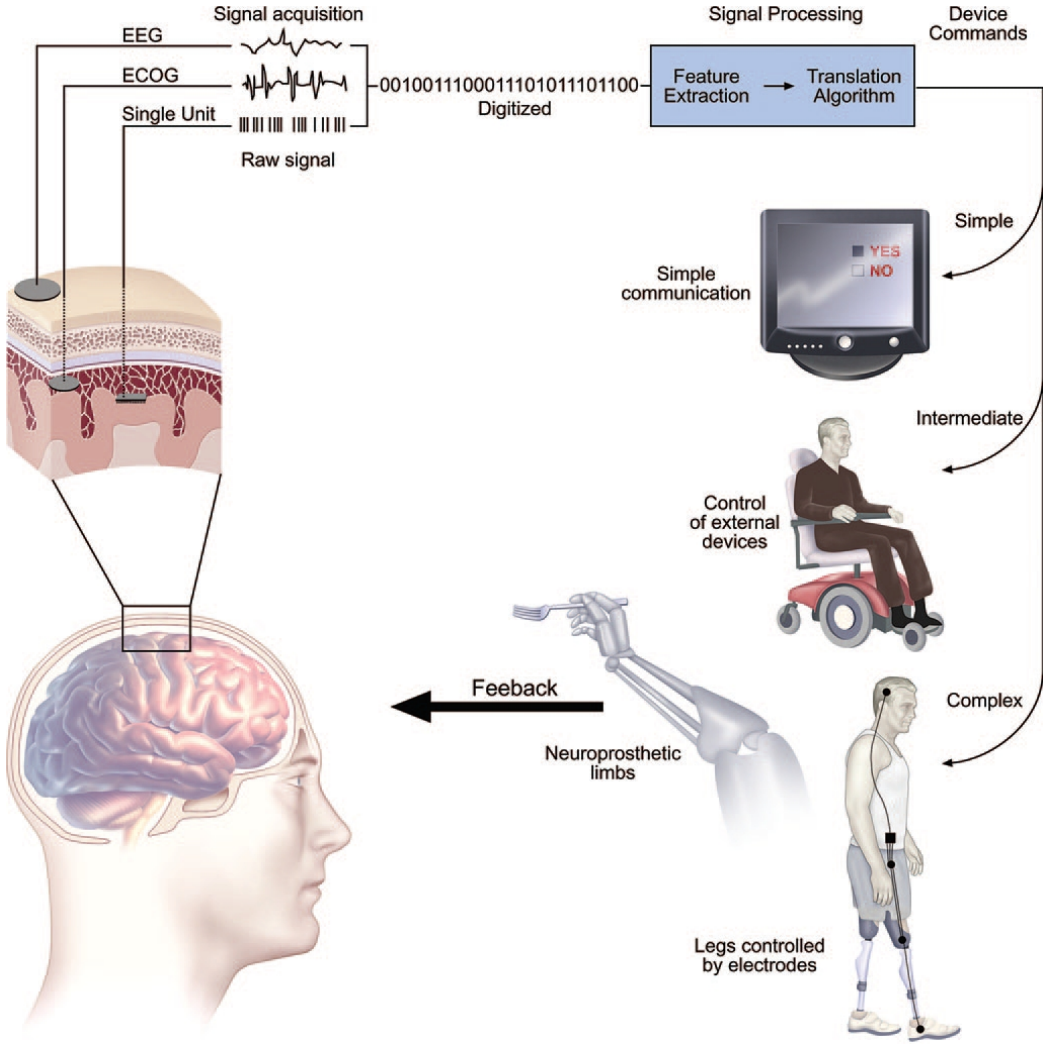

Fig. 3.1 Schematic representation of electrophysiological signal acquisition and processing from non-invasive or invasive brain-computer interfaces into device commands. Brain signals are acquired by electrodes non-invasively from scalp-recorded electroencephalographic (EEG) activity, or invasively either from subdural or epidural electrocorticographic (ECoG) activity or from single unit-based systems implanted into the brain parenchyma. Signals are digitised, processed and translated into device commands ranging from simple to higher levels of control. Sensory feedback improves the performance by altering electrophysiological signals (Leuthardt et al., 2006).

Neural interface systems are however not solely intended to restore mobility, but also to restore sensory information in blind or deaf people by means of sensory neuro-prostheses. Cochlear implants (Loeb, 1990;Wilson et al., 1991), auditory brain stem implants (O'Driscoll et al., 2011;Matthies et al., 2014) or midbrain implants (Lenarz et al., 2006) have been developed as auditory prostheses, as well as visual prostheses that stimulate retinal neurons, the optic nerve or the visual cortex (Pezaris and Eskandar, 2009).

Electrode implantation is also necessary for deep brain stimulation (DBS), which is of remarkable therapeutic benefit in disorders such as chronic pain, Parkinson's disease, tremor and dystonia. DBS also proved useful for the treatment of affective and related disorders, including depression, obsessive-compulsive disorder, Tourette's syndrome, chronic pain or cluster headache (Kringelbach et al., 2007).

Further potential applications of chronically implanted intracranial electrodes are in epilepsy to monitor, detect and treat seizures by means of automatic seizure-prediction algorithms that trigger automatic therapeutic interventions before convulsions and the loss of consciousness occur (Nicolelis, 2001).

3.1.2 Animal models

In animal models microinjections via chronically implanted stainless steel guide cannulae **(Fig. 3.2)** represent a common method in basic research to study transmitter systems and receptor subtypes as well as drug effects on the behaviour (Krase et al., 1993;Koch et al., 2000). The contribution of specific brain areas to certain behaviours or diseases by means of permanent or reversible inactivation of that brain area is a further field of application for chronic brain implants (Fendt et al., 1994;Koch et al., 1996;Feja et al., 2014). Reversible inactivation differs from permanent inactivation by permitting an examination of functional deficits immediately following the tissue inactivation without any "recovery of function". In permanent tissue inactivation the animal has to cope with the inactivated tissue permanently and often develops compensatory strategies, or relies upon secondary cortical circuits to accomplish the task which makes it more difficult to evaluate the results in chronic settings. In reversible inactivation experiments no recovery of function takes place since the inactivation lasts for limited time only (Lomber, 1999). In this work an initial reversible inactivation study by means of the $GABA_A$ agonist muscimol was also conducted in

order to examine the acute behavioural deficits in a skilled reaching task and the precise function of the motor cortical area chosen for the follow-up experiments.

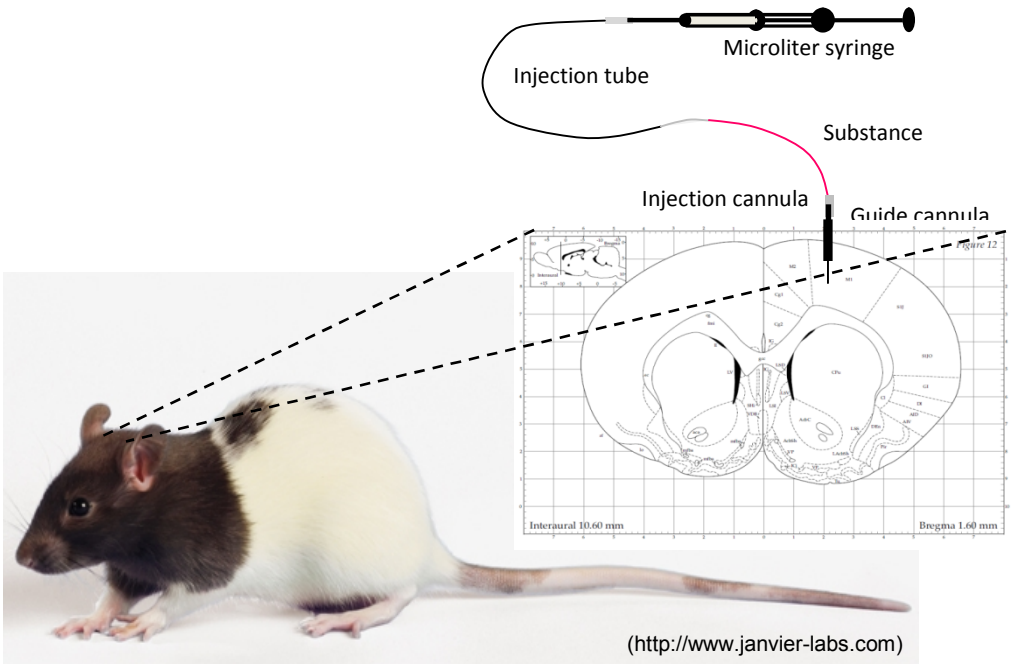

Fig. 3.2. Chronic cannula implantation in animal models. Guide cannulae are chronically implanted by means of stereotactic devices to enable insertion of injection cannulae which are connected to a microliter syringe via an injection tube. Substances can be precisely injected into specific brain areas, as depicted here for the caudal forelimb area of the primary motor cortex in Lister Hooded rats on a schematic drawing from the rat brain atlas (Paxinos and Watson, 1998).

However, chronic cannula implantations used for microinjections are not the only application of chronic brain implants in animal models. Optical imaging via the insertion of micro-optical probes into surgically implanted guide tubes works similarly and is a further field of application that serves to examine brain processing or disease progression by tracking neurons or gliomas, vasculature structures or microcirculatory speed (Barretto et al., 2011).

Moreover, BCIs are not only of clinical relevance, but can also contribute to real-time neurophysiological investigations of neural circuits in behaving animals and to quantification of physiological changes that take place in learning of sensorimotor and cognitive tasks (Nicolelis et al., 2003). Electrodes are also in use as biosensors in order to investigate transmitter release and receptor activity in the absence and presence of pharmacological

agents (Nguyen et al., 2010) and are inevitably required in preclinical basic research for the application of DBS therapies (Gong et al., 2015).

3.1.3 Obstacles for clinical application

Although there has been immense progress in the field of BCI research and some first human trials were successful, several hurdles have yet to be overcome. A lot of basic research in device implantation is still necessary to better understand and control the tissue response to indwelling devices and to ensure that chronic electrode implantation in clinical application is safe and beneficial enough to take the risk of the surgical intervention. Besides improving electrode designs, microelectronics, power management, real-time computational modelling and robotics, the biocompatibility of the implants remains a major problem for long-term clinical applications (Nicolelis et al., 2003;Polikov et al., 2005). The tissue response that is also referred to as “foreign body response” involves the formation of a glial scar around the implant that is accompanied by progressive neurodegeneration. Both contributes to inconsistent performance of recording electrodes in humans and results in a loss of recorded electrical potentials (Polikov et al., 2005).

Previous attempts to minimise the foreign body response examined different electrode designs and implantation techniques (Edell et al., 1992;Turner et al., 1999;Szarowski et al., 2003;Nicolelis et al., 2003;Kim et al., 2004;Biran et al., 2005), as well as different surface coatings with biocompatible (Ignatius et al., 1998;Kam et al., 2002;He et al., 2006) or immunosuppressant molecules (Maynard et al., 2000;Shain et al., 2003;Kim and Martin, 2006;He et al., 2007). However, a satisfactory control of the foreign body response is still not available (Polikov et al., 2005;Griffith and Humphrey, 2006).

3.2 Cells involved in the immune response of the brain

The foreign body response is a protective mechanism by the immune system with different cell types being involved. The CNS tissue consists of neurons, glial cells (oligodendrocytes, astrocytes and microglia) and vascular-related tissue. Glial cells are evolutionarily conserved, existing in similar forms in simple invertebrates as well as in vertebrates such as humans. The proportion of glial cells to neurons seems to be correlated to the animal’s taxonomical organisation, with the brain of fruit flies consisting to 25% of glia, of rodents to roughly 65%

and of humans to about 90% (Allen and Barres, 2009). In post-mortem studies of human cortices, a glia to neuron ratio of 1.32 and 1.49 for males and females, respectively, has been observed, with males exhibiting a 28% higher number of cortical glial cells and a 19% higher number of cortical neurons. For rats, the cortical glia to neuron ratio was suggested to be slightly higher with about twice as much glial cells compared to neurons. The ratio of the different types of glial cells was suggested to be about 75% oligodendrocytes, 20% astrocytes and 5% microglia (Pelvig et al., 2008). The oligodendrocytes in the CNS are the equivalent of the Schwann cells in the peripheral nervous system (PNS) and provide mechanical support and electric insulation to neuronal axons. By extending processes around multiple axons, they are metabolically coupled to neurons and form myelin sheaths that are essential for saltatory conduction of action potentials (Simons and Nave, 2015). However, the main effectors in the brain's immune response are microglia and astrocytes.

3.2.1 Microglia

Microglial cells constitute the resident macrophages of the brain and constantly screen the brain tissue in their "resting" state for pathologic events. They exhibit a ramified morphology with highly mobile processes that are continually rebuilt (*de novo* formation) and retracted in order to thoroughly scan the environment. The complete brain parenchyma is monitored every few hours without translocation of microglial cell bodies. This high "resting mobility" serves as housekeeping function to control the microenvironment and to clear the parenchyma of metabolic products or deteriorated tissue components (Nimmerjahn et al., 2005;Hanisch and Kettenmann, 2007). A transformation from their surveillant "resting" state to an "activated" state takes place in response to disturbances of tissue homeostasis, such as after microlesions or traumatic injuries as well as in neurodegenerative diseases, stroke or brain tumors. The mediation of the rapid baseline dynamics of their processes as well as of injury-induced chemotactic responses necessarily involves the nucleotide adenosine triphosphate (ATP) (Davalos et al., 2005).

Four distinct morphological phenotypes of microglia can be distinguished according to their degree of activation: ramified, primed, reactive and amoeboid. Ramified microglial cells display a small but defined cell body with several highly branched processes that correspond to resting microglia. Primed microglia cells have fewer higher-order branches and wider cell bodies and are an intermediate phenotype. Reactive microglia are the next

level of intermediate phenotypes in the sequence of complete activation with amoeboid-shaped cell bodies and only few processes that are generally longer than the cell body. Fully activated amoeboid microglia cells also have the characteristic amoeboid-shaped cell body and are either devoid of processes or have a few unbranched processes within the length of the cell body. Microglia can either transform into an intermediate phenotype and return to the ramified morphology or transform into the amoeboid phenotype along the complete activation sequence (Torres-Platas et al., 2014).

Activated microglia can be further distinguished according to their functionality into "classically activated" pro-inflammatory (type-1) microglia or "alternatively activated" anti-inflammatory (type-2) microglia. Depending on the type and extend of pathological event, microglia shift from their homeostatic surveillant "resting" state into an "activated" state of type-1 or type-2 (Kigerl et al., 2009). Upon tiny homeostatic disturbances, such as microlesions of vessels or tissue, microglia rapidly respond with a directed reorganisation of processes and the production of neurotrophic factors, like nerve growth factor (NGF), brain derived neurotrophic factor (BDNF), glial-derived neurotrophic factor (GDNF) and neurotrophin-3 (NT-3), to support endangered neurons and promote regenerative processes, which are mediated by anti-inflammatory type-2 microglia **(Fig. 3.3)** (Hanisch and Kettenmann, 2007). Under these acute conditions of minor disturbances, microglia cells are able to limit further damage and restore normal homeostasis, which thus remains largely unrecognised. However, after stronger insults to the CNS, such as infectious challenges or significant tissue injury, more drastic changes are triggered in the functional phenotype, which then surfaces overt symptoms. These stronger insults trigger the transformation of microglia cells towards the type-1 phenotype that releases pro-inflammatory molecules including excitatory amino acids, such as glutamate or aspartate, reactive oxygen intermediates, such as hydrogen peroxide (H_2O_2) or superoxide anion (O^{2-}), reactive nitrogen intermediates, such as nitric oxide (NO), and diverse pro-inflammatory cytokines, such as interleukin-1 (IL-1), IL-6 or tumor necrosis factor alpha (TNFα). Excessive acute, sustained or maladaptive responses of microglia cause failure of protection and trigger neurotoxic damaging cascades (Polikov et al., 2005;Hanisch and Kettenmann, 2007).

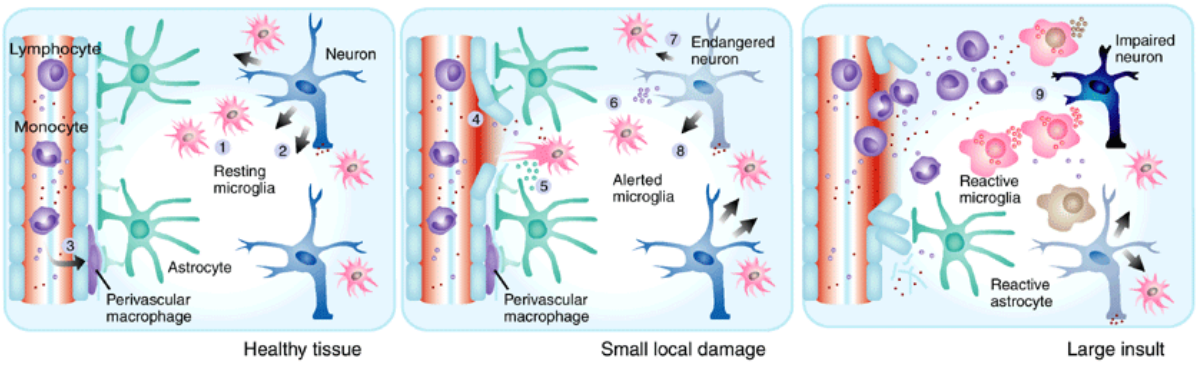

Fig. 3.3. Activity states of microglia. Left, "resting" microglia actively scan their environment (1) for signals released by neurons (2) or pathological events disturbing homeostasis. Perivascular macrophages (3) also scan for disruption of blood vessels. **Middle**, tiny microlesions (4) trigger microglial "activation" into anti-inflammatory type-2 microglial cells that are supported by neighbouring astrocytes (5). Type-2 microglia release neurotrophic factors (6) in order to support endangered neurons, which are recognised by a disruption of ongoing communication (7) or by emission of signals indicating disturbed functions (8). **Right**, stronger insults trigger microglial transformation into pro-inflammatory type-1 microglia (9) that actively contribute to neurotoxic damaging cascades (Hanisch and Kettenmann, 2007).

3.2.2 Astrocytes

Astrocytes are the second cell type involved in the immune response of the brain and contribute to homeostasis in the healthy brain by removing neurotransmitters from the synaptic cleft and providing neurons with energy and substrates for neurotransmission. They exhibit cellular extensions giving them a star-like appearance with end feet abutting capillary walls serving the transfer of nutrients across the blood-brain-barrier (BBB). Astrocytes provide mechanical support to neuronal networks and can be subdivided into protoplasmatic astrocytes in the grey matter associated with cell bodies and synapses and into fibrous astrocytes in the white matter associated with axons. When activated by an injury or other pathological event, they transform into a "reactive" phenotype. They proliferate, migrate to the site of injury and are characterised by hypertrophy and an up-regulation of their intermediate protein GFAP (glial fibrillary acid protein). Astrocytes possess many of the same neurotransmitter receptors as neurons, and neurotransmitter release activates Ca^{2+}-based signalling cascades between astrocytes. They interact and communicate with neurons by means of feed-back loops and inhibit or enhance the neuronal activity (Polikov et al., 2005;Allen and Barres, 2009). Astrocytes are coupled by gap

junctions composed of two connexons (connexin hemichannels), by which they mediate intercellular transfer of metabolites (e.g. adenosine diphosphate (ADP), glucose and glutathione), second messengers (e.g. cyclic adenosine monophosphate (cAMP) and inositol 1,4,5-trisphosphate (IP_3)) and ions (e.g. Na^+, K^+ and Ca^{2+}). This formation of a functional syncytium allows intercellular communication and spatial buffering of ions and metabolites (Montero and Orellana, 2015).

Far reaching communication via Ca^{2+}-wave propagation has been shown to depend largely on extracellular release of ATP, which acts as an the intercellular messenger (Guthrie et al., 1999) via purinergic pore-forming $P2X_7$ receptors (Ballerini et al., 1996;Suadicani et al., 2006) and to be independent in its propagation from intracellular Ca^{2+} and IP_3 (Wang et al., 2000). Extracellular ATP binds to purinergic P2 receptors on adjacent cells that can be subdivided into P2X receptors, a family of ligand-gated ion channels selectively permeable to Na^+, K^+ and Ca^{2+} with seven subtypes, and P2Y receptors, a family of G-protein-coupled receptors (GPCRs) with eight subtypes. A second class of purinergic receptors are the P1 receptors, a family of GPCRs with four subtypes, that bind the metabolite adenosine (Fields and Burnstock, 2006;Burnstock, 2008). Binding of extracellular ATP to purinergic P2 receptors on adjacent cells, results in Ca^{2+} transmembrane influx via the P2X receptor channel and in cell depolarisation. Moreover, P2Y receptor activation triggers the production of IP_3 via a G-protein-mediated mechanism, which causes the release of Ca^{2+} from the endoplasmatic reticulum (Goodenough and Paul, 2003;Fischer et al., 2009). ATP-induced ATP release from astrocytes is required for the propagation of intercellular Ca^{2+}-signals (Anderson et al., 2004). Ca^{2+}-wave propagation in astrocytic communication in response to any kind of pathological event that causes disturbances of the homeostasis is indispensable of ATP.

Since astrocytes express a large variety of neurotransmitter receptors, they sense neuronal activity as well as microenvironmental changes. They respond to changes with the release of ATP as the most important “gliotransmitter” in astrocyte communication, as well as with the release of further bioactive molecules, such as glutamate, aspartate, adenosine, GABA or D-serine (Montero and Orellana, 2015). The release of the excitatory amino acids glutamate and aspartate from astrocytes is also dependent on Ca^{2+}-release from internal stores (Jeremic et al., 2001) which results in a non-vesicular efflux of glutamate and aspartate through the pore-forming $P2X_7$ receptor (Duan et al., 2003). However, glutamate

release can additionally be mediated by reversal of uptake by plasma membrane glutamate transporters, by volume-regulated anion channel opening induced by cell swelling, by exchange via cystine-glutamate antiporter or by hemichannels on the cell surface as well as by Ca^{2+}-dependent vesicular exocytosis (Malarkey and Parpura, 2008). Since ATP release from astrocytes has also been shown to be evoked by glutamate receptor activation (Queiroz et al., 1997), there seems to be a positive feedback loop between the release of glutamate and ATP by astrocytes (Jeremic et al., 2001).

3.3 The foreign body response

The immune response of the brain to a chronically implanted foreign body such as an electrode array or a cannula can be subdivided into an acute phase that is caused by the mechanical trauma of insertion and a chronic phase due to enduring inflammatory processes at the interface (Polikov et al., 2005).

3.3.1 Mechanical trauma of insertion (acute phase)

The acute immune response of the brain is a one to three week process that is initiated by the mechanical trauma due to device implantation and the release of cellular contents by injured cells. In the acute phase of the wound healing response, especially resident microglia and infiltrated macrophages are activated to clear cellular debris and excessive fluid, but also reactive astrocytes start to insulate the implant and the damaged tissue from the surrounding healthy tissue (Polikov et al., 2005). In addition to the release of cellular contents from injured and dying cells, activated microglial cells release neurotoxic and pro-inflammatory molecules, which causes secondary cell death to neurons and neuronal “die-back” zones around implants (Biran et al., 2005;Potter et al., 2012). The neuronal cell loss is accompanied by the formation of a glial scar that occurs faster than re-growth of neuronal processes (Turner et al., 1999). Within two weeks after implant insertion, the formation of a loosely organised glial sheath is observed with scattered reactive microglial cells and reactive astrocytes that extend their processes towards the insertion site up to 500 µm from the implant **(Fig. 3.4A)** (Turner et al., 1999;Szarowski et al., 2003).

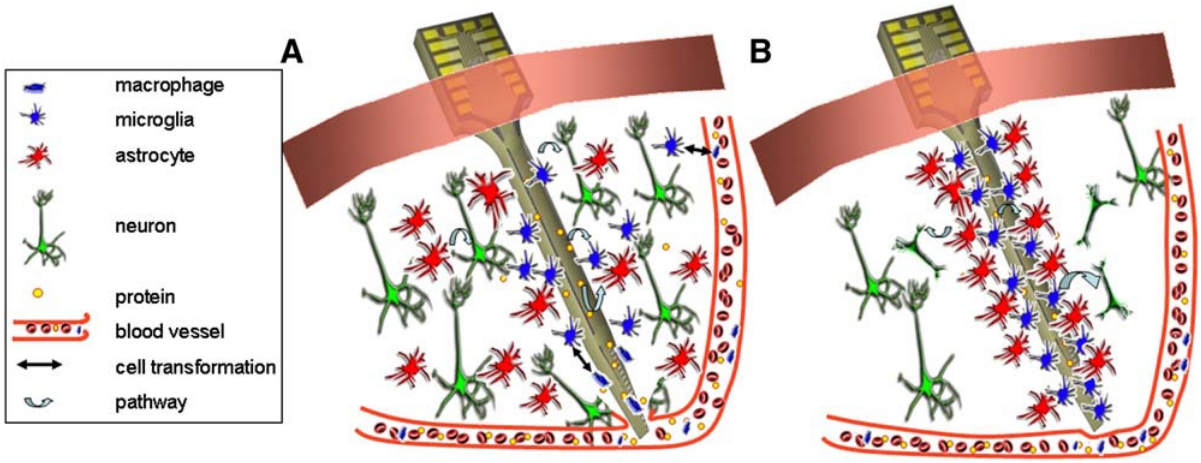

Fig. 3.4. Schematic representation of the acute and chronic tissue response following device implantation. A) The acute tissue response is characterised by neuronal and glial cell injury and the damage of blood vessels, which infiltrates macrophages and activates microglial cells and astrocytes. **B)** The chronic response is characterised by "frustrated phagocytosis" of the microglial cells and enduring inflammatory processes at the implant surface, accompanied by reactive astrocytes forming a dense encapsulating layer to separate the healthy tissue from the enduring inflammation (Schwartz et al., 2006).

3.3.1.1 Glutamate-mediated excitotoxicity

During the insertion of an implant into the brain, neurons and glial cells in the tract are injured and blood vessels are damaged. The disruption of blood vessels in the implantation tract impairs the oxygen and glucose supply of neurons, which results in energy-depletion followed by ionic imbalance. Uncontrolled membrane depolarisation and massive changes in the concentration gradients of Na^+ and K^+ across the cell membrane result in a sustained release of the excitatory amino acid glutamate (Iadecola and Anrather, 2011;Bretón and Rodríguez, 2012). Glutamate released from neurons is either Ca^{2+}-dependently released from neuronal vesicles, K^+-dependently through swelling-activated anion channels or Na^+-dependently by a reversed operation of glutamate transporters (Rossi et al., 2000). Moreover, the damage of neurons causes leakage of excitotoxic amounts of glutamate from necrotic cells, which triggers a cascade of apoptotic and necrotic events (Bonfoco et al., 1995). The accumulation of glutamate in the extracellular space results in an overstimulation of glutamate receptors with the N-methyl-D-aspartate (NMDA) receptor playing a key role in

excitotoxic cell death due to its high permeability for Ca^{2+} (Lipton and Rosenberg, 1994;Lynch and Guttmann, 2002).

The two major subtypes of NMDA receptors in the adult forebrain are the NR2A subunit containing receptor (NR2AR) and the NR2B subunit containing receptor (NR2BR). NR2ARs are primarily located at the synapse and are essential for synaptic transmission and plasticity with its activation triggering intracellular processes resulting in neuronal survival. NR2BR are primarily located at extrasynaptic sites and their activation triggers the activation of downstream cascades that result in neuronal cell death (Hardingham et al., 2002;Lai et al., 2011;Vizi et al., 2013). Hence, neurotoxicity is not solely mediated by the extent of NMDA receptor activity and Ca^{2+}-overload *per se*, but rather by the Ca^{2+}-flow through extrasynaptically located NR2BRs (Leveille et al., 2008). Although both receptor subtypes cause Ca^{2+}-increase in the neuron, they activate different intracellular pathways. Synaptic NR2AR activation triggers the phosphorylation of the extracellular signal-regulated kinase (ERK) and thereby the activation of the ERK pathway. Subsequent phosphorylation of the cellular transcription factor cAMP response element-binding protein (CREB) induces the transcription of genes linked to neuroprotection against apoptotic and excitotoxic insults, such as the neurotrophin BDNF, which promotes neuronal survival, or activity-regulated inhibitors of death (AID), that render mitochondria more resistant to stress and toxic insults. Activation of extracellular NR2BRs has opposing effects and promotes ERK dephosphorylation and thereby an inhibition of gene transcription by CREB, with the extrasynaptic ERK “shut-off” signal being dominant over the synaptic “on” signal (Hardingham and Bading, 2010). This causes a suppression of pro-survival pathways, and instead triggers the expression of pro-apoptotic proteins **(Fig. 3.5)** (Ehrnhoefer et al., 2011).

The excessive rise in Ca^{2+}-levels also triggers further processes involved in neurotoxicity that include the production of excessive amounts of NO, which serves as substrate for free radical production. NO is produced in neurons by the neuronal nitric oxide synthase (nNOS) that catalyses the conversion of the amino acid L-arginine to L-citrulline by oxidative deamination (Burgner et al., 1999). In the healthy brain, NO is involved in synaptic plasticity and neuronal signalling. However, excessive amounts of NO that are produced by NMDA receptor overactivation majorly contribute to glutamate-mediated neurotoxicity (Dawson and Dawson, 1996;Habib and Ali, 2011). High levels of NO induce necrosis due to cellular energy depletion via the inhibition of cytochrome C oxidase. This inhibition impairs

the mitochondrial respiratory chain and ATP production via the formation of peroxynitrite that induces mitochondrial permeability transition resulting in ATP-hydrolysis and via the formation of reactive oxygen species (ROS) and reactive nitrogen species (RNS) that cause DNA strand breaks. ATP depletion causes failure of ATP-driven Ca^{2+}- and Na^{+}-pumps and results in osmotic rupture of the plasma membrane. Since caspase activation is also ATP-dependent, its depletion prevents apoptosis and usually causes necrosis instead (Brown, 2010).

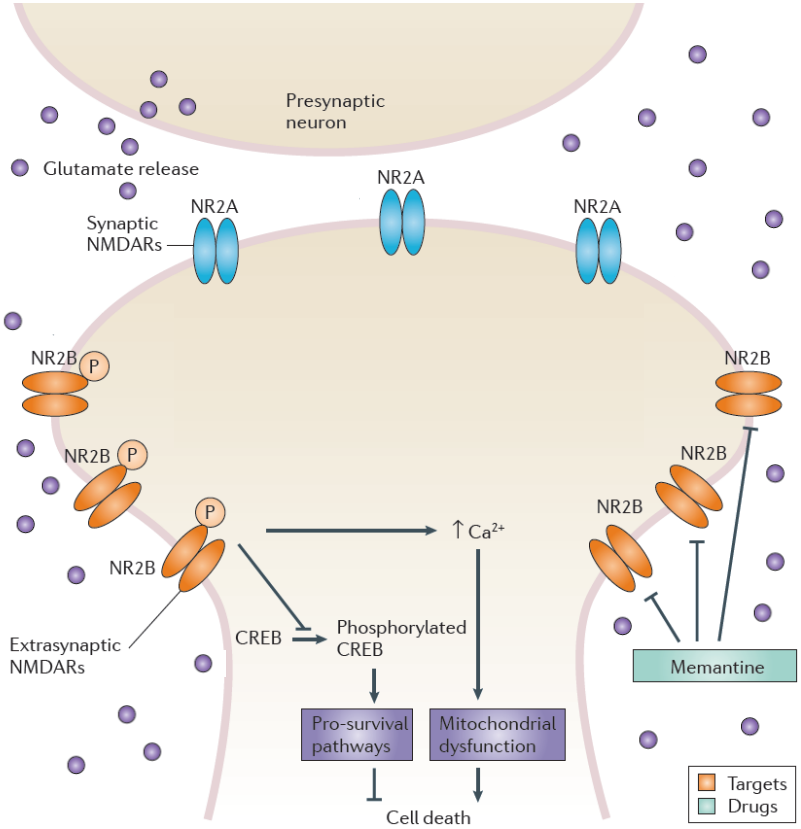

Fig. 3.5. Glutamate-mediated excitotoxicity. The accumulation of glutamate in the extracellular space after tissue damage results in an overstimulation of glutamate receptors with opposing actions of synaptically located NR2A subunit containing N-methyl-D-aspartate (NMDA) receptors and extrasynaptically located NR2B receptors. Excessive activation and Ca^{2+}-influx into the cells via extrasynaptic NR2B receptors causes mitochondrial dysfunction and cell death via an overproduction of reactive oxygen species (ROS), cell membrane rupture and DNA fragmentation. Moreover, NR2B receptor activation promotes extracellular signal-regulated kinase (ERK) dephosphorylation and inhibits the transcription factor cAMP response element-binding protein (CREB), which results in the inhibition of pro-survival pathways and excitotoxic cell death of apoptotic or necrotic nature. These cell death promoting effects can be counteracted by the low-affinity, open-channel blocker memantine (from Ehrnhoefer et al., 2011).

NMDA receptors in neurons have been shown to interact with multi-protein complexes known as postsynaptic densities (PSDs) that contain several PDZ (postsynaptic density-95/discs large/zonula occludens-1) protein interaction domains. The most prominent protein component in the PDZ complex is the protein PSD-95, that contains three PDZ domains, of which the first two (PDZ1 and PDZ2) interact with the NR2B subunit, that is linked via these domains to nNOS. Activation and Ca^{2+}-influx into the cells via this receptor causes binding of the allosteric activator calmodulin to nNOS, which initiates complex formation of NMDA receptor/PSD-95/nNOS. Under sustained conditions, this leads to the production of excessive amounts of NO, which serves as substrate for highly free radical production and is a major component of excitotoxicity (Bretón and Rodríguez, 2012). Inhibition of PSD-95/nNOS interaction has also proven beneficial in reducing excitotoxic damage (Zhou and Zhu, 2009;Zhou et al., 2010).

Moreover, the overstimulation of extrasynaptically located NR2BRs and the concomitant rise in Ca^{2+}-levels causes the activation and overstimulation of proteases, lipases, phosphatases and endonucleases. Mitochondrial dysfunction, which is a consequence of the excessive Ca^{2+}-influx, results in the formation of ROS and caspase activation, cell membrane rupture, cytoskeletal breakdown and DNA fragmentation that also results in excitotoxic cell death (Bretón and Rodríguez, 2012). The necrotic cells release further glutamate that spills over to nearby cells that had survived the original trauma. This causes secondary damage to originally uninjured cells by consecutive depolarisation, cell swelling, lysis and the further release of cellular contents, including glutamate, into the parenchyma. This autodestructive cascade of progressive cell death mediated particularly via extrasynaptically located NR2BR can continue for hours or even days after a severe insult primarily by necrotic-like mechanisms (Lipton, 2004). Memantine, as an uncompetitive, low-affinity, open-channel blocker with a preference for extrasynaptically located NR2BRs over synaptically located NR2ARs, has been shown to be neuroprotective and to inhibit glutamate-mediated excitotoxicity (Lipton, 2004;Lipton, 2006;Xia et al., 2010).

3.3.1.2 NO and ATP in glial cell activation

The primary damage of brain tissue after insertion of an implant is coupled to the release of cellular contents that can either directly cause damage to the brain tissue or indirectly via the activation of pro-inflammatory microglial cells. In addition to the release of cellular

contents and nNOS activation, several further forms of NOS are up-regulated that produce large amounts of NO (Conti et al., 2007).

In addition to nNOS, that is immediately up-regulated after cell injury, a second form of constitutively expressed NOS is up-regulated, which is called endothelial NOS (eNOS) according to its location in the endothelium of blood vessels (Alderton et al., 2001). Unlike nNOS, eNOS which is activated by sheer forces has been suggested to have a neuroprotective role. By promoting vasodilatation, it lowers the blood pressure in the vessels and maintains local blood flow and nutrients supply. Moreover, it inhibits microvascular aggregation, adhesion and vasospasm and is suggested to reduce neuronal cell loss following ischemia. Compared to total brain NOS activity, eNOS contributes to only a fraction of NO production (Wei et al., 1999;Gewaltig and Kojda, 2002;Conti et al., 2007).

A third form of NOS is the inducible form of NOS (iNOS) that is expressed in all cell types in response to a pathological event including astrocytes and microglia. This inducible form synthesises about 100-1000 times more NO than the constitutively expressed enzymes (Alderton et al., 2001). After the first short toxic peak of NO production by nNOS that is reached within one hour, there is a second increase of NO in damaged tissue that goes back to the activation of iNOS. Its activation is induced by pro-inflammatory cytokines within two hours after an injury and its amount grows progressively for a few days (Conti et al., 2007). The expression of iNOS is regulated at the transcriptional level and does not require Ca^{2+} for its activity. The enduring release of large amounts of NO is not only harmful for surrounding neurons but has also been demonstrated to be an important chemoattractant for microglial cells to migrate to the site of injury. However, it has also been shown that NO is only an effective chemoattractant in the presence of ambient ATP (Dibaj et al., 2010).

An increase in extracellular ATP concentration has been shown to rapidly mediate the microglial response towards the site of injury (Davalos et al., 2005). Initially released from the damaged tissue, high levels of ATP persist in the peritraumatic zone for many hours after an insult, thereby triggering irreversible increases of cytosolic Ca^{2+} and cell death of even healthy neurons through purinergic receptor activation with an important role for the $P2X_7$ receptor (Wang et al., 2004). Moreover, the high levels of extracellular ATP also trigger an increase of Ca^{2+}-levels in astrocytes (Wang et al., 2000), which results in the release of regenerative ATP from internal pools (Anderson et al., 2004). This ATP-induced ATP release from astrocytes is not only responsible for far reaching communication via Ca^{2+}-wave

propagation between astrocytes, but also enhances the directional chemotactic response of microglial cells (Davalos et al., 2005). Microglial activation is accompanied by the release of pro-inflammatory cytokines, which further amplifies the immune response resulting in a self-perpetuating cycle of cell death after a severe insult **(Fig. 3.6)** (Bianco et al., 2005;Schwartz and Shechter, 2010). In addition to ATP release, astrocytes also release glutamate in response to ATP binding, which exacerbates the glutamate-mediated excitotoxicity and further contributes to neuronal cell loss (Lipton and Rosenberg, 1994;Lynch and Guttmann, 2002). The ATP-induced ATP release from astrocytes is required for the activation and migration of microglial cells to the site of injury, which exacerbates secondary cell death and the immune response after severe tissue damage. This microglial activation has been shown to be reduced by the enzyme apyrase, an ATPase that hydrolyses extracellular ATP and ADP (Davalos et al., 2005).

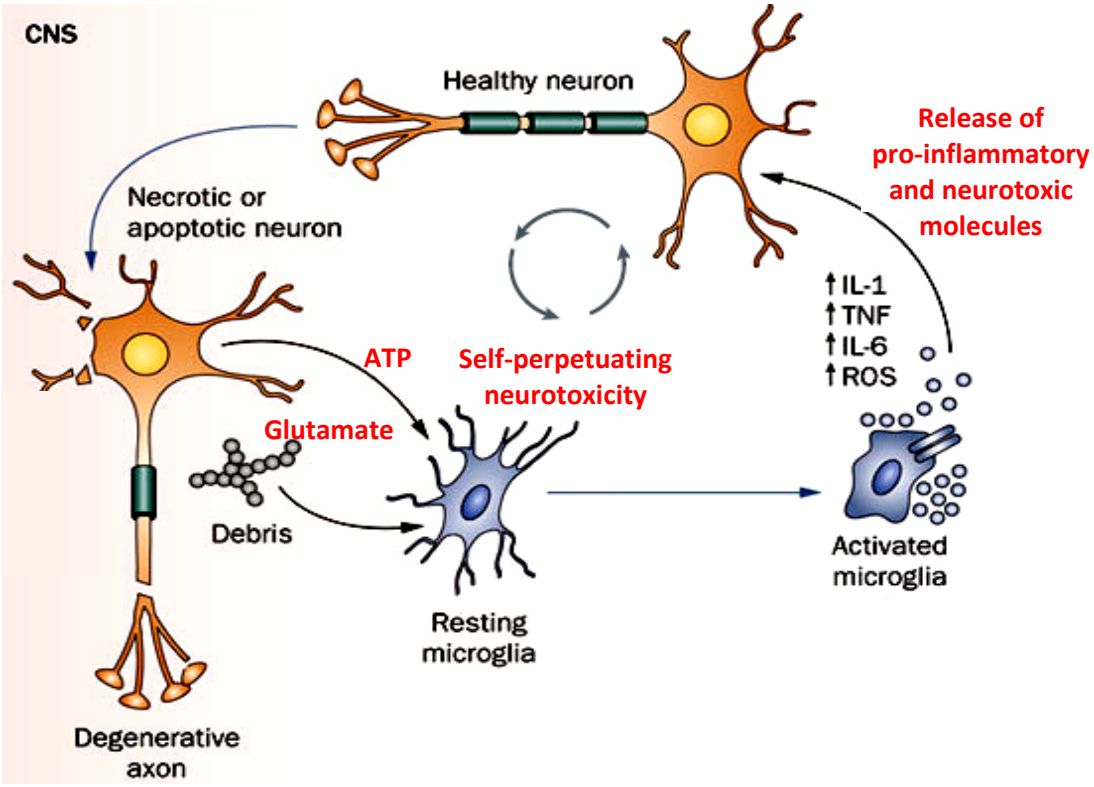

Fig. 3.6. Self-perpetuating cycle of cell death. Neuronal damage results in the leakage of excitotoxic glutamate and adenosine triphosphate (ATP) from injured cells. This induces the activation of microglial cells (also referred to as reactive microgliosis). The activated microglia phagocytose neuronal debris while concurrently releasing pro-inflammatory cytokines, such as interleukin (IL)-1, tumor necrosis factor (TNF) and IL-6, and neurotoxic molecules, such as reactive oxygen species (ROS), that contribute to a cycle of self-sustaining neurotoxicity involving the loss of surrounding neurons and the activation of further microglial cells (from Schwartz and Shechter, 2010).

3.3.1.3 Self-perpetuating cycle of cell death

The initial activation and migration of microglial cells is beneficial after tiny microlesions in the protection against infectious agents and the repair of the damaged tissue by means of producing neurotrophic substances and cell adhesion molecules, which support injured neurons. Similar, the activation and proliferation of astrocytes helps to separate healthy from necrotic tissue (Eddleston and Mucke, 1993;Marin and Fernandez, 2010). However, under severe acute or chronic conditions an overactivation of microglial cells causes secondary tissue damage due to the release of pro-inflammatory and neurotoxic molecules. Also the activation of astrocytes that form a barrier hinders neuroregenerative processes, such as neurite outgrowth, and instead, pushes neuronal cell bodies further away from the implant surface (Turner et al., 1999;Leach et al., 2010).

The large amounts of cellular contents released after an injury contribute not only directly to cell damage, but are moreover important chemoattractants for microglial cells. The activation and migration of microglial cells in response to glutamate (Liu et al., 2009) is accompanied by a fourfold increase in ATP-release of microglial cells. NO, that has been demonstrated to be a chemoattractant for microglial cells as long as ambient ATP is available, induces the immediate attraction of microglial cell processes, followed by cell migration and subsequent morphological changes to amoeboid-like cells (Dibaj et al., 2010). In severe acute as well as in chronic conditions, as it is the case for chronic cannula implantation, microglia become a source of toxic factors due to an overproduction of pro-inflammatory cytokines and free radicals that evoke a self-perpetuating cycle of neurotoxicity (Schwartz and Shechter, 2010). Activated microglia cells phagocytose the debris of dying and dead cells, but concurrently secrete pro-inflammatory cytokines, like IL-1, IL-6 and TNFα, that contribute to the progressive activation of further microglial cells as well as of astrocytes. Pro-inflammatory cytokines either stimulate the release of ROS and RNS from microglial cells or are directly toxic to neurons and oligodendrocytes (Hanisch, 2002). The activation of microglial cells has been shown to be inhibited by the semi-synthetic, second-generation tetracycline minocycline, an antibiotic with a broad range of anti-inflammatory and anti-apoptotic properties that reduces the amount of activated glial cells and thereby inhibits the release of neurotoxic and pro-inflammatory substances (Elewa et al., 2006).

3.3.2 Long-term inflammation (chronic phase)

Once the acute immune response subsides, a chronic response is initiated that is characterised by enduring inflammatory processes at the interface between the implant and the brain tissue **(Fig. 3.4B)**. In contrast to stab wounds, the chronic foreign body response is associated with persistent microglial activity around the implant that is accompanied by neuronal cell loss (Biran et al., 2005). The inability of the microglia and of the infiltrated macrophages to phagocytose the insoluble foreign body results in a state of "frustrated phagocytosis" of the microglial cells (Polikov et al., 2005). This state is characterised by the persistent release of pro-inflammatory and neurotoxic substances that causes microglia-induced secondary cell death. The loss of neurons around chronic implants does not result solely from the mechanical trauma of insertion, as no such loss is observed in stab wounds, but rather in combination with the chronic inflammation at the interface (Biran et al., 2005). Due to the persistent presence of the insoluble foreign body, the microglia cells constitutively release neurotoxic substances trying to degrade the implant, thereby evoking a self-perpetuating cycle of neurotoxicity and ongoing neuron damage (Block et al., 2007;Schwartz and Shechter, 2010). The activated microglia adhere to the implant surface and try to degrade the foreign material by secreting lytic enzymes and ROS, as well as pro-inflammatory cytokines that activate further astrocytes that form a dense, organised sheath around the implant and push surviving neurons even further away (Leach et al., 2010). For optimal device function neuronal survival within the first 50 µm surrounding electrodes is imperative to separate spike amplitudes of neurons (Buzsaki, 2004). The glial sheath formation is suggested to be complete six weeks after foreign body implantation and to remain stable thereafter, with reactive microglial cells constituting the first two layers around the implant and reactive astrocytes extending only 50-100 µm around the insertion site (Turner et al., 1999;Szarowski et al., 2003).

3.4 Neuronal substrates of skilled reaching

The impact of the inflammatory cascade and secondary cell death following the chronic implantation of a foreign body into the motor cortex may also be measurable on the behavioural level. In this regard, cannula implantation into the motor cortex may cause motor deficits that can be measured by a task that is sensitive enough.

Since the skilled reaching task has been shown to be very sensitive to disturbances of the motor cortex, it has evolved into a model system to analyse the functionality of the motor cortex by means of an elaborated movement scoring system (Alaverdashvili et al., 2008). The hand shaping movements during skilled reaching for food have been shown to be similar in rats and humans, and probably share a common origin in early tetrapods. Skilled forelimb movements seem to derive from food-handling behaviour and are described as homologous as they occur at the same spatial and temporal sequence (Iwaniuk and Whishaw, 2000;Sacrey et al., 2009). Different brain regions, such as the corticospinal tract, the sensorimotor cortex and the caudate-putamen, as well as nigrostriatal dopamine have been demonstrated to be involved in skilled forelimb movement. Lesions in these brain regions produce pronounced impairments in the use of the contralateral limb in skilled motor performance, such as reaching for a food pellet, while relatively sparing unskilled behaviours, such as walking, grooming, swimming and even holding a food pellet. This has been suggested to result from a common underlying circuitry that is involved in the control of independent limb use. This circuitry includes cortical motor areas and their projections to the striatum, which in turn projects back to the motor cortex via the globus pallidus and the thalamus. This pathway is considered to be the major route via which the basal ganglia influence movements. The dopaminergic nigrostriatal projection from the substantia nigra pars compacta to the dorsal striatum has also been shown to be particularly involved in the production of movement as a further part of the basal ganglia motor loop. The substantia nigra pars reticulata, which is also an important output nucleus of the basal ganglia to the thalamus, moreover has modulatory efferents to the extrapyramidal system that also contributes to the control of complex movements (Whishaw et al., 1986;Whishaw et al., 1993). Cortical and subcortical lesions have not only been demonstrated to impair skilled reaching for a food pellet, but also to impair skilled walking on a rung ladder (Metz and Whishaw, 2002;Metz and Whishaw, 2009). The forelimb region of the motor cortex has evolved into an important study target, since it has proven appropriate for the investigation of neural plasticity and compensation strategies after stroke (Alaverdashvili and Whishaw, 2010), as well as for the investigation of cortical reorganisation of movement representation and synaptogenesis during motor learning (Kleim et al., 2004). Moreover, it has proven as interesting target to study strain-related differences in topographical mapping and

behavioural, physiological and anatomical organisation of the motor system (VandenBerg et al., 2002;Whishaw et al., 2003).

3.4.1 The motor cortex

The motor cortex, which is considered the main target for BCIs, is part of the frontal lobe and is involved in planning, control and execution of voluntary movements. In primates and humans, it can be subdivided into M1, which is the main contributor in the execution of voluntary movements, the premotor cortex, which is mainly involved in the preparation for movements and in the spatial and sensory guidance, and the supplementary motor area, which is involved in the initiation, selection and planning of movements and the coordination of both body sides. M1, also referred to as Brodmann area 4 in humans, is located in the dorsal portion of the frontal lobe and works in association with the other cortical areas to plan and execute movements. Inter- and intrahemispheric connections between these motor areas ensure their coordination and interaction in the execution of movements (Roland et al., 1980;Sadato et al., 1997).

The motor cortex in rats can be historically subdivided into a medial agranular zone (Agm) and a lateral agranular zone (Agl) (Colechio and Alloway, 2009). Moreover, topographical investigation of the motor cortex by means of intracortical stimulation studies in rats demonstrated the existence of two separate forelimb areas: a rostral (RFA) and a caudal forelimb area (CFA) (Neafsey and Sievert, 1982). The RFA is much smaller that the CFA and is located in the Agm near the frontal pole. It is considered due to its location, cellular organisation and projections to correspond to the premotor cortex in primates with some overlap in function with the supplementary motor area. The CFA is larger and begins at bregma. It is located in the Agl and largely corresponds to M1 of primates with a broader layer V compared to the Agm and larger and denser distributed cells (Colechio and Alloway, 2009;Deffeyes et al., 2015). Both areas, however, are known to have direct corticospinal projections, and have recently been demonstrated to exhibit a specialisation and segregation of complex movement representation. In a detailed topographical investigation of the forelimb movement representation, the RFA has been shown to primarily elicit grasping movements, including digit flexion, while the CFA has been found to primarily elicit reaching movements, including forelimb elevation, advance and retraction **(Fig. 3.7)**. This

functional and topographical dissociation suggests a conserved homology of independent grasp and reach circuitries that are also found in primates (Brown and Teskey, 2014).

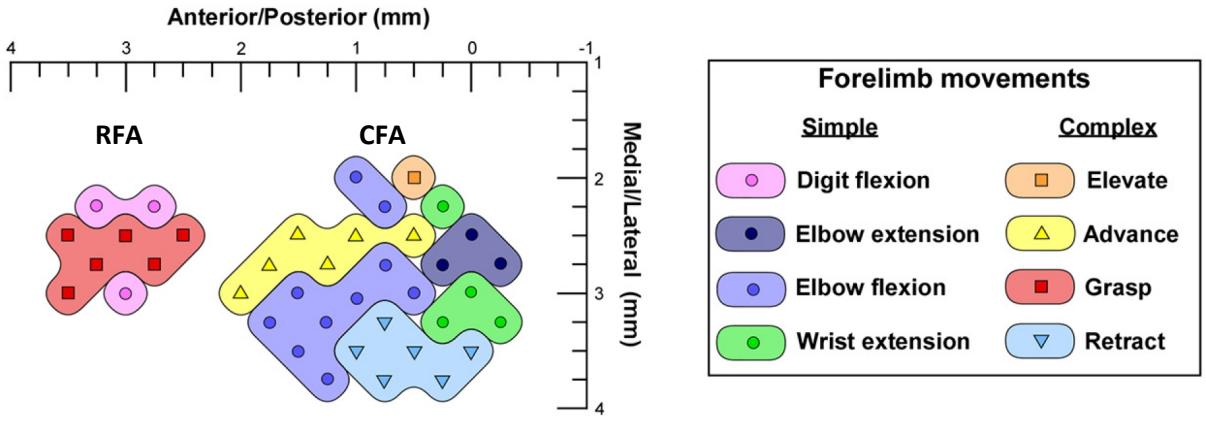

Fig. 3.7. The rostral (RFA) and the caudal forelimb area (CFA) of the primary motor cortex in rats. Detailed topography of forelimb movement representation in reach-trained rats was recently derived from a cortical deactivation study by a reversible cooling technique. Accordingly, grasping representation, including digit flexion, is primarily localised in the RFA, while reaching representation, including elevation, advance and retraction is primarily found in the CFA (Brown and Teskey, 2014).

It has been shown that the size of the cortical representation of the different forelimb areas can vary between rat strains as well as between different levels of experience. Quantitative and qualitative differences have been described in reach movements especially between pigmented and unpigmented strains, with pigmented strains being most widely used for studies of the neuronal substrates of movements, while unpigmented rats are most widely used for the study of movement impairments in neurological diseases. The quality of movements of unpigmented rat strains has been described to resemble the movement of pigmented rats after motor system injury (VandenBerg et al., 2002;Whishaw et al., 2003).

3.4.2 Connectivities of the CFA

The CFA of M1 receives most of its cortical input from the ipsilateral primary somatosensory area (S1), which is important for motor behavioural functions of the forelimbs that strongly depend on somatosensory feedback. The feedback includes cutaneous input from the skin as well as kinaesthetic inputs from joints and muscles. The second most cortical input, the CFA

receives via callosal connections from homotopic regions in the contralateral M1 that are important for bilaterally coordinated forelimb movements (Colechio and Alloway, 2009). Moreover, it has numerous reciprocal connections with the RFA and both regions project to several common targets which allows them to interact at multiple levels, with a modulatory influence of the RFA on CFA control of forelimb movements (Rouiller et al., 1993). Furthermore, the CFA receives projections from the ipsilateral thalamus (Colechio and Alloway, 2009), carrying cerebellar and basal ganglionic information (Weiler et al., 2008). The posterior parietal cortex and the claustrum also send a few projections to the CFA (Colechio and Alloway, 2009).

Major outputs from the CFA include the reciprocal corticocortical connections with homotopic regions in the contralateral M1 as well as with the RFA, as described above. Reciprocal connections also exist with the thalamus, with the CFA being mainly interconnected with the ventromedial thalamic nucleus. Moreover, the CFA sends efferent projections to the basal ganglia, with a very dense projection to the lateral portion of the ipsilateral caudate putamen, but also to the substantia nigra and to the subthalamic nucleus. The red nucleus, tectum, pontine nuclei, inferior olive, brain stem and spinal cord are also innervated by CFA projections (Rouiller et al., 1993;Weiler et al., 2008). The projections to the spinal cord are referred to as the corticospinal tract. This tract is the principle motor system for controlling movements that require skill and flexibility (Martin, 2005).

3.4.3 Cellular organisation of M1

The mature rat motor cortex can be subdivided into the conventional six layers with approximate thicknesses as estimated for lamina (L) 1 through 6: 210, 230, 180, 190, 520 and 550 µm (Skoglund et al., 1997). Most cortical neurons are excitatory glutamatergic pyramidal cells (70-80%) which are the projection neurons of the cortex. The remaining 20-30% of cortical neurons are interneurons, that are mostly GABAergic and inhibitory in nature (Markram et al., 2004). Excitatory glutamatergic pyramidal cells are located in all layers except in L1. There is an upper-layer circuit from L2/3 to L5A/B that supplies feed-forward excitation to lower-layer circuits that include corticospinal, corticothalamic, corticostriatal and other subcortical projections. L5A also projects back to L2/3 representing local circuits in rodent cortices that also exist within all laminae as intralaminar horizontal connections (Weiler et al., 2008). Corticospinal neurons, also known as Betz cells in humans,

are the largest pyramidal cells and are located exclusively in L5B in the motor cortex. They have a large pyramidal cell body with a single apical dendrite extending toward L1 and majorly branching within L2/3 with numerous basal dendrites and a very long axon that constitutes a direct monosynaptic pathway from the cortex to the motor neurons of the spinal cord (Terashima, 1995;Jara et al., 2014). However, only a fraction of the corticospinal tract arises from M1 with further input arising from the premotor cortex and the somatosensory cortex. As the tract courses from the cortex to the spinal cord, most axons decussate to the contralateral side in the lower brain stem (medullary pyramid) and descend in the contralateral white matter as the lateral corticospinal tract (Martin 2005). Less than 5% of the axons do not decussate in the medullary pyramid and descend in the ipsilateral white matter as the ventral corticospinal tract, which is why muscles are largely innervated by the contralateral side of the cortex (Carmel and Martin, 2014). Therefore, to measure behavioural deficits that are caused by the chronic implantation of a foreign body into the motor cortex, the motor performance of the contralateral body side has to be evaluated.

3.5 Aim of the thesis

The aim of this thesis was to further understand and control the foreign body response of the brain to chronically indwelling devices such as electrodes, which is crucial for the widespread clinical application of BCIs. For this purpose, the excitotoxic and inflammatory cascades after cannula implantation in the motor cortex of Lister Hooded rats was further investigated and intended to be suppressed at a very early stage to promote the survival of neurons in the vicinity of the implant. The experiments in this work served as a proof-of-principle investigation to mimic the implantation of a device, such as an electrode array, into the cortex with all substances being applied during the implantation of the cannula to mimic the local drug delivery from coated electrodes. Due to the high sensitivity of the skilled reaching task to motor cortical disturbances, the impact of glial scar formation and neuronal cell death following the chronic implantation of a foreign body into the CFA was suggested to be also measurable on the behavioural level in this task. In this regard, a reversible inactivation study by means of the $GABA_A$ agonist muscimol was initially conducted in order to examine the acute deficits in the skilled reaching task and the precise function of the CFA in Lister Hooded rats. Subsequently, cannula implantation was accompanied by local substance administration, in order to antagonise the foreign body response. Regular

behavioural investigations in the skilled reaching task, in a skilled walking task and in the open field before and once weekly after cannula implantation, as well as immunohistological tissue examination in the acute and chronic phase, served to examine the efficacy of the substances.

4 Suppression of excitotoxicity and foreign body response by memantine in chronic cannula implantation into the rat brain

Linda Hayn and Michael Koch

4.1 Abstract

Chronic brain implants are accompanied by a tissue response that causes the loss of neurons in the vicinity of the implant and the formation of a glial scar that is also referred to as foreign body response. Despite immense progress in the field of brain-computer interface (BCI) research the biocompatibility of chronic brain implants remains a primary concern in device design. Excitotoxic overstimulation of NMDA-receptors by extrasynaptic glutamate plays a pivotal role in cell death in the acute phase of the tissue response. In this study, we examined the effect of the uncompetitive NMDA-receptor antagonist memantine locally applied during cannula implantation in the caudal forelimb area (CFA) of the motor cortex (M1) in Lister Hooded rats on their behavioural performance in a skilled reaching and a rung-ladder task as well as in the open field. Moreover, the distribution of neurons and glial cells in the vicinity of the implant were assessed. Memantine improved the performance in the behavioural paradigms compared to controls and increased the number of surviving neurons in the vicinity of the implant even above basal levels accompanied by a reduction in astrocytic scar formation directly around the implant with no effect on the microglia/macrophage activation two and six weeks after cannula implantation. These findings suggest that memantine is a potential therapeutic agent in the acute phase of chronic foreign body implantation in the motor cortex in terms of increasing the viability of neurons adjacent to the implant and of improving the behavioural outcome after surgery.

4.2 Introduction

In the last decades, immense progress has been made in the field of BCI research. Neuroprosthetic devices that restore mobility in patients suffering from paralysis or amputations have been developed, and moreover, have demonstrated functionality even years after an injury to the central nervous system (CNS) (Hochberg et al., 2012;Jackson, 2012). Despite this technological progress, the biocompatibility of these chronic brain implants still remains a major problem and a demanding field of research. Different

electrode designs as well as implantation techniques have been investigated (Edell et al., 1992;Turner et al., 1999;Szarowski et al., 2003;Nicolelis et al., 2003;Kim et al., 2004;Biran et al., 2005), complemented by different surface coatings with biocompatible (Ignatius et al., 1998;Kam et al., 2002;He et al., 2006) or immunosuppressant molecules (Maynard et al., 2000;Shain et al., 2003;Kim and Martin, 2006;He et al., 2007). However, a satisfactory control of the foreign body response that may impair the functioning of the implants is still not available (Polikov et al., 2005;Griffith and Humphrey, 2006).

The implantation into the brain of a chronically indwelling device, such as an electrode array, is accompanied by two different phases of tissue response: an acute and a chronic response (Turner et al., 1999;Szarowski et al., 2003). The acute response is caused by the rupture of blood vessels in the implantation tract and the damage of neurons and glial cells (Szarowski et al., 2003;Potter et al., 2012). Similar to stroke, the disruption of blood vessels in the implantation tract impairs the oxygen and energy supply of neurons which causes an ionic imbalance that is followed by sustained release of glutamate due to uncontrolled membrane depolarisation (Iadecola and Anrather, 2011;Bretón and Rodríguez, 2012). Glutamate is suggested to be either Ca^{2+}-dependently released from neuronal vesicles, K^{+}-dependently through swelling-activated anion channels from astrocytes or Na^{+}-dependently by a reversed operation of glutamate transporters (Rossi et al., 2000). The accumulation of glutamate in the extracellular space overstimulates glutamate receptors with N-methyl-D-aspartate (NMDA) receptors playing a pivotal role in excitotoxic cell death (Lipton and Rosenberg, 1994;Lynch and Guttmann, 2002). The two major subtypes of NMDA receptors in the adult forebrain are the NR2A subunit containing receptor that is primarily located at the synapse activating intracellular processes resulting in neuronal survival, and the NR2B subunit containing receptor that is primarily located at extrasynaptic sites activating downstream cascades resulting in neuronal death (Hardingham et al., 2002;Lai et al., 2011;Vizi et al., 2013). Excessive Ca^{2+}-influx into the cells via extracellular NR2BRs induces an overproduction of highly reactive free radicals, mitochondrial dysfunction, cell membrane rupture and DNA fragmentation, which results in excitotoxic cell death of apoptotic or necrotic nature depending on the severity of the insult (Bretón and Rodríguez, 2012). Moreover, the injury of neurons causes further leakage of excitotoxic amounts of the amino acid glutamate, enhancing the cascades of apoptotic and necrotic processes by NMDA receptor overstimulation. The large amounts of glutamate spill over to nearby cells that had

survived the original trauma and cause them to depolarise, swell, lyse and to release their cellular contents into the parenchyma. This autodestructive cascade continues for hours or even days (Bonfoco et al., 1995;Lipton, 2006). The necrotic brain tissue and the accumulation of fluid in the acute phase accompanied by the release of early neuronal "danger signals" like the nucleotide ATP by the injured cells activates microglia cells that migrate to the site of injury in order to clear the necrotic tissue and to degrade the foreign body by releasing pro-inflammatory molecules (Davalos et al., 2005;Iadecola and Anrather, 2011). This in turn activates astrocytes that extend their processes towards the implantation site to separate the healthy tissue from the injured. These early reactive responses of the glial cells are supposed to be complete about two weeks after the implantation (Turner et al., 1999;Szarowski et al., 2003). In contrast to stab wounds though, these acute responses are followed by long-term inflammatory processes around the implant in chronic settings with microglia cells trying to degrade the foreign body by means of enduring release of inflammatory mediators (Biran et al., 2005;Potter et al., 2012). About six weeks after the implantation, the glial scar is highly compact and remains constant in size after this time point to isolate the healthy brain tissue from the enduring inflammatory processes at the interface (Turner et al., 1999;Szarowski et al., 2003). For optimal device function of brain electrodes the survival of neurons within the first 50 µm around the implant is of special importance (Buzsaki, 2004). However, device implantation followed by the neurotoxic cascade and the enduring inflammation processes, results in a neuronal "kill zone" around the implantation site (Edell et al., 1992;Biran et al., 2005), followed by the formation of a glial scar that pushes the surviving neurons even further away. Moreover, the glial scar prevents the regrowth of neuronal processes into the implantation site, since this process takes longer than sheath formation itself (Turner et al., 1999).

The current study serves as a proof-of-principle investigation mimicking the implantation of a device such as an electrode array into the motor cortex by means of a steel cannula. We aimed to block the initial steps of the foreign body response and to counteract the extent of neurotoxicity at the implantation site by a single local application of the uncompetitive NMDA receptor antagonist memantine. The relatively low-affinity, open-channel blocker memantine, is the first clinically successful NMDA receptor antagonist that is used for the treatment of Alzheimer's disease (Scarpini et al., 2003;Lipton, 2006;Wenk et al., 2006) and also shows some potential therapeutic benefit in patients with Huntington's

disease (Fan and Raymond, 2007) with a more favourable side-effect profile than high affinity uncompetitive NMDA receptor antagonists (Parsons et al., 1999). The progressive cell death due to NMDA receptor overactivation gets inhibited by memantine without affecting the physiological functions at the synapse due to its fast off-rate kinetics (Parsons et al., 1999;Lipton, 2004) and its preference for extrasynaptically located NR2BRs over synaptically located NR2ARs (Xia et al., 2010). In the context of this study, memantine administration during cannula implantation may mimic the local drug delivery from coated electrodes and is expected to facilitate the survival of neurons in the vicinity of the implant and to suppress the density of the glial scar. We investigated the skilled reaching performance of rats based on the behavioural paradigm of Whishaw and colleagues (Whishaw et al., 1986;Whishaw and Pellis, 1990), the skilled walking performance on a rung ladder in different conditions (Metz and Whishaw, 2002;Antonow-Schlorke et al., 2013) and the locomotor behaviour of rats in an open field box before and after the implantation of a cannula in the caudal forelimb area (CFA) of the motor cortex (M1). Moreover, the spatial distribution of neurons, and glial cells was immunohistologically analysed at the implantation site two weeks after cannula implantation when the glial sheath is supposed to be less organised and extends furthest around the implantation site (acute phase), and six weeks after implantation when the glial sheath is most densely organised and remains constant for the duration of the implantation (chronic phase) (Polikov et al., 2005).

4.3 Materials and methods

4.3.1 Animals

A total of 60 naive adult male Lister Hooded rats (Charles River Laboratories, Germany) weighing 200-220 g were used in this study. Rats were group-housed under standard conditions in Makrolon cages (type IV) on a 12 h light/dark cycle (lights on at 7:00 a.m.) with controlled temperature and humidity. All rats received tap water *ad libitum* and were restricted to 12 g standard diet rodent chow (Altromin, Germany) per rat per day as soon as the training started. The experiments were conducted in compliance with the ethical guidelines of the National Institute of Health for the care and use of laboratory animals for experiments and were approved by the local animal care committee (Senatorische Behörde, Bremen, Germany).

4.3.2 Timeline

The study was designed to assess the effects of acute memantine treatment locally administered during the implantation of a foreign body in the CFA of M1. Therefore, the rats were habituated and individually trained in the single-pellet boxes (Whishaw et al., 1986;Whishaw and Pellis, 1990) at least four weeks before the experiments started. After reaching a stable baseline of at least 75 % the rats were pseudo-randomly assigned to six groups, receiving either artificial cerebrospinal fluid (aCSF) which served as the control or memantine in a low dose (20 µg/µl) or in a high dose (50 µg/µl). Brains were removed for histological analysis either two or six weeks after cannula implantation. All animals were tested in the single-pellet reaching box and in the open field the day before cannula implantation and once a week after the implantation. Moreover, the 2-week group was tested on a ladder rung walking task for further analysis of the rats' skilled walking ability and received one week of previous training.

4.3.3 Single-pellet reaching task

The single-pellet reaching task was chosen to define the preferred forepaw of each rat and to analyse the functionality of the motor cortex contralateral to this paw before and after cannula implantation.

4.3.3.1 Single-pellet reaching boxes

The single-pellet boxes **(Fig. 4.1A)** were made of clear polycarbonate (40.0 cm long x 14.0 cm wide x 31.0 cm high) with a vertical slot at the centre of the front wall, 1 cm wide extending from 2 cm above the floor to a height of 15 cm. On a shelf in the front of the slot, 2.5 cm above the floor, casein pellets (45 mg Dustless Precision Pellets, Bio-Serv®, UK) were placed in one of two indentations. These indentations were located 2 cm from the inside of the wall aligned with the edges of the slit in order to prevent the rats using the tongue to lap the pellet and to ensure that they only reach the pellet in the indentation contralateral to the preferred paw. After the habituation phase, two additional polycarbonate side walls were inserted in the box with a distance of 6 cm to each other to ensure that the rats directly approach the slot with their body postures always in a similar orientation **(Fig. 4.1B)**.

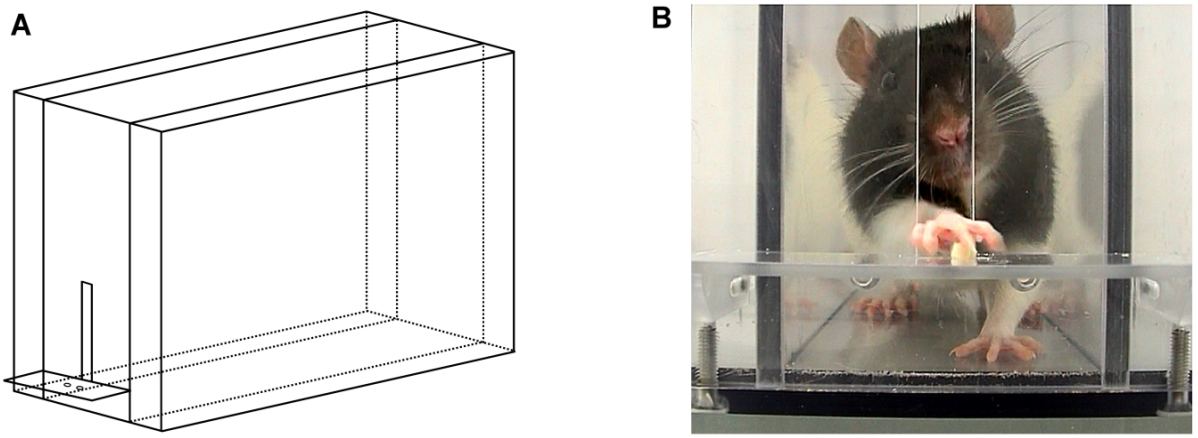

Fig. 4.1. Single-pellet box. Schematic representation of the skilled reaching box with additionally inserted side walls **(A)**. Photograph of a rat reaching for a pellet (Subelement: *Pronate*/*Grasp*) **(B)**.

4.3.3.2 Training and testing

The first week of training in the skilled reaching box consisted of daily 10 min training sessions per rat. After box habituation pellets were placed on the shelf to introduce their retrieval. As soon as the rats successfully retrieved pellets from the shelf, these were moved to the indentations to force the rats to use the paws for their retrieval. The paw that was most often and most precisely used usually emerged to be the preferred paw of the rat and was then trained by placing individual pellets into the indentation contralateral to that paw. When demonstrating a paw preference, inter-trial intervals were introduced during which the rats had to turn around and walk to the rear wall of the box to receive a further pellet as a reward for every pellet they gained from the indentation in the front and to initiate a new trial. After this habituation phase to the procedure two additional polycarbonate side walls were inserted in the box to ensure that the rats directly approach the slot and avoid major variations in their body posture when reaching for the pellets. The rats were trained to walk to the rear wall of the box after every trial to initiate the next one, though, only the trials in which they successfully reached a pellet in the first attempt were rewarded by the additional pellet in the back. On semi-random trials pellets on the shelf were withheld to ensure that the rats sniff for and orient to the pellet. Training sessions in the following weeks consisted of daily 5-10 min sessions per rat for about 4-5 weeks until they reached a stable baseline of at least 75% correct responses.

The 2-week group with the cannula explantation two weeks post-surgery was tested in the reaching box the day before the surgery and once weekly for two weeks post-surgery. The 6-week group with cannula explantation six weeks post-surgery was also tested the day before the surgery and then once weekly for six weeks post-surgery to investigate short- and long-term effects of cannula implantation in the CFA of M1 on the behavioural performance.

4.3.3.3 Behavioural analysis

The reaching performance in the single-pellet boxes was recorded for 5 min on each test day using a Panasonic NV-DS60 digital video camera (shutter speed 1/50 s) and a cold-light source for improved subsequent frame-by-frame analysis (25 frames/s). All experiments were performed with the experimenter being blind to the treatment protocol.

Quantitative analysis:

Hit-reach-ratio. The success rate of each rat was calculated from the total number of hits compared to the total number of reaches. Reaching attempts were scored as long as the pellet was in the respective indentation. A successful reach was scored as a *hit* ("1 hit") when the pellet was grasped and consumed in the first attempt. If the pellet was grasped, but dropped in the box an *incomplete hit* ("0.5 hits") was scored. An *incomplete hit* was also scored when the rat had missed the pellet, which was scored as a *miss* ("1 miss"), but then grasped the pellet from the indentation without priorly withdrawing the paw through the slot. Repeated, unsuccessful attempts without paw withdrawal from the shelf were scored as *repeated misses* ("0.5 misses") with the first miss being scored as complete *miss*. Moreover, attempts in which the rat approached the slot, but dropped the paw on the inner edge of the slot, were scored as *incomplete attempts* ("0.5 misses").

The hit-reach-ratio was calculated by the sum of *hits* and *incomplete hits* divided by the total number of attempts. Each *hit* as well as each *incomplete hit* was counted as one attempt as well as the complete *misses* which was hence scored as "1 reach". Only *repeated misses* and *incomplete attempts* were counted as half attempts and were hence scored as "0.5 reaches".

$$\text{Hit - reach - ratio} = \frac{\text{Total number of hits}}{\text{Total number of reaches}}$$

Qualitative analysis:

Movement pattern analysis. Each forelimb movement during a successful hit in the single-pellet box consists of 12 movement subelements (Alaverdashvili et al., 2008;Alaverdashvili and Whishaw, 2010). When initiating a trial the rat moves from the back of the box to the front where it sniffs for the pellet in the indentation contralateral to the preferred paw. This element is referred to as *orientation to locate the food pellet* (1) with the head and the snout targeting the pellet, accompanied by further postural adjustments and a raise of the head when initiating the movement. As the rat begins to reach for the pellet by *lifting the limb* (2) the tips of the digits are aligned with the midline of the body. The palm is supinated with the *digits semiflexed or closed* (3). *Aiming* (4) at the food pellet involves the adduction of the elbow to the midline of the body with the digits remaining positioned on the body midline. As the paw *advances* (5) through the slot the *digits extend and open* (6) in the end of the movement when the paw is over the pellet. In a *pronation* (7) movement over the pellet the digits fully extend and open with the outer digit through the inner digit sequentially contacting the shelf by an abduction of the elbow and a rotation of the wrist. *Grasping* (8) consists of the flexion and closure of the digits around the pellet followed by an extension at the wrist and the raise of the pellet. The supination movement of the paw consists of two phases: *Supination I* (9) involves the rotation of the paw by 90 ° around the wrist as it is withdrawn through the slot, followed by *supination II* (10), the rotation of the paw so the palm with the pellet faces the mouth. By opening the digits the pellet is finally *released* (11) into the mouth and the paw is *replaced* (12) on the floor or on the wall when rearing or turning around to initiate the next trial.

The first five attempts on each test day before and after the surgery were analysed for these 12 subelements and rated using a three-point scale. A successful normal subelement was rated “0”, when the subelement was present but abnormal it was rated “0.5”, and when it was absent or incomplete and resulted in a miss or of loss of the pellet it was rated “1”. Scoring was achieved by means of frame-by-frame analysis.

4.3.4 Open field

The locomotor activity of the rats was analysed in infrared-controlled activity chambers (44.7 cm x 44.7 cm x 44.0 cm; ActiMot-system, TSE, Bad Homburg, Germany) by the total

distance travelled [m] that was measured from the rats' horizontal activity for 30 min the day before surgery and once weekly after surgery.

4.3.5 Ladder rung walking task

For further analysis of the rats' preferred forelimb the skilled walking ability of the 2-week group was tested on a ladder rung walking task in horizontal, upward and downward conditions according to a modified version of Antonow-Schlorke et al. (2013) analysing the rats' preferred forelimb contralateral to the cannula implantation side.

4.3.5.1 Ladder rung walking test apparatus

The test apparatus was manufactured according to Metz and Whishaw (2002) by in-house mechanics of the University of Bremen. The rung ladder was 1 m in length with metal rungs 3 mm in diameter linking the side walls that were made of clear polycarbonate with a height of 25 cm and a distance of about 8 cm to each other. During the training phase the rungs were placed at a regular arrangement with a distance of 2 cm between the rungs to habituate the rats to the setting. In the horizontal condition the ladder was elevated about 1 m above the floor with a platform at both ends. The angle of inclination of the rung ladder for the upward and the downward condition was about 38.32°, due to the one end of the ladder being elevated about 62 cm. Rats were supposed to walk from a neutral platform across the ladder to a platform on the other side with a small reward which were three casein pellets in the horizontal condition and four pellets in the upward and downward conditions.

4.3.5.2 Training and testing

After a short training phase of 2-3 days on the regular pattern single rungs were removed to receive an irregular pattern with rung-to-rung distances of 2-6 cm **(Fig. 4.2)**. The original regular pattern with rungs spaced at 2 cm intervals was further applied for the last 20 cm on each side of the ladder to enable the rats to enter and leave the alley, since they often stopped in these regions for orienting behaviour. Two templates of irregular patterns, pattern A and B, were applied for the middle part of 60 cm to prevent the rats from learning the pattern. After the rats enabled to cross the ladder fluently, without too many stops, they were video recorded the day before the surgery on pattern A for the horizontal and the

upward condition and pattern B for the downward condition. One week after the surgery the animals were tested on pattern B for the horizontal and the upward condition and on pattern A for the downward condition. In the second post-surgery week the same patterns from before the surgery were applied.

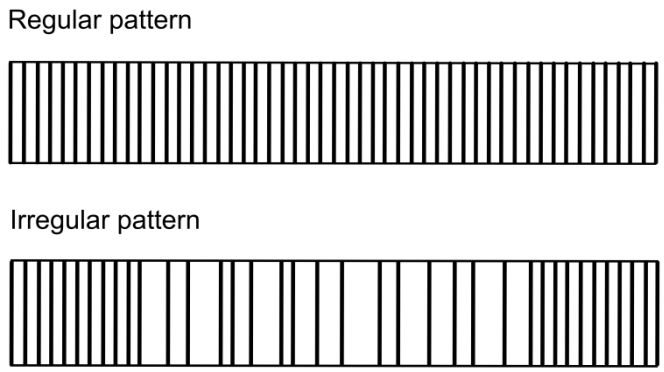

Fig. 4.2. Horizontal ladder. Arrangement of ladder rungs: regular and irregular pattern.

4.3.5.3 Foot fault scoring

The skilled walking performance was evaluated qualitatively by means of frame-by-frame analysis using a seven-category scale according to previous studies (Metz and Whishaw, 2002;Antonow-Schlorke et al., 2013): a *correct placement* of the paw on the rung with full weight support on its midportion was rated “6 points”; a *partial placement* of the paw on the rung with the wrist or digits was rated “5 points”; a *correction* of the limb that aimed for a rung, but was then quickly repositioned without touching the first rung was rated “4 points”; the replacement of the paw, touching a rung without weight bearing, being quickly lifted and placed on another rung was rated “3 points”; a *slight slip* off a rung with the animal maintaining its balance and a continued coordinated walk was rated “2 points”; a *deep slip* off a rung due to weight bearing on the slipping paw was rated “1 point”; a *total miss* of a rung that resulted in a fall was rated “0 points”. Only the forelimb that was preferred in the reaching box and that was contralateral to the cannula implantation site was rated. When different errors occurred at the same time, the lowest of the scores was given. In case of a fall, the preferred forelimb was only rated when it initiated the fall otherwise no score was given until the rat repositioned all limbs. The scores for the preferred forelimb of each rat and of each treatment group were averaged for the horizontal, for the upward and the downward condition respectively and compared within and in between the treatment groups before and after the surgery.

4.3.6 Cannula implantation and drug administration

Substances administered during the implantation of the cannula were either aCSF (in mM: 133.3 NaCl, 3.4 KCl, 1.3 $CaCl_2$, 1.2 $MgCl_2$, 0.6 NaH_2PO_4, 32.0 $NaHCO_3$ and 3.4 glucose; with pH adjusted to 7.4) serving as vehicle or memantine in a low (20 µg/µl) or in a high dose (50 µg/µl) dissolved in aCSF (with pH adjusted to 7.4). ACSF was aliquoted and stored in the freezer. Memantine solutions were freshly prepared before cannula implantation. Substance administration occurred in a pseudorandom order by a treatment-blind experimenter.

Rats of all groups were implanted with a blunted stainless steel 27 gauge injection cannula (0.4 mm diameter, Braun, Melsungen, Germany) in the CFA of M1 contralateral to the preferred forelimb. Drugs were administered during the implantation procedure. For this purpose, animals were anesthetised by intraperitoneal (i.p.) injections of 60 mg/kg pentobarbital (Sigma Aldrich, Steinheim, Germany) and 10 mg/kg xylazine (Rompun®; Bayer, Leverkusen, Germany). To mitigate the respiratory depressive effects of pentobarbital 0.1 mg/kg atropine (Braun, Melsungen, Germany) were administered subcutaneously (s.c.). Rats were fixed in a stereotaxic apparatus (Kopf Instruments, Tujunga, CA, USA) in a flat skull position. After a midsagittal incision of the skin and removal of the periosteum, jeweler's screws were anchored in the skull to fix the cannula. A small hole was drilled above the contralateral CFA and 0.5 µl of either aCSF or memantine in its low or high dose were administered on the cortical surface from the injection cannula that was connected with a microlitre syringe (SGE Scientific Glass Engineering, Darmstadt, Germany) via polyethylene tubes. Subsequently, further 0.5 µl were administered during the implantation of the injection cannula into the CFA (0.1 µl/30 s). Coordinates for implantation (anteroposterior: +1.5 mm; mediolateral: ±2.3 mm; dorsoventral: -2.3 mm from bregma) were derived from previous mapping studies (Neafsey et al., 1986;Hyland, 1998;Colechio and Alloway, 2009) and further pretests of our workgroup using the GABA (γ-aminobutyric acid)$_A$-agonist muscimol (0.5 µg/0.3 µl and 1 µg/0.3 µl; Biozol, Eching, Germany) to temporarily inactivate this region. After implantation the cannula was left in place and was embedded in dental acrylic. The polyethylene tubes were removed as soon as the cannula was fixed to the skull and then closed by the acrylic cap. After surgery the rats were kept on a warming plate until recovered from anaesthesia.

4.3.7 Perfusion and tissue collection

Upon completion of the last test, the rats were euthanised with a lethal dose of pentobarbital (200 mg/kg; i.p.) and transcardially perfused with 250 ml PBS (phosphate buffered saline; pH 7.4) followed by 250 ml 4% paraformaldehyde (PFA; Serva Electrophoresis, Heidelberg, Germany) in 0.1 M phosphate buffer (pH 7.4). The brains were removed from the skull and post-fixed for 24 h in PFA followed by cryoprotection in 30% sucrose solution for 48 h. Subsequently, six series of horizontal 40 µm sections of the rats' cortex including the implantation site in the CFA were cut on a cryostat (Jung CM 3000, Leica Instruments GmbH, Nussloch, Germany).

4.3.8 Histology

Brain slices of the first series were used to visualise the injection site. They were mounted onto gelatinised glass slides and Nissl-stained with thionin and coverslipped for subsequent analysis of the implantation site using a light microscope (Zeiss; Göttingen, Germany) and a rat brain stereotaxic atlas (Paxinos and Watson, 1998). The extent of inflammation and the number of the neurons around the implantation site were analysed by immunohistological staining of free-floating sections. The second series of sections was stained for neurons (neuronal nuclei; NeuN), the third series for astrocytes (glial fibrillary acid protein; GFAP) and the fourth series for microglia/macrophages (ionised calcium binding adaptor molecule 1; IBA-1). Free-floating sections were rinsed three times (for 10 min each) at room temperature in PBS, followed by 1 h tissue blocking at room temperature in 10% normal goat serum (NGS; Linaris, Dossenheim, Germany) blocking buffer containing 0.05% Triton-X 100 (Sigma, Steinheim, Germany) to rehydrate the tissue and to increase the permeability of the cell membranes for the antibodies. Following blocking, the tissue sections were incubated in the respective primary antibody dilutions for 72 h at 4 °C which were either mouse anti-NeuN (1:1000; Millipore, Darmstadt, Germany), rabbit anti-GFAP (1:5000; DAKO, Hamburg, Germany) or rabbit anti-IBA-1 (1:2000; WAKO, Neuss, Germany). Next, after 3 rinses in PBS (10 min per rinse), followed by 1 h blocking at room temperature in PBS containing 0.2% bovine serum albumin (PBSA; Sigma, Steinheim, Germany), sections were transferred to their secondary antibody dilutions for 48 h at 4 °C. Secondary antibodies, which were either biotinylated goat anti-rabbit IgG (1:2000; DAKO, Hamburg, Germany) for the astrocytes as well as for the microglia/macrophages or Alexa Fluor 488 goat anti-mouse IgG (1:1000;

Dianova, Hamburg, Germany) for the neurons, were diluted in PBSA blocking buffer. After immunostaining with the secondary antibodies and 3 further rinses with PBS the tissue sections stained for the neurons were mounted onto sodium azide-gelatinised glass slides and dried in the dark for 3 days. The sections stained for astrocytes and microglia/macrophages were treated again for 1 h with PBSA blocking buffer and were then incubated in PBSA containing Cy3-labeled streptavidin (1:2000; Sigma, Steinheim, Germany) for 24 h at room temperature. After 3 further rinses in PBS theses series were as well mounted on microscope slides and dried in the dark.

To eliminate background immunofluorescence and autofluorescence of lipofuscin the sections were treated for 20 min with 0.5% filtered Sudan Black (Acros, New Jersey, USA) solution prepared in 70% ethanol. After 3 rinses in 0.2 M PB (10 min each), they were coverslipped with fluorescence mounting medium (DAKO, Glostrup, Denmark) for imaging.

4.3.9 Image analysis

Fluorescent images of tissue sections from layers V of the cortex near the tip of the cannula were taken using a Zeiss Axioskop fluorescent microscope (Göttingen, Germany) with adequate band pass filter sets (excitation and emission peaks: Cy2 at 492 nm and 510 nm (green); Cy3 at 550 nm and 570 nm (red)) and a digital camera RT Slider Spot connected to the image analysis software Metamorph 4.6 (Visitron Systems GmbH, Puchheim, Germany). Z-stack images were captured with a 20 x objective around the implantation site for the neurons as well as for the microglia/macrophages to individually count the cells and with a 10 x objective for astrocytes to examine the distribution of the astrogliotic scar. Exposure times and gamma values were held constant for each cellular marker. Quantification was performed following the acquisition of 16-bit tagged image files (TIFs) using the image processing software FIJI. The implant region was manually delineated and regions of interest (ROIs) were defined in 50 µm concentric circles up to 300 µm from the interface for neurons and microglia/macrophages and up to 500 µm for astrocytes. Large blood vessels or other irregularities were excluded from the ROIs. To improve visual display images in this report have been pseudo-coloured.

To quantify the neuronal population surrounding the implantation site the neurons in each ROI around the implantation site were manually counted by means of the cell counter plug-in and the average number of neurons [n] for bins of 50 µm² was calculated for each

treatment. The same procedure was applied to the images of the microglia/macrophages. The motor cortex of the hemisphere contralateral to the implantation site of aCSF-treated animals served as the control and the average number of neurons and of microglia/macrophages in the CFA was determined from the untreated hemispheres, with the same ROI sets as used on the contralateral implantation site.

The distribution of the astrocytic scar was examined by converting the images into 8-bit images to level them (enhancement of contrast: 0.3%), followed by the application of an auto local threshold (method: median; radius: 80 pixel; correction value (c): -30) in order to obtain binary images. The average area covered with astrocytes [%] was calculated for each ROI. Again the motor cortex of the hemisphere contralateral to the implantation site of aCSF-treated animals served as the control and the average area covered with astrocytes in the CFA was determined from the untreated hemispheres with the same ROI sets as used on the contralateral implantation site.

4.3.10 Statistical analysis

Descriptive statistics are based on means and variances indicated as standard error of the mean (+S.E.M.). Statistical analyses were run using the statistical software SigmaStat (version 2.03 for Windows) using a two-way repeated measures analysis of variance (2-way RM ANOVA) for the behavioural tests with the factors treatment and test day within the 2-week group and within the 6-week group and for the immunohistological investigations with the factors treatment and distance from the implantation site for each marker within the 2-week group and within the 6-week group. Post-hoc pairwise comparisons using a Tukey's t-test were defined to be significant at $P<0.05$. Animals that did not reach a stable baseline performance of 75% correct responses in the skilled reaching task or lost the acrylic cap after cannula implantation were excluded from further analysis.

4.4 Results

4.4.1 Behavioural experiments

A total of eight animals were excluded from the experiments either due to a loss of the acrylic cap (n=5) or due to not reaching a stable baseline of at least 75% correct responses in the single-pellet reaching task (n=3). Data of all 52 participating animals (aCSF: *n*=16; Mem

low: *n*=18; Mem high: *n*=18) are included in the bar plots and statistics of the 2-week group for all behavioural experiments except for the ladder rung walking task that was exclusively applied to the 2-week group and contains the data of the 26 animals that remained for two weeks in the experiment. Bar plots and statistics of the 6-week group contain only the data of 26 animals that remained in the experiment up to the sixth week with each treatment group containing half of the animals. Start differences within the groups go back to individual differences in different behavioural patterns of the animals.

4.4.1.1 Single-pellet reaching task

Hit-reach-ratio. Before cannula implantation into the CFA contralateral to the preferred forelimb, rats of all treatment groups showed a stable baseline in the reaching boxes with a hit-reach-ratio of at least 75%. Local vehicle treatment during cannula implantation decreased the performance not only within the first two post-surgery weeks, but also at later time points as shown by the 6-week group. Both doses of memantine reversed this impairment to about baseline levels in the 6-week group. The statistical data analysis revealed for the first two weeks **(Fig. 4.3A)** a significant main effect of drug treatment ($F_{2,98}$=3.549; P=0.036) and time point of measurement ($F_{2,98}$=54.371; P<0.001), as well as a significant interaction drug x time point of measurement ($F_{4,98}$=4.973; P=0.001). Further post-hoc comparisons showed that cannula implantation into the CFA caused a decrease of the hit-reach-ratio within the first two weeks that was significant for all treatment groups when compared to pre-surgery (P<0.01). Both doses of memantine significantly improved the performance in the first post-surgery week compared to vehicle (P<0.01). In the second post-surgery week the high dose of memantine also significantly increased the performance compared to vehicle (P=0.014), although the effect of the low dose of memantine did not reach statistical significance (P=0.096). Statistical data analysis of the hit-reach-ratio for the 6-week animals **(Fig. 4.3B)** also revealed a significant main effect of drug treatment ($F_{2,138}$=8.276; P=0.002) and time point of measurement ($F_{6,138}$=12.254; P<0.001) as well as a significant interaction drug x time point of measurement ($F_{12,138}$=2.105; P=0.020). Post-hoc comparisons revealed that vehicle treatment significantly decreased the hit-reach-ratio in all post-surgery weeks compared to pre-surgery (P<0.001), in contrast to memantine treatment that resulted in a decrease only in the second post-surgery week compared to pre-surgery (P<0.05). Both doses of memantine improved the performance significantly in most post-

surgery tests compared to vehicle treatment (P<0.05) and returned to about baseline levels after the second post-surgery week, with the low dose of memantine significantly improving the performance from the second to the sixth post-surgery week (P=0.045).

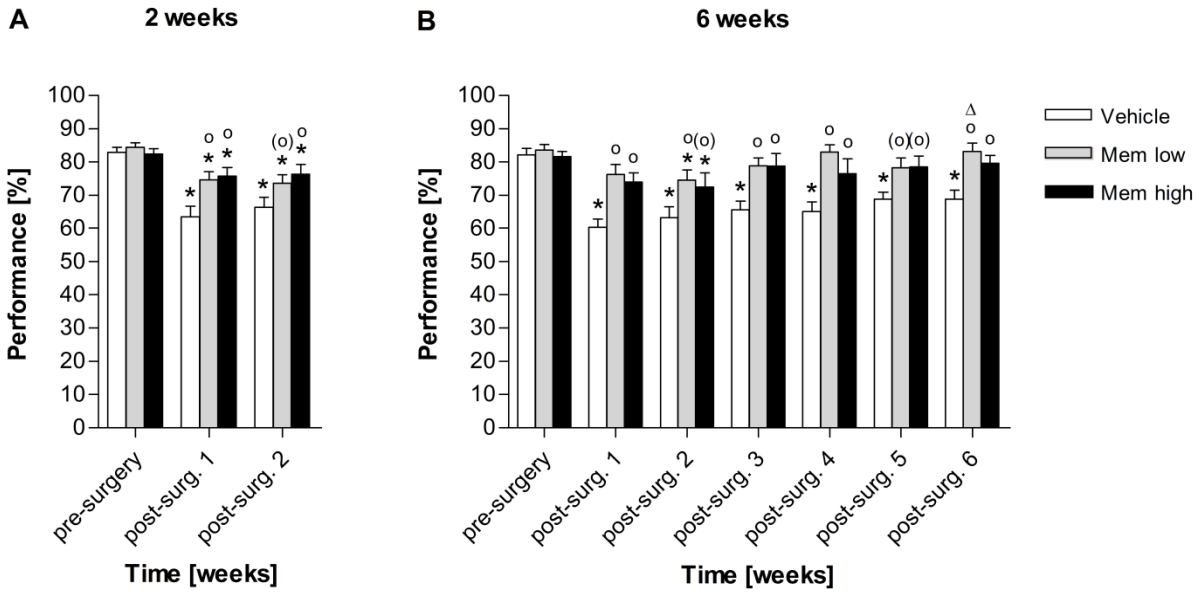

Fig. 4.3. Hit-reach-ratio. Quantitative data analysis of the rats' performance in the skilled reaching task before and once weekly after the implantation of a cannula into the CFA contralateral to the preferred forepaw accompanied by either local vehicle treatment (aCSF) or local memantine treatment in a low (20 µg/µl) or a high dose (50 µg/µl) two (n=52) **(A)** and six weeks (n=26) post-surgery **(B).** Data are means +S.E.M. *Asterisks* denote a significant difference (Tukey's t-test; P<0.05) between pre- and post-surgery tests of a certain treatment. Significant differences on a certain test day compared to vehicle are illustrated by *circles*. A significant postsurgery effect of a certain treatment is illustrated by the *triangle* (here: from post-surgery week 2 to 6). *Brackets* () indicate a trend of significance (Tukey's t-test; P<0.1).

Movement pattern analysis. In addition to the quantitative hit-reach-ratio analysis, the qualitative movement pattern analysis of the first five trials revealed that the subelements most impaired were the *advancing* of the paw through the slot, the *pronation* of the paw over the pellet, as well as the *release* of the pellet into the mouth. The other subelements were unaffected by the surgery suggesting that *advancing*, *pronation* and *release* are most vulnerable to the implantation-induced tissue damage. In compliance with the results of the hit-reach-ratio-analysis, vehicle treatment caused the strongest increase in errors with the highest error scores within the first two post-surgery weeks. Both doses of memantine reduced these error scores.

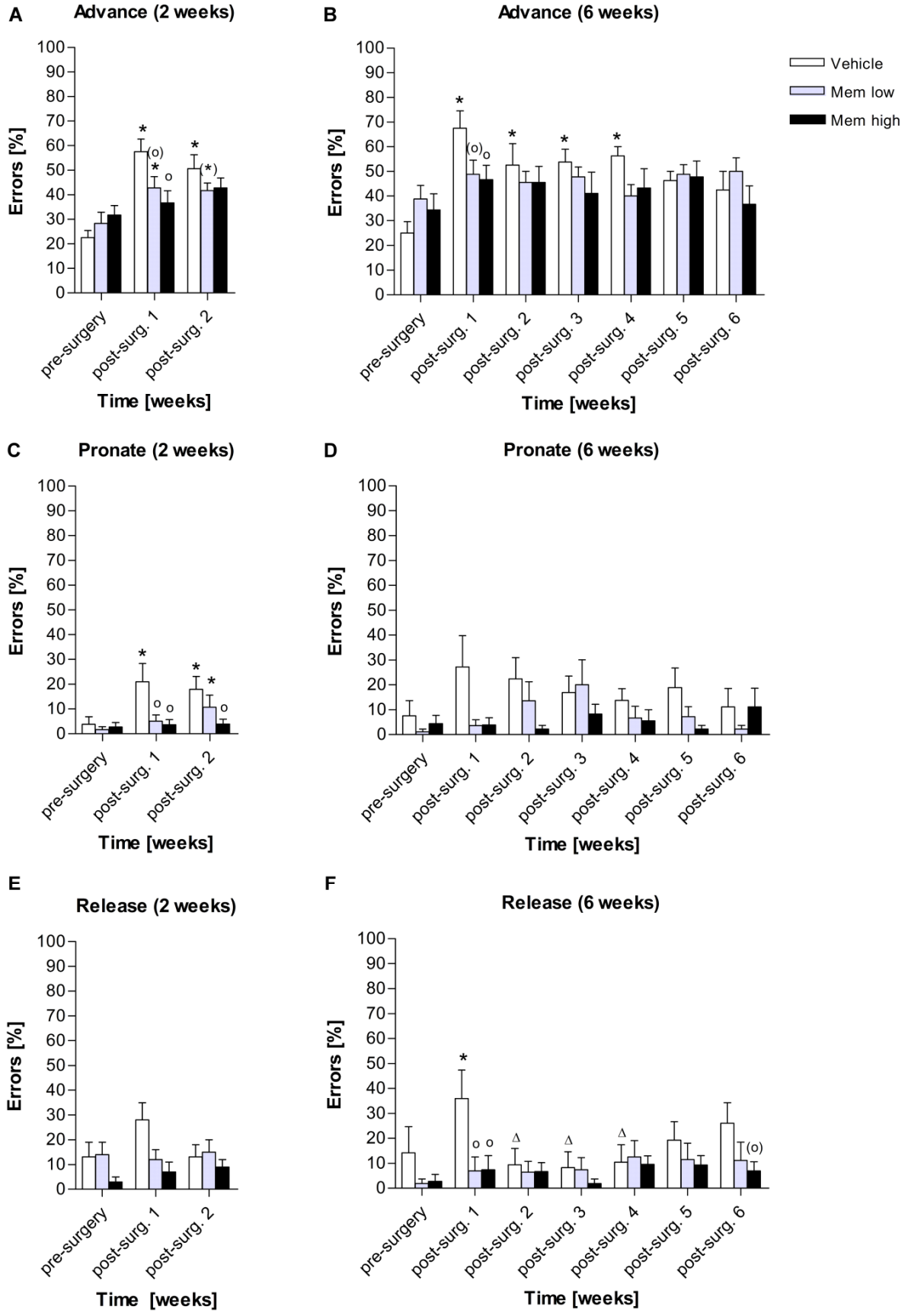
A
Advance (2 weeks)
B
Advance (6 weeks)
Vehicle
Mem low
Mem high
C
Pronate (2 weeks)
D
Pronate (6 weeks)
E
Release (2 weeks)
F
Release (6 weeks)
Errors [%]
Time [weeks]
pre-surgery
post-surg. 1
post-surg. 2
post-surg. 3
post-surg. 4
post-surg. 5
post-surg. 6

Fig. 4.4. Movement pattern analysis. Qualitative data analysis of the most impaired subelements within the first five trials in the skilled reaching task before and once weekly after cannula implantation accompanied by local vehicle or memantine treatments two (*n*=52) **(A,C,E)** and six weeks (*n*=26) post-surgery **(B,D,F).** Data are means +S.E.M. *Asterisks* denote a significant difference (Tukey's t-test; *P*<0.05) between pre- and post-surgery tests of a certain treatment. Significant differences on a certain test day compared to vehicle are shown by *circles*. A significant post-surgery effect of a certain treatment is indicated by the *triangle* (here: from post-surgery week 1 to 2, 3 and 4). *Brackets* () denote a trend of significance (Tukey's t-test; *P*<0.1).

The error rate of the subelement *advance* was increased after cannula implantation in all treatment groups with the animals often advancing the paw not far enough through the slot to reach the pellet or swept the pellet off the shelf when touching it only with the tips of the digits. Vehicle treatment showed the strongest increase in errors up to four weeks post-surgery. Memantine again amended this motor impairment. The statistical data analysis revealed for the first two weeks **(Fig. 4.4A)** a significant main effect of time point of measurement ($F_{2,98}$=18.622; *P*<0.001) and of the interaction drug x time point of measurement ($F_{4,98}$=3.432; *P*=0.011). Further post-hoc comparisons showed that the increase in the number of errors in this subelement was significant for vehicle treatment (*P*<0.001) and the low dose of memantine (*P*=0.035) in the first post-surgery week compared to pre-surgery. For vehicle treatment this increase remained significant in the second post-surgery week compared to pre-surgery (*P*<0.001), in contrast to memantine that only tended to increase the error rate in the low dose (*P*=0.057), although not in the high dose. The high dose improved the performance significantly compared to vehicle in the first post-surgery week (*P*=0.003). The decrease of errors with the low dose of memantine compared to vehicle did not reach statistical significance (*P*=0.052) in the first post-surgery week. For the 6-week animals **(Fig. 4.4B)** only a significant main effect of time point of measurement was revealed ($F_{6,138}$=4.284; *P*<0.001). Further post-hoc comparisons revealed that the increase in errors continued to be significant for vehicle treatment for the first four post-surgery weeks (*P*<0.05) with a significant decrease in the number of errors from the first to the sixth post-surgery week (*P*=0.034). Memantine slightly improved motor performance within the first four post-surgery weeks compared to vehicle, but reached statistical significance only in the first post-surgery week in the high dose (*P*=0.044), although not in the low dose (*P*=0.082).

The error rate of the subelement *pronate* was not that pronounced, but increased post-surgically with especially the vehicle-treated rats either not fully extending and opening their digits or omitting the rotation of the wrist, and hence missing the pellet or grasping the pellet with a lateral swipe of the paw. This effect was again most intense in the first two post-surgery weeks and improved by memantine. Within these first two post-surgery weeks **(Fig. 4.4C)** a significant main effect of drug treatment ($F_{2,98}$=3.3341; P=0.044) and time point of measurement ($F_{2,98}$=8.307; P<0.001) was revealed as well as a significant interaction drug x time point of measurement ($F_{4,98}$=3.185; P=0.017). Further post-hoc comparisons revealed a significant increase of errors in this subelement after vehicle treatment in both post-surgery weeks (P≤0.001) as well as after the low dose of memantine in the second post-surgery week (P=0.043) compared to pre-surgery. The high dose of memantine significantly improved the performance in the first (P=0.005) as well as in the second post-surgery week (P=0.027) compared to vehicle, similar to the low dose of memantine in the first post-surgery week (P=0.011). An increase in the number of errors was also obvious in the 6-week groups especially after vehicle treatment in the first post-surgery week **(Fig. 4.4D)**, though without reaching statistical significance.

The error rate of the subelement *release* also showed its strongest increase in the first post-surgery week after vehicle treatment, with the animals often showing difficulties to open their paw and release the pellet into the mouth. Statistical data analysis of the first two weeks **(Fig. 4.4E)** including all animals neither showed a significant main effect of drug treatment or time point of measurement nor of their interaction for this subelement. Though, for the 6-week group **(Fig. 4.4F)** data analysis revealed a significant main effect of time point of measurement ($F_{6,138}$=2.460; P=0.027). Post-hoc comparisons indicated a significant increase in the number of errors after vehicle treatment in the first post-surgery week compared to pre-surgery (P=0.033), but in post-surgery weeks 2-4 a significant decrease of errors (P<0.01) occurred compared to the first post-surgery week. A significant lower error rate was revealed after memantine treatment in both doses in the first post-surgery week compared to vehicle (P<0.01) and a trend of decrease (P=0.072) with high dose of memantine in the sixth post-surgery week.

The other subelements were not impaired within the first five trials. The subelement replace exhibited a mean error rate of 41.09% (± 5.03%) already pre-surgery and revealed no significant differences post-surgery.

4.4.1.2 Open field

The analysis of the rats' locomotor activity measured by the total distance travelled [m] in 30 min served as a control paradigm and did not reveal any treatment effects neither within the first two weeks **(Fig. 4.5A)** nor within the 6-week group **(Fig. 4.5B)**. Only a significant main effect of the time point of measurement was revealed for the 6-week group ($F_{6,138}$=2.589; P=0.021), with further post-hoc comparisons revealing a significant overall decrease in the total distance travelled in the first post-surgery week compared to pre-surgery (P=0.017) and again a significant increase from the first to the sixth post-surgery week (P=0.048) independent of the treatment. Further post-hoc comparisons revealed for the low dose of memantine a significant increase in the distance travelled from the first to the sixth post-surgery week (P=0.005), similar to the high dose that tended to increase motor behaviour (P=0.072).

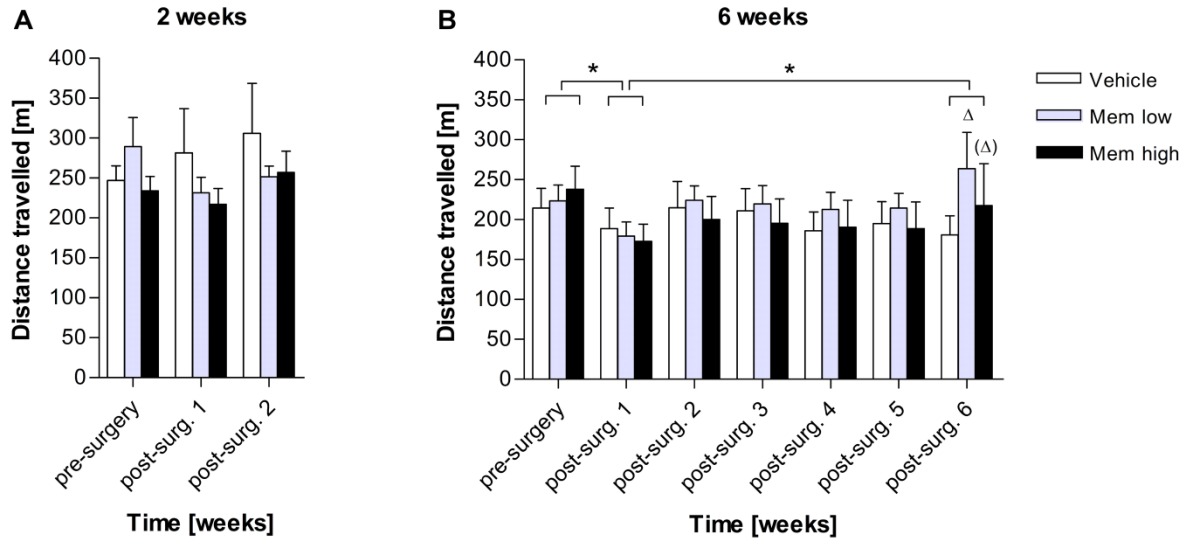

Fig. 4.5. Open field. Analysis of the rats' total distance travelled [m] within 30 min on the day before and once weekly after cannula implantation two (n=52) **(A)** and six weeks (n=26) post-surgery **(B)**. Data are means +S.E.M. *Triangles* denote significant post-surgery differences (Tukey's t-test; P<0.05) within a certain treatment (here: from post-surgery week 1 to 6). *Brackets* () indicate a trend of significance (Tukey's t-test; P<0.1).

4.4.1.3 Ladder rung walking task

The data analysis of the foot placement scores of the 2-week animals on the rung ladder revealed the ladder's diagonal conditions to be more difficult than the horizontal condition

(Fig. 4.6A). Vehicle treatment caused a slight decrease of performance in the ladder's upward **(Fig. 4.6B)** as well as in the ladder's downward condition **(Fig. 4.6C)** that was improved by memantine. Statistical analysis revealed a significant main effect of the factor treatment ($F_{2,46}$=4.909; P=0.017) only for the ladder's upward condition. Further post-hoc comparisons indicated a significantly decreased locomotor activity in the first post-surgery week after vehicle treatment compared to the low dose (P=0.002) or the high dose of memantine (P=0.010). In the second post-surgery week vehicle-treated animals improved again significantly compared to the first post-surgery week (P=0.036). No significant impairments were observed in the horizontal and downward conditions. The results of the vehicle treatment in the ladder's downward condition indicate a stronger decline in the animals' post-surgery performance compared to memantine treatment, but this effect failed to reach statistical significance.

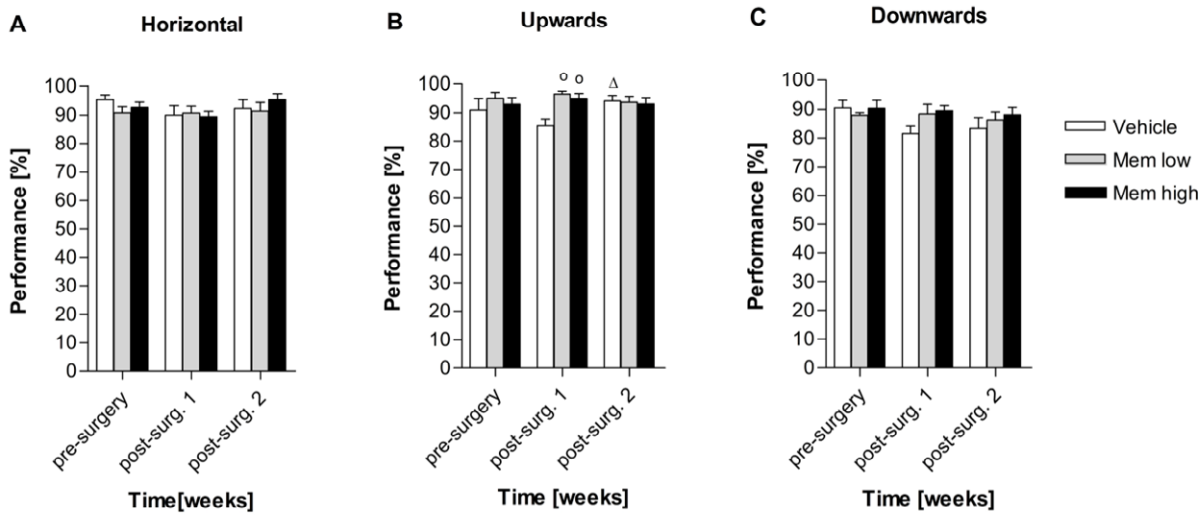

Fig. 4.6. Ladder rung walking task. Analysis of the rats' skilled walking ability on the rung ladder in horizontal **(A)**, upward **(B)** and downward **(C)** conditions on the day before and once weekly after the implantation of a cannula two weeks post-surgery (n=26)**.** Data are means +S.E.M. *Circles* denote a significant difference (Tukey's t-test; P<0.05) on a certain test day compared to vehicle. Significant post-surgery differences within a certain treatment are indicated by *triangles* (here: from post-surgery week 1 to 2).

4.4.2 Histology

The microscopic examination of the Nissl-stained sections revealed that all implantation sites were located within the CFA. Data analysis for histological examination included at least 2-3 sections from 4-5 rats per treatment group and per time point.

4.4.2.1 Neuronal distribution

The distribution of neurons in the CFA without **(Fig. 4.7A)** and with a cannula accompanied by aCSF **(Fig. 4.7B)** or memantine treatment was assessed by immunostaining for NeuN, a nuclear antigen found in neurons. Two as well as six weeks after the implantation of the cannula a reduction in neuronal nuclei within a zone of 50 µm from the implant was observed after vehicle treatment. In contrast, memantine treatment increased the number of neurons within this zone reaching neuron numbers above baseline.

Statistical analysis revealed a significant main effect of the interaction drug x distance ($F_{15,70}$=5.932; P<0.001) for the number of neurons in the 2-week animals **(Fig. 4.7C)**. Further post-hoc comparisons for the vehicle treatment show a significant reduction in the average number of neurons in the first 50 µm around the implantation site compared to all further intervals up to 300 µm (P<0.001) as well as compared to the contralateral hemisphere with no intervention (P=0.004) . The average number of neurons within the first 50 µm was increased significantly with the low (P=0.001) as well as with the high dose (P<0.001) of memantine compared to vehicle. Moreover, the high dose also revealed an increased average number of neurons within this first interval compared to the interval 250-300 µm from the implantation site (P=0.037). For the 6-week animals **(Fig. 4.7D)** a significant main effect in the interaction drug x distance was also revealed ($F_{15,65}$=2.995; P=0.001). Further post-hoc comparisons indicated a significant reduction in the average number of neurons within the first 50 µm compared to intervals from 150-300 µm after vehicle treatment (P<0.05), although not when compared to the hemisphere with no intervention. Memantine significantly increased the number of neurons within this interval in the low (P=0.009) and in the high dose (P=0.003) with the high dose showing again a slight-to-significant increase in the average number of neurons within these first 50 µm compared to the intervals further away from the implantation site (150-200 µm, P=0.063; 200-250 µm, P=0.003; 250-300 µm, P=0.052). Contralateral to the implantation site the average number of neurons was about the same two and six weeks post-surgery.

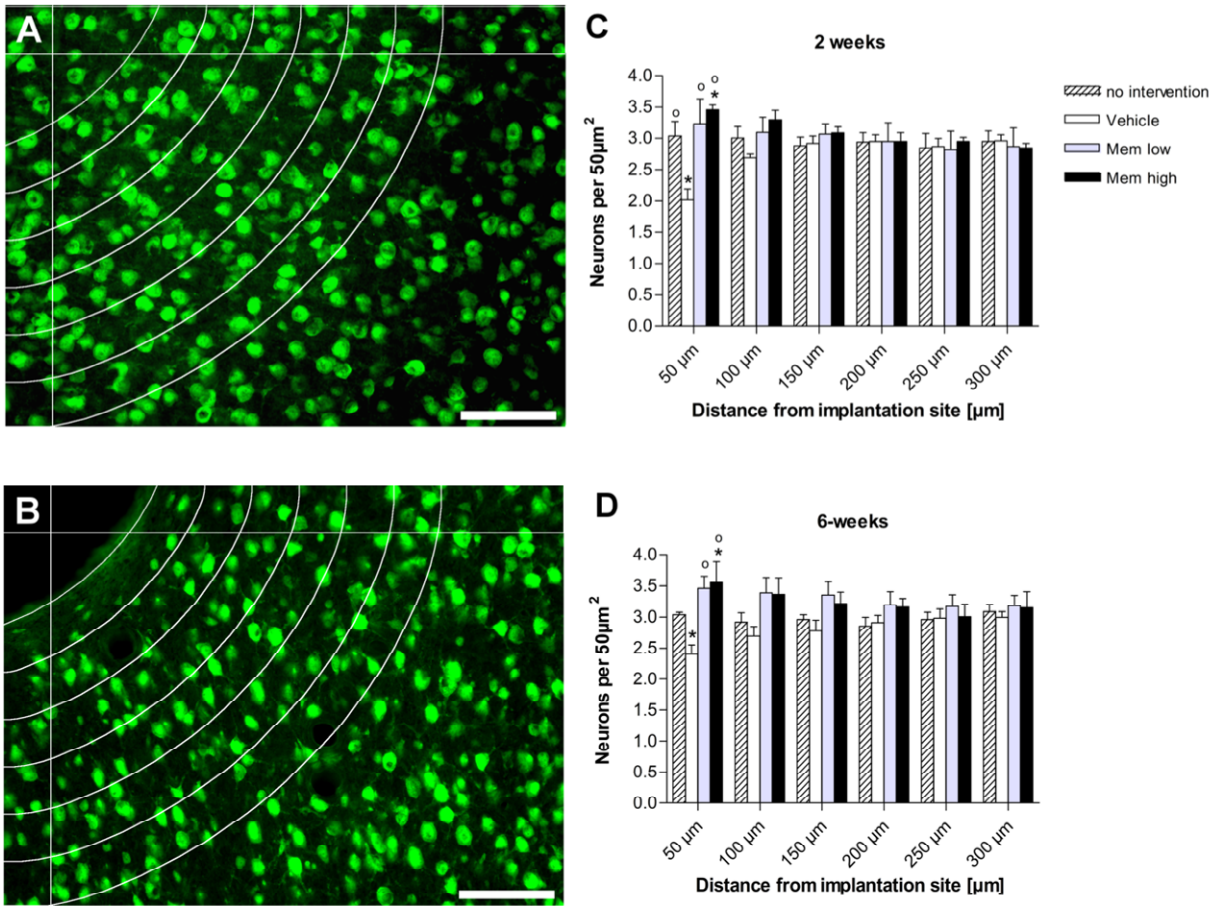

Fig. 4.7. Average number of NeuN$^+$ nuclei. Representative immunohistological images showing NeuN expression in the CFA of controls in the hemisphere without intervention **(A)** and with cannula implantation illustrated with an appropriate set of ROIs **(B)** two weeks post-surgery. Quantification of the average number of neuronal nuclei, as a function of distance from the implantation site, is shown two **(C)** and six weeks post-surgery **(D)**. Data are means +S.E.M. *Asterisks* denote a significant difference (Tukey's t-test; P<0.05) between the first interval of 50 µm and an interval further away (up to 300 µm) of a certain treatment. *Circles* denote a significant difference within a certain interval compared to vehicle. *Scale bar* = 100 µm.

4.4.2.2 Microglial/Macrophagial distribution

The distribution of microglia/macrophages in the CFA without **(Fig. 4.8A)** and with a cannula accompanied by aCSF **(Fig. 4.8B)** or memantine treatment was assessed by immunostaining for IBA-1, an antigen that is specifically expressed in microglia and macrophages, and is up-regulated upon activation during inflammation. Two and six weeks after cannula implantation, a strong increase in microglia/macrophages within the first 50 µm from the

implant was observed independent of the treatment with an overall increase in the number of microglia/macrophages two weeks compared to six weeks after the implantation.

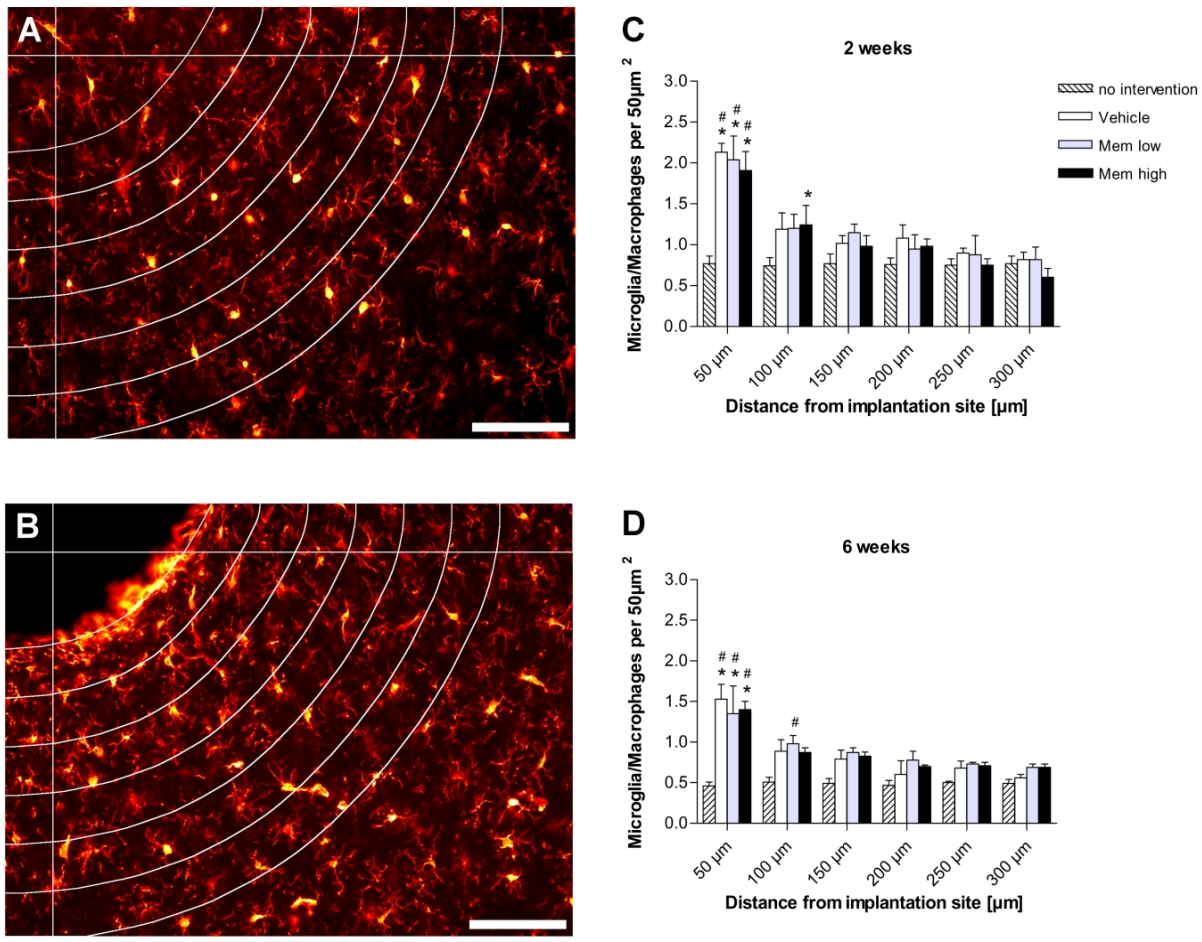

Fig. 4.8. Average number of IBA-1$^+$ cells. Representative immunohistological images showing IBA-1 expression in the CFA of controls in the hemisphere without intervention **(A)** and with cannula implantation illustrated with an appropriate set of ROIs **(B)** two weeks post-surgery. Quantification of the average number of microglia/macrophages, as a function of distance from the implantation site, is shown two **(C)** and six weeks postsurgery **(D)**. Data are means +S.E.M. *Asterisks* denote a significant difference (Tukey's t-test; P<0.05) between an interval close to the implantation site and any interval further away (up to 300 µm) of a certain treatment. A significant difference of any treatment compared to no intervention within a certain interval is indicated by a *rhomb*. *Scale bar* = 100 µm.

Statistical analysis revealed a significant main effect of drug treatment ($F_{3,70}$=3.807; P=0.035) and distance ($F_{5,70}$=47.706; P<0.001) as well as of their interaction ($F_{15,70}$=6.041; P<0.001) for the microglia/macrophage distribution of the 2-week animals **(Fig. 4.8C)**. Further post-hoc comparisons indicated a significantly increased number of microglia/macrophages in the first 50 µm around the implantation site for all treatments (P<0.001) compared to all further

distances and when compared to the hemisphere without interventions (P<0.001). The interval of 50-100 µm comprised a significantly increased number of microglia/macrophages for the high dose of memantine compared to 200-250 µm (P=0.018) and 250-300 µm (P<0.001). Six weeks after cannula implantation **(Fig. 4.8D)** a significant main effect of drug treatment ($F_{3,65}$=7.440; P=0.004) and distance ($F_{5,65}$=25.770; P<0.001) as well as of their interaction ($F_{15,65}$=3.397; P<0.001) was observed. Post-hoc comparisons revealed again a significant increase in the number of microglia/macrophages in the first 50 µm for all treatments compared to all further distances (P<0.001) and when compared to the hemisphere without interventions (P<0.001). Moreover, within a distance of 50-100 µm there was a significant increase of microglia/macrophages after the low dose of memantine compared to the untreated hemisphere (P=0.016), that did not reach statistical significance after vehicle treatment or the high dose of memantine. Moreover, a significant main effect of the time point of measurement was evident in the untreated hemisphere ($F_{1,35}$=8.453; P<0.023) with an overall increase of microglia/macrophages two weeks compared to six weeks post-surgery.

4.4.2.3 Astroglial distribution

The distribution of astrocytes in the CFA without **(Fig. 4.9A)** and with a cannula accompanied by aCSF **(Fig. 4.9B)** or memantine treatment was assessed by immunostaining for GFAP, an antigen that is expressed in the intermediate filaments of astrocytes, and is up-regulated upon activation during inflammation. Two and six weeks after cannula implantation, an increased astrocytic immunoreactivity around the implant was observed independent of the treatment with an overall increase two weeks compared to six weeks after the implantation and a further expansion of scar tissue two weeks post-surgery. Statistical analysis revealed for the 2-week animals **(Fig. 4.9C)** a significant main effect of drug treatment ($F_{3,126}$=7.288; P=0.004) and distance ($F_{9,126}$=213.097; P<0.001) as well as of their interaction ($F_{27,126}$=29.817; P<0.001). Further post-hoc comparisons show for the first 50 µm, that vehicle treatment significantly enhanced astrocyte density compared to the low dose of memantine (P=0.002) which also tended to be enhanced compared to the high dose (P=0.068). Within the first 100 µm all treatments caused significantly enhanced intensity profiles compared to no intervention, with memantine exhibiting an enhancement up to 150 µm (P<0.05). Within the 50-100 µm interval the high dose of memantine revealed significantly enhanced GFAP

immunoreactivity compared to vehicle (P=0.012) and within the 100-150 µm interval the low dose of memantine significantly enhanced astrocyte density compared to vehicle (P=0.019), similar to the high dose of memantine (P=0.076), which did not reach the level of significance though. Moreover, a significant increase in fluorescent intensity was revealed for the low dose of memantine up to 200 µm around the implantation site (P<0.01) and for vehicle and the high dose of memantine up to 250 µm (P<0.05) compared to intervals further away than 400 µm. 400-450 µm from the implantation site significantly less GFAP immunoreactivity was found after vehicle treatment compared to the untreated hemisphere (P=0.028), similar to the interval of 450-500 µm, which also tended to be decreased (P=0.059). Statistical analysis of the 6-week animals **(Fig. 4.9D)** revealed a significant main effect of distance ($F_{9,117}$=240.016; P<0.001) and of the interaction drug x distance ($F_{27,117}$=28.021; P<0.001), as well as a trend for a significant main effect of drug treatment ($F_{3,117}$=3.346; P=0.053). Further post-hoc comparisons show that vehicle-treated animals exhibited significantly enhanced astrocyte density within the first interval compared to the low (P=0.044) or the high dose of memantine (P<0.001). Moreover, within the first 50 µm all treatments revealed significantly enhanced GFAP immunoreactivity compared to no intervention (P<0.001) with the high dose of memantine exhibiting this increase as well 50-100 µm from the implantation site (P=0.008). A significant increase in GFAP immunoreactivity was found up to 150 µm from the implantation site for memantine (P<0.05) and up to 200 µm for vehicle (P<0.05) compared to intervals further away than 400 µm. 200-500 µm around the implantation site vehicle treatment either tended to (P<0.1) or caused significantly less (P<0.05) fluorescent intensity compared to the hemisphere without intervention. The low dose of memantine revealed a significant decrease in GFAP immunoreactivity (P=0.009) only for the last interval of 450-500 µm compared to no intervention. Moreover, again a significant main effect of the time point of measurement was evident in the untreated hemisphere ($F_{1,63}$=10.169; P=0.015) with an overall increase of astrocytes two weeks post-surgery compared to six weeks post-surgery.

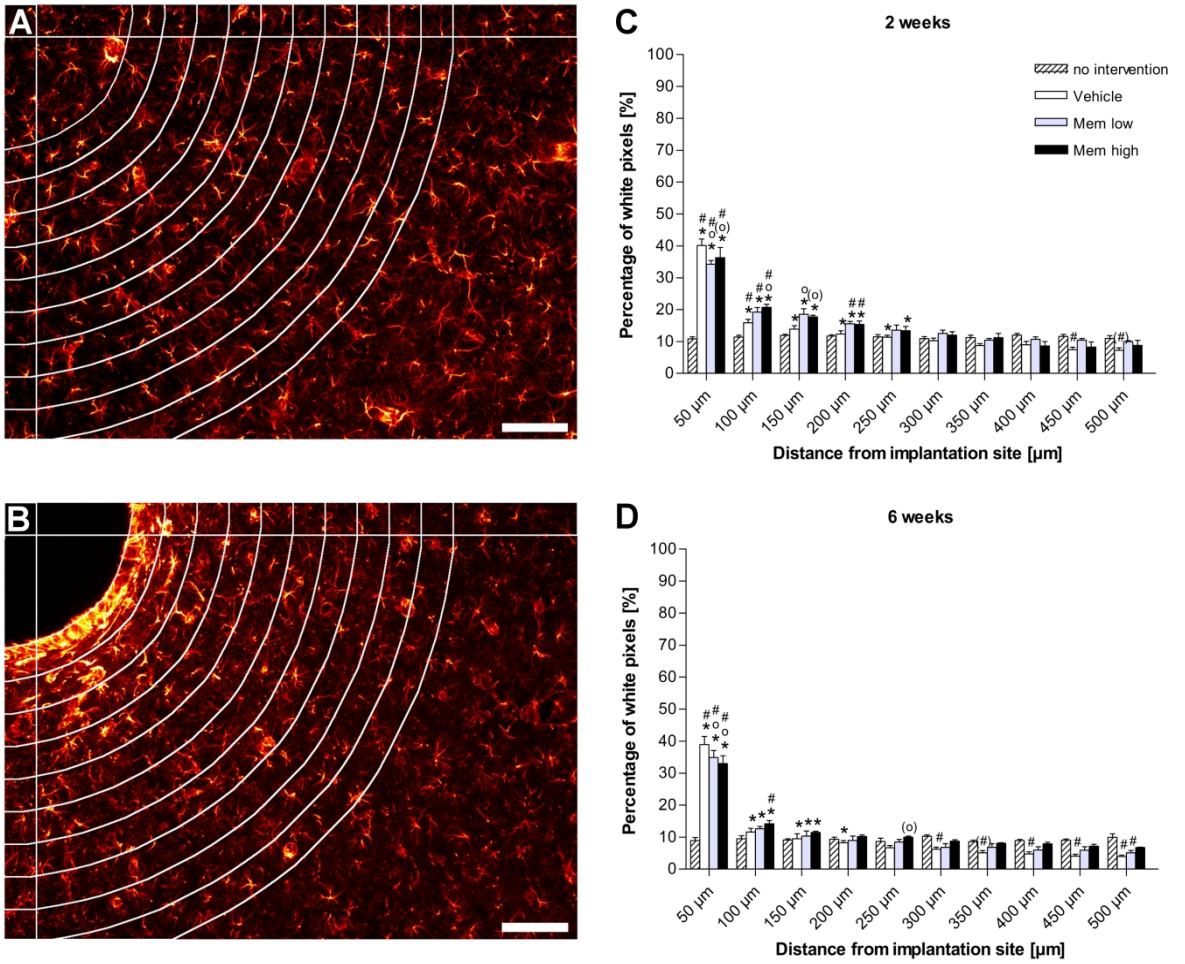

Fig. 4.9. Average distribution of GFAP$^+$ cells. Representative immunohistological images showing GFAP expression in the CFA of controls in the hemisphere without intervention **(A)** and with cannula implantation illustrated with an appropriate set of ROIs **(B)** two weeks post-surgery. Quantification of the average distribution of astrocytes, as a function of distance from the implantation site, is shown two **(C)** and six weeks post-surgery **(D).** Data are means +S.E.M. *Asterisks* denote a significant difference (Tukey's t-test; $P<0.05$) between an interval close to the implantation site and any interval further away (up to 500 µm) of a certain treatment. A significant difference of any treatment compared to no intervention within a certain interval is indicated by a *rhomb*. *Circles* denote a significant difference within a certain interval compared to vehicle. *Brackets* () indicate a trend of significance (Tukey's t-test; $P<0.1$). *Scale bar* = 100 µm.

4.5 Discussion

This study demonstrates that local memantine treatment during cannula implantation in the CFA increases the vicinity and the number of neurons adjacent to the implant accompanied by an improved motor behaviour compared to controls. The effect on the glial scar

formation is only minor revealing no effect on the microglia/macrophage activation, but a slight reduction in astrocytic scar formation directly around the implant.

Glutamatergic NR2B subunit containing NMDA-receptors play a key role in the neurodegeneration associated with glutamate-induced excitotoxicity, with memantine being the only clinically approved drug that preferentially blocks this predominantly extrasynaptically located NMDA receptor subtype (Vizi et al., 2013;Lopes et al., 2013). The NR2BR has been found to contribute to a number of pathological events including Alzheimer's disease (Maher et al., 2014) and epilepsy (Zhu et al., 2015), as well as Huntington's disease, schizophrenia, hypoxia/ischemia and others as reviewed by (Loftis and Janowsky, 2003;Waxman and Lynch, 2005). The neuroprotective properties of memantine by blocking NR2B receptor induced excitotoxicity are supposed to be additionally enhanced by an increased production of the glial cell line-derived neurotrophic factor (GDNF) from astrocytes which promotes neuronal survival, as well as by an inhibition of microglia activation and a reduction in production of pro-inflammatory molecules that exacerbate the inflammation (Wu et al., 2009). Here, we report that memantine has also neuroprotective potential when locally applied during cannula implantation into the CFA accompanied by an improvement in motor behaviour.

Our results show that neuronal cell loss persists around an implant in rat motor cortex over a 6-week period after vehicle treatment as measured by NeuN immunoreactivity. Two as well as six weeks after cannula implantation a reduction in neurons was observed that was restricted to an arc of 50 µm surrounding the cannula. These findings have also been described in previous studies at these or similar time points (Winslow and Tresco, 2010;Winslow et al., 2010;Potter et al., 2012) and indicate that the loss of neurons is a locally restricted phenomenon. Neuronal cell loss seemed to be more intense two weeks after the implantation compared to six weeks, suggesting that neurons slightly re-approach the lesion after the acute phase of the foreign body response. Larger neuronal "die-back" has also been observed by Potter and colleagues (Potter et al., 2012) two weeks after electrode implantation recovering by four to eight weeks with another relapse at 16 weeks though. The initial cell loss is in line with the results of the glial cells that are spread further and more intense around the implantation site two weeks after the implantation, with the sheath getting more compact after six weeks. Memantine, as an uncompetitive NMDA-receptor antagonist, appears to effectively interrupt the cascade of

progressive neurodegeneration given locally during the implantation of the cannula. Two as well as six weeks post-surgery there is an increase in the average number of neurons close to the implant when treated with memantine compared to vehicle, suggesting that neurons in the implantation tract are pushed aside by the implant and survive this original trauma after memantine treatment without getting implicated in and exacerbating the neurotoxic cascade by secondary cell death.

We also provide evidence that the spatial distribution of glial cells does not increase over time, but becomes denser and more organised six weeks compared to two weeks after cannula implantation, indicating a contraction of the glial sheath around the implant at later time points which has already been suggested previously (Winslow and Tresco, 2010;Potter et al., 2012). Moreover, it was reported that the microglia/macrophages attach to the implant as early as 6 h post-implantation, then increase in number and constitute a layer of 1-2 cells covering the length of the implant (Polikov et al., 2006). After the implantation of a foreign body into the rat cerebral cortex a scattered distribution of reactive microglia and hypertrophic astrocytes has been postulated in the initial wound healing response, followed by an encapsulating sheath with clustering of microglia and hypertrophic astrocytes extending in previous studies up to 500 µm from the implant two weeks after the implantation (Turner et al., 1999;Szarowski et al., 2003). A continuous presence of microglia in a tight cellular sheath has been observed six weeks after the implantation with a compact astrocytic sheath extending 50-100 µm around the implant that remains constant after this time point. The inability of the microglia/macrophages to clear the insoluble implant material has been describes as “frustrated phagocytosis” that is characterised by persistent, constitutive release of inflammatory products, surrounded by astrocytes in an encapsulation layer to separate the region of enduring inflammation from the healthy tissue (Polikov et al., 2005;Biran et al., 2005). These findings are in line with the results of our study with an increase of microglia/macrophage activity two weeks after the implantation and clustering in the first 50 µm around the implant. Six weeks after the implantation the number of microglia/macrophages had slightly decreased. The hypertrophic astrocytes extended in our study up to 100-200 µm from the implant two weeks after the implantation, surrounded by a region of hypotrophy within a distance of 400-500 µm in controls. Six weeks after the implantation the hypertrophic region seemed to be restricted to the first 50 µm surrounded by a region of hypotrophy ranging from 250-500 µm. Staining for IBA-1 revealed a thin layer

of microglia/macrophages cells that were irregularly distributed along the length of the cannula providing further evidence that the microglia/macrophages constitute the most inner layer and adhere to the implant, therefore being partly removed with the cannula by implant extraction which also has been reported previously (Szarowski et al., 2003). Memantine treatment resulted only in minor reductions in the glial scar formation around the implant. There was a decrease of the astrocytic scar tissue in the first 50 µm around the implant accompanied by a reduction of the hypotrophic regions surrounding the scar, but no differences in the microglia/macrophage activation compared to vehicle. Hence, these results are in line with the concept that the cell loss in the acute phase with a principally beneficial immune response is to a large extend independent of the more adverse long-term foreign body response with persistent inflammatory processes at the interface (Biran et al., 2005;Marin and Fernandez, 2010). Although the astroglial response is only reduced by memantine in the first 50 µm in our study, this may not be a major problem, since the vicinity and the number of the neurons is increased above baseline adjacent to the implant and moreover the reactive astrocytes are not predominantly harmful, but depend in their function strongly on the type of injury. Astrocytes are supposed to exhibit primarily beneficial, protective function after ischemia-related injuries expressing high levels of neurotrophic factors and cytokines that help to repair and rebuild lost synapses, as well as the blood-brain barrier and limit immune cell influx and neuronal death (Zamanian et al., 2012). Furthermore, they are essential to remodel the extracellular space and to protect the neurons from the enduring inflammatory processes at the interface and to restrict the spread of inflammation into surrounding tissue serving as anti-inflammatory barrier (Sofroniew, 2015).

Irrespective of the glia cell distribution adjacent to the implant we found an overall increase of microglia/macrophages as well of astrocytes in the untreated contralateral hemisphere of the vehicle-treated controls two weeks compared to six weeks post-surgery, suggesting widespread inflammatory processes enduring during this time span. Activation of microglia in the contralateral hemisphere has also been described in previous studies after cerebral ischemia (Marks et al., 2001), and were suggested to be either due to far-ranging signals sent from microglia around the site of damage stimulating the activation, proliferation and migration to the site of damage, or become activated as a result of diaschisis, i.e. functional changes in brain structures remote from, but connected to the site

of brain damage (Seitz et al., 1999). The interhemispheric connectivity via transcallosal fibers connecting the primary motor cortices (M1-M1) that is also important in motor recovery after stroke (Lindenberg et al., 2012) may also induce the activation of microglia in the contralesional CFA. Alternatively, contralateral microglia activation may be enhanced due to enduring brain swelling causing physical deformation also of the contralateral hemisphere (Loddick et al., 1998). In support of these assumptions is the finding that not only microglia but also astrocytes are increased two compared to six weeks after cannula implantation. Intensification of GFAP staining in the contralateral hemisphere following injury has also been noted previously (Badan et al., 2003), with a peak of microglial and astrocyte activation on average after one to two weeks.

In accordance with the neuronal cell loss after vehicle treatment in the vicinity of the implant, that is even more severe two weeks after the implantation compared to six weeks, the results of the behavioural experiments suggest the most severe decline in the rats' performance in the first two post-surgery weeks and a slight recovery thereafter. The data from the reaching box confirm that the increase in neurons around the implant after memantine treatment positively influences the performance two as well six weeks after cannula implantation. Although showing an increased number of neurons even above baseline levels after memantine treatment, the performance is still significantly decreased within the first two post-surgery weeks when compared to pre-surgery. It can be hypothesised that the neurons in the vicinity of the implant, that are presumably pushed aside during cannula implantation, survived the initial trauma due to memantine treatment, but may have partly lost their synaptic connectivity and the neuronal networks they had established. Four to six weeks after implantation the memantine-treated animals had recovered to a large extent and reached baseline levels again, probably benefitting from the surviving neurons and the repair of synapses and neuronal networks by astrocytes. In general, after local brain injury, recovery occurs spontaneously also without rehabilitative training due to behavioural compensations. Over the ensuing weeks a redistribution of the representation of the affected area occurs by neuroanatomical changes such as local axonal sprouting, dendritic spine expansion and synaptogenesis in the regions surrounding the lesion. Neurite outgrowth into intact motor areas surrounding the lesion occurs as well as remote cortical neurons that project to the lesion site contribute to a reassembly of inter- and intra-areal cortical networks and functional recovery. The transfer of functional

responsibility takes about 4-8 weeks, although still comprising significant deficits when not undergoing rehabilitative training (Maldonado et al., 2008;Nudo, 2013). Since rats in our study did not receive daily rehabilitative training after cannula implantation the slight increase in performance during the six post-surgery weeks was most probably due to a combination of spontaneous recovery and weekly testing as a form of rehabilitative training.

The subelement most impaired was the advancing of the paw through the slot with the rats either reaching not far enough to hit the pellet or sweeping the pellet off the shelf when touching it only with the tips of the digits. The strongest increase in errors was found after vehicle treatment in the first post-surgery week enduring up to the fourth week. Memantine amended this motor impairment. In the fifth and sixth post-surgery week the increase in errors in this subelement was compensated or had recovered by the weekly testing. As examined previously the cortical area for wrist and digit presentation is predominantly the RFA, with the CFA being largely responsible for elbow and shoulder movement and partly for wrist movement without being involved in digit coordination (Neafsey and Sievert, 1982;Neafsey et al., 1986). After skilled reach training, the movement representation in the CFA changes in responsibility to an increase in wrist representation and, to some extend, as well to digit representation accompanied by a decrease in elbow and shoulder representation (Kleim et al., 1998). Since the mere repetitive motor use of a limb has been shown to result in no net change in movement topography, the increase in wrist and digit representation in the CFA goes back to skill acquisition (Nudo et al., 1997). The increase in wrist representation in the CFA might be responsible for the increase in error rate in the subelements pronate and release which depend on wrist movement. That these subelements are not as heavily impaired as the advancing and only in the first or the first two post-surgery weeks is probably due to the fact that the CFA in which the cannula was implanted is still primarily responsible for elbow and shoulder movement. According to several previous studies (Neafsey and Sievert, 1982;Neafsey et al., 1986;Colechio and Alloway, 2009) and unpublished preliminary inactivation experiments in our lab, using the $GABA_A$ agonist muscimol, we decided for the actual coordinates used in this study. Moreover, a recent microstimulation study (Brown and Teskey, 2014) suggests the coordinates used in the present study to be majorly involved in the advancing of the paw, which is perfectly in line with the results of our study.

The results of the ladder rung walking task show, that the most difficult condition was the upward walk followed by the downward walk with a decrease in performance especially in the first week after vehicle treatment that was again mitigated by memantine. Since according to the reaching box experiment the elbow and shoulder movements were most impaired after vehicle treatment during surgery, this would suggest that the rats have problems exactly coordinating the affected forepaw when reaching for the next rung, which becomes obvious from a decline in the paw placement accuracy. The diagonal conditions of the rung ladder have been described as more challenging by Antonow-Schlorke et al. (2013) with forelimb motor impairments being reflected by enhanced error scores with challenging requirements in foot placement accuracy, interlimb coordination and balance. Since the impairments in this task were minor and only present in the first week, the animals in the six week group were not tested in this task.

The open field test was used to assess the locomotor behaviour of the animals by the total distance travelled pre-as well as post-surgery. The overall decrease in the distance travelled in the first post-surgery week of the 6-week animals followed by an increase to the sixth week is probably due to the preceding surgery and an incomplete overall behavioural recovery at that time point, which would be in line with the behaviour of the animals in their home cages sleeping or resting a lot the week after the surgery.

In summary, the results of the present study show that memantine has neuroprotective potential when locally applied during cannula implantation by promoting the survival of neurons in the vicinity of the implant. This effect is accompanied by a reduction in astrocytic scar formation directly around the implant in the motor cortex with no effect on the microglia/macrophage activation. Moreover, memantine mitigated the lesion-induced behavioural deficits especially in the skilled reaching task. These findings suggest that memantine treatment is effective in reducing the foreign body response in the brain. It needs to be elucidated in further studies whether coating of electrodes with memantine improves the biocompatibility and long-term recording quality of BCIs in a similar way.

5 Suppression of the foreign body response and neuroprotection by apyrase and minocycline in chronic cannula implantation

Linda Hayn, Linda Deppermann, Michael Koch

5.1 Abstract

Chronic implantation of electrodes or cannulae into the brain is accompanied by a tissue response that is referred to as foreign body response. Persistent inflammation at the interface between the implant and the brain tissue enhances the formation of a glial scar that involves reactive microglial cells and astrocytes. The constitutive release of pro-inflammatory molecules and cytotoxic substances by microglial cells in chronic settings exacerbates neuronal death and tissue damage. An important signal molecule released by injured or dying cells is ATP that activates the microglial cells which exacerbates tissue damage and the immune response. In this study, we examined the effect of the ATP-hydrolysing enzyme apyrase and the antibiotic minocycline on the foreign body response, when locally applied during cannula implantation in the caudal forelimb area (CFA) of the motor cortex (M1) in Lister Hooded rats. The rats' behavioural performance was assessed in a skilled reaching and a ladder rung walking task as well as in the open field. Moreover, the distribution of neurons and glial cells in the vicinity of the implant was examined. Minocycline as well as apyrase increased the number of surviving neurons and reduced microglia/macrophage activation. However, minocycline most effectively improved the skilled motor performance and, moreover, caused a temporary reduction in astrogliosis. Local minocycline application proved sufficiently beneficial to suggest it as a promising therapeutic candidate for improving the biocompatibility of chronic brain implants.

5.2 Introduction

Rehabilitation of sensory or motor functions in patients suffering from neurological diseases or brain injury has been pursued for several decades now (Lebedev and Nicolelis, 2006;Jackson, 2012). Brain computer interfaces that substitute motor, sensory or cognitive functions by stimulating or recording the activity of individual or small populations of neurons after electrode implantation have been developed to restore lost nervous system

function and have demonstrated feasibility even years after an injury to the central nervous system (CNS) (Hochberg et al., 2012;Jackson, 2012). However, the implantation of an electrode device into the brain is accompanied by a tissue response, also known as foreign body response, that impedes the maintenance of neuronal signals over time (Polikov et al., 2005;Griffith and Humphrey, 2006).

The foreign body response that accompanies the implantation of an indwelling device into the brain can be classified into an acute and a chronic response. The acute response is a 1 to 3-week long process and is initiated by the mechanical trauma caused by device implantation which disrupts the BBB and injures neurons and glial cells in the implantation tract. This in turn induces a wound healing response that includes activated microglia and infiltrated macrophages to clear cellular debris and excessive fluid, as well as reactive astrocytes to insulate the implant and the damaged tissue from the surrounding healthy tissue (Polikov et al., 2005). Once the acute inflammatory response declines, a chronic response ensues that is characterised by astroglial encapsulation of the implant accompanied by chronic inflammation at the interface. This is exacerbated by the activated microglia and infiltrated macrophages that are in a state of “frustrated phagocytosis” due to their inability to remove the foreign body, which results in a persistent release of pro-inflammatory molecules (Polikov et al., 2005;Biran et al., 2005). Biran et al. (2005) suggested that a large amount of cell loss does not solely result from the mechanical trauma of insertion, but from the interplay with the chronic inflammation at the interface, which was confirmed by further studies (Winslow and Tresco, 2010;Potter et al., 2012). For optimal device function neuronal survival within the first 50 µm surrounding electrodes is imperative to separate spike amplitudes of neurons (Buzsaki, 2004). The glial sheath formation is suggested to be complete six weeks after foreign body implantation and remains stable thereafter (Turner et al., 1999;Szarowski et al., 2003).

In the acute phase of trauma injured and dying cells release early neuronal “danger signals” like the nucleotide adenosine triphosphate (ATP) which increases within minutes after an injury, due to neuronal and glial depolarisation or simply due to leakage through damaged cell membranes (Davalos et al., 2005;Kono and Rock, 2008;Iadecola and Anrather, 2011). ATP and its metabolite ADP are important activators of glial cells (Davalos et al., 2005) by binding to purinergic P2 receptors (Fields and Burnstock, 2006;Burnstock, 2008). Astrocytes as well as microglia contain diverse subtypes of purinergic receptors which

depend in their activation on the amount of released ATP (Inoue, 2002;Hanisch and Kettenmann, 2007). Activated microglia proliferate and migrate to the site of injury to clear cellular debris, with ATP inducing the chemotaxic response of their processes and the movement of these cells to the site of injury (Haynes et al., 2006;Burnstock, 2008). On the one hand, after microinjury and homeostatic disturbances, such as tiny vascular or tissue damages, microglia are known to phagocyte foreign material and cellular debris and to secrete predominantly neurotrophic factors, that promote neuronal growth and survival. However, under excessive acute or chronic conditions, such as at an interface, they persistently release pro-inflammatory molecules as well as of cytotoxic factors due to their enduring activity and their inability to degrade the foreign material (Inoue, 2002;Polikov et al., 2005;Hanisch and Kettenmann, 2007).

Initially released from the damaged tissue high levels of ATP persist in the peritraumatic zone for many hours after an insult which triggers cell death of even healthy neurons by irreversibly increasing cytosolic Ca^{2+}-levels and neuronal degeneration (Wang et al., 2004). Extracellular ATP also triggers intercellular Ca^{2+}-levels in astrocytes (Wang et al., 2000) and the release of regenerative ATP from internal pools (Anderson et al., 2004). In turn, astrocytes release ATP through regulated pathways to mediate intercellular Ca^{2+}-wave propagation to distant cells. This ATP-triggered ATP release from astrocytes was suggested to be an important mediator of the directional chemotactic response of the microglia (Davalos et al., 2005) that is followed by the release of pro-inflammatory cytokines such as IL-1β, IL-6 and TNFα (Bianco et al., 2005). Moreover, in addition to ATP release from astrocytes, they also release the excitatory transmitter glutamate. Glutamate-mediated excitotoxicity further contributes to neuronal cell loss especially via the overstimulation of extrasynaptically localised N-methyl-D-aspartate (NMDA) receptors (Lipton and Rosenberg, 1994;Lynch and Guttmann, 2002). The contribution of glutamate-mediated excitotoxicity to the foreign body response has previously been investigated using the uncompetitive NMDA receptor antagonist memantine (Hayn and Koch, 2015).

Since ATP, and to a lesser extent also ADP, are able to induce a rapid microglial response (Davalos et al., 2005), in the present study we decided to use the ATP/ADPase apyrase that hydrolyses extracellular nucleoside triphosphates as well as diphosphates. We intended to suppress the extent of immune response by interrupting the inflammatory cascade at a very early stage to also promote the survival of neurons. Moreover, we used

the semi-synthetic second-generation tetracycline minocycline with a broad range of anti-inflammatory, anti-apoptotic and glutamate-antagonist properties (Elewa et al., 2006). Time-points chosen for tissue examination were two and six weeks constituting the end of the acute and of the chronic phase of the immune response.

The present study aimed to further understand and control the foreign body response and serves as a proof-of-principle investigation mimicking the implantation of a device such as an electrode array into the motor cortex by means of a steel cannula. The initial steps of the foreign body response are considered to be of particular relevance and were intended to be blocked to counteract the extent of neurotoxicity and inflammation at the implantation site by a single local application of either apyrase or minocycline during cannula implantation in order to mimic local drug delivery from coated electrodes. The extent of tissue damage in M1 of rats was investigated on the behavioural level using the skilled reaching task (Whishaw et al., 1986;Whishaw and Pellis, 1990), the ladder rung walking task (Metz and Whishaw, 2002;Antonow-Schlorke et al., 2013) and the open field box. Rats were tested before and once a week after the implantation of a cannula into the CFA of M1. Moreover, the spatial distribution of neurons and glial cells was immunohistologically analysed at the implantation site two weeks as well as six weeks after cannula implantation.

5.3. Materials and Methods

The materials and methods used in this study have already been described in detail previously (Hayn and Koch, 2015) and are only briefly addressed here.

5.3.1 Animals

A total of 60 naive adult male Lister Hooded rats (Charles River Laboratories, Germany) weighing 200-220 g were used in this study. Rats were group-housed under standard conditions in Makrolon cages (type IV) on a 12 h light/dark cycle (lights on at 7:00 a.m.) with controlled temperature and humidity. All rats received tap water *ad libitum* and were restricted to 12 g standard diet rodent chow (Altromin, Germany) per rat per day as soon as the training started. The experiments were conducted in compliance with the ethical guidelines of the National Institute of Health for the care and use of laboratory animals for experiments and were approved by the local animal care committee (Senatorische Behörde, Bremen, Germany).

5.3.2 Timeline

The study was designed to assess the effects of acute apyrase (grade VII apyrase from potato; *A 6535*; Sigma Aldrich, Steinheim, Germany) treatment with an ATPase/ADPase ratio of approximately 1 as well as minocycline (minocycline hydrochloride; *M 9511*; Sigma Aldrich, Steinheim, Germany) treatment locally administered during the implantation of a cannula into the CFA of M1. For this purpose, the rats were habituated and individually trained in the single-pellet reaching boxes (Whishaw et al., 1986;Whishaw and Pellis, 1990) at least four weeks before the experiments started. After reaching a stable baseline with a hit-reach-ratio of at least 75 % the rats were pseudo-randomly assigned to six groups, receiving either artificial cerebrospinal fluid (aCSF), which served as the control, apyrase (0.3 U/µl) or minocycline (20 µg/µl). Brains were removed for histological analysis either two or six weeks after cannula implantation. All animals were tested in the single-pellet reaching box and in the open field the day before cannula implantation and once a week after the implantation. Moreover, the 2-week group was tested on a ladder rung walking task for further analysis of the rats' skilled walking ability and received one week of previous training for this task.

5.3.3 Single-pellet reaching task

The single-pellet reaching task was chosen to define the preferred forepaw of each rat and to analyse the functionality of the motor cortex contralateral to this paw before and after cannula implantation.

5.3.3.1 Single-pellet reaching boxes

The single-pellet boxes **(Fig. 5.1)** had a vertical slit at the centre of the front wall, and a shelf in the front of the slit, on which casein pellets (45 mg Dustless Precision Pellets, Bio-Serv®, UK) were placed in one of two indentations. These indentations were located 2 cm from the inside of the wall aligned with the edges of the slit in order to prevent the rats using the tongue to lap the pellet and to ensure that they only reach the pellet in the indentation contralateral to the preferred paw. After the habituation phase, two additional polycarbonate side walls were inserted in the box to ensure that the rats directly approach the slot with their body postures always in a similar orientation.

Fig. 5.1. Single-pellet reaching box. Photograph of the skilled reaching box with additionally inserted side walls.

5.3.3.2 Training and testing

Training sessions in the skilled reaching box consisted of a habituation phase in which the preferred paw was identified. The rats were trained to walk to the rear wall of the box after every trial to initiate the next one, however, only trials in which they successfully reached a pellet in the first attempt were rewarded by an additional pellet in the back. Training sessions consisted of daily 5-10 min sessions per rat for about 4-5 weeks until they reached a stable baseline of at least 75% correct responses.

5.3.3.3 Behavioural analysis

The reaching performance in the single-pellet boxes was recorded for 5 min on each test day using a Panasonic NV-DS60 digital video camera (shutter speed 1/50 s) and a cold-light source for improved subsequent frame-by-frame analysis (25 frames/s). All experiments were performed with the experimenter being blind to the treatment protocol.

Quantitative analysis:

Hit-reach-ratio. The success rate of each rat was calculated from the total number of hits compared to the total number of reaches. Reaching attempts were scored as long as the pellet was in the respective indentation. A successful reach was scored as a *hit* (“1 hit”) when the pellet was grasped and consumed in the first attempt. If the pellet was grasped, but

dropped in the box an *incomplete hit* (“0.5 hits”) was scored. An *incomplete hit* was also scored when the rat had missed the pellet, which was scored as a *miss* (“1 miss”), but then grasped the pellet from the indentation without previously withdrawing the paw through the slot. Repeated, unsuccessful attempts without paw withdrawal from the shelf were scored as *repeated misses* (“0.5 misses”) with only the first miss being scored as complete *miss*. Moreover, attempts in which the rat approached the slot, but dropped the paw on the inner edge, were scored as *incomplete attempts* (“0.5 misses”).

The hit-reach-ratio was calculated by the sum of *hits* and *incomplete hits* divided by the total number of reaches. Each *hit* as well as each *incomplete hit* was counted as one attempt as well as the complete *misses* and was hence scored as “1 reach”. Only *repeated misses* and *incomplete attempts* were counted as half attempts and were hence scored as “0.5 reaches”.

Qualitative analysis:

Movement pattern analysis. Each forelimb movement during a successful hit in the single-pellet box consists of 12 movement subelements: *Orientation*, *limb lift*, *digits flexion*, *aim*, *advance*, *digits extension and opening*, *pronation*, *grasp*, *supination I*, *supination II*, *release* and *replace* (Alaverdashvili et al., 2008;Alaverdashvili and Whishaw, 2010;Hayn and Koch, 2015). The first five attempts on each test day before and after the surgery were analysed for these 12 subelements and rated using a three-point scale. A successful normal subelement was rated “0”, when the subelement was present but abnormal it was rated “0.5”, and when it was absent or incomplete and resulted in a miss or of loss of the pellet it was rated “1”. Scoring was achieved by means of frame-by-frame analysis.

5.3.4 Open field

The locomotor activity of the rats was analysed in infrared-controlled activity chambers (44.7 cm x 44.7 cm x 44.0 cm; ActiMot-system, TSE, Bad Homburg, Germany) by the total distance travelled [m] that was measured from the rats’ horizontal activity for 30 min the day before cannula implantation and once weekly after the implantation.

5.3.5 Ladder rung walking task

For further analysis of the rats' preferred forelimb, the skilled walking ability of the 2-week group was tested on a ladder rung walking task in a horizontal condition (Metz and Whishaw, 2002), and additionally, in a diagonal condition according to a modified version of Antonow-Schlorke et al. (2013) to further analyse the performance of the rats' preferred forelimb contralateral to the cannula implantation site.

5.3.5.1 Ladder rung walking test apparatus

The test apparatus was manufactured according to Metz and Whishaw (2002) by in-house mechanics of the University of Bremen. The rung ladder was 1 m in length with metal rungs linking the side walls. During the training phase the rungs were placed at a regular arrangement with a distance of 2 cm between the rungs. In the horizontal condition **(Fig. 5.2A)** the ladder was elevated about 1 m above the floor with a platform at both ends. The angle of inclination of the rung ladder for the upward and the downward condition **(Fig. 5.2B)** was about 38.32°. Rats crossed the ladder from a neutral platform to a platform on the other side with casein pellets as reward.

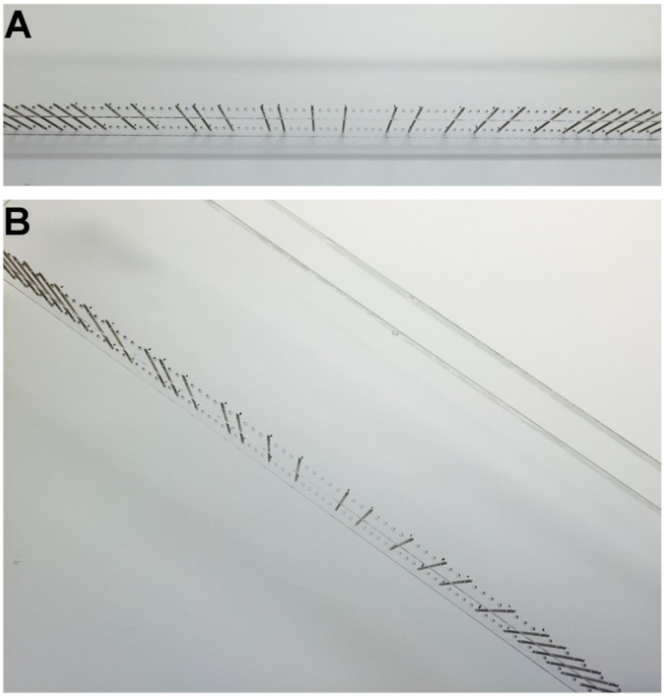

Fig. 5.2. Ladder rung walking test apparatus. Irregular arrangement of rungs in horizontal **(A)** and diagonal directions **(B).**

5.3.5.2 Training and testing

After a short training phase on the regular pattern single rungs in the middle part of 60 cm were removed to receive an irregular pattern with rung-to-rung distances of 2-6 cm. Two templates of irregular patterns, pattern A and B, were applied to prevent the rats from learning the pattern. After the rats accomplished to cross the ladder fluently, they were video recorded the day before the surgery and once a week for two weeks after the surgery.

5.3.5.3 Foot fault scoring

The skilled walking performance was evaluated qualitatively by means of frame-by-frame analysis using a seven-category scale: *Correct placement*, *partial placement*, *correction*, *replacement*, *slight slip*, *deep slip and total miss* (Metz and Whishaw, 2002;Antonow-Schlorke et al., 2013;Hayn and Koch, 2015). Scores from 6 to 0 points were given and only the forelimb that was preferred in the reaching box was rated. When different errors occurred at the same time, the lowest score was given. In case of a fall, the preferred forelimb was only rated when it initiated the fall.

5.3.6 Cannula implantation and drug administration

Substances administered during the implantation of the cannula were either aCSF which served as control, or apyrase or minocycline dissolved in aCSF (with pH adjusted to 7.4). Substances were freshly prepared before surgery and administration occurred in a pseudorandom order by a treatment-blind experimenter.

Rats of all groups were anesthetised by intraperitoneal (i.p.) injections of 60 mg/kg pentobarbital (Sigma Aldrich, Steinheim, Germany) and 10 mg/kg xylazine (Rompun®; Bayer, Leverkusen, Germany). To mitigate the respiratory depressive effects of pentobarbital 0.1 mg/kg atropine (Braun, Melsungen, Germany) were administered subcutaneously (s.c.). Rats were fixed in a stereotaxic apparatus (Kopf Instruments, Tujunga, CA, USA) and were implanted with a blunted stainless steel 27 gauge injection cannula of 0.4 mm in diameter (Braun, Melsungen, Germany) into the CFA of M1 contralateral to the preferred forelimb. Drugs were administered during the implantation procedure with 0.5 µl being applied to the cortical surface and further 0.5 µl being administered during the implantation of the cannula. Coordinates for implantation according to bregma (AP: +1.5 mm; ML: ±2.3 mm; DV: -2.3 mm) were derived from previous mapping studies (Neafsey et al., 1986;Hyland, 1998;Colechio and Alloway, 2009) and additional pre-tests of our workgroup using the GABA (γ-aminobutyric acid)$_A$-agonist muscimol to temporarily inactivate this region.

5.3.7 Perfusion and tissue collection

Upon completion of the last test, the rats were euthanised with a lethal dose of pentobarbital (200 mg/kg; i.p.) and transcardially perfused with 4% PFA. The brains were removed from the skull and post-fixed for 24 h followed by cryoprotection in 30% sucrose solution for 48 h. Subsequently, six series of horizontal 40 µm sections of the cortical implantation site were cut on a cryostat (Jung CM 3000, Leica Instruments GmbH, Nussloch, Germany).

5.3.8 Histology

Brain slices of the first series were Nissl-stained to control the coordinates of the implantation site by means of a rat brain stereotaxic atlas (Paxinos and Watson, 1998). The extent of inflammation and the number of the neurons around the implantation site were analysed by immunohistological staining for neurons (neuronal nuclei; NeuN) with mouse anti-NeuN (Millipore, Darmstadt, Germany), for astrocytes (glial fibrillary acid protein; GFAP) with rabbit anti-GFAP (DAKO, Hamburg, Germany) and for microglia/macrophages (ionised calcium binding adaptor molecule 1; IBA-1) with rabbit anti-IBA-1 (1:2000; WAKO, Neuss, Germany). Secondary antibodies were biotinylated goat anti-rabbit IgG (DAKO, Hamburg, Germany) followed by Cy3-labeled streptavidin (Sigma, Steinheim, Germany) for the astrocytes as well as for the microglia/macrophages and Alexa Fluor 488 goat anti-mouse IgG (Dianova, Hamburg, Germany) for the neurons. Sections were mounted on microscope slides and counterstained with Sudan Black (Acros, New Jersey, USA) to eliminate background immunofluorescence and autofluorescence before being coverslipped for imaging.

5.3.9 Image analysis

Fluorescent images of tissue sections from layers V of the cortex near the tip of the cannula were taken using a Zeiss Axioskop fluorescence microscope (Göttingen, Germany). Z-stack images were captured with a 20 x objective around the implantation site for neurons and for microglia/macrophages to individually count the cells and with a 10 x objective for astrocytes to examine their distribution. Exposure times and gamma values were held constant for each cellular marker. Quantification was performed using the image processing software FIJI (ImageJ). The implantation region was manually delineated and regions of interest (ROIs) were defined in 50 µm concentric circles up to 300 µm from the interface for

neurons and microglia/macrophages and up to 500 µm for astrocytes. Large blood vessels or other irregularities were excluded from the ROIs. In order to improve visual display images in this report have been pseudo-coloured **(Fig. 5.3)**.

Quantification of the neuronal population surrounding the implantation site **(Fig. 5.3A)** was accomplished by manually counting the neurons in each ROI around the implantation site and by calculating the average number of neurons [n] for bins of 50 µm² for each treatment. The same procedure was applied to the images of the microglia/macrophages **(Fig. 5.3B)**. The motor cortex of the hemisphere contralateral to the implantation site of aCSF-treated animals served as the control.

The distribution of the astrocytic scar **(Fig. 5.3C)** was examined by an enhancement of contrast by 0.3%, followed by the application of an auto local threshold (method: median; radius: 80 pixel; correction value (c): -30) in order to obtain binary images. The average area covered with astrocytes [%] was calculated for each ROI. Again the motor cortex of the hemisphere contralateral to the implantation site of aCSF-treated animals served as the control.

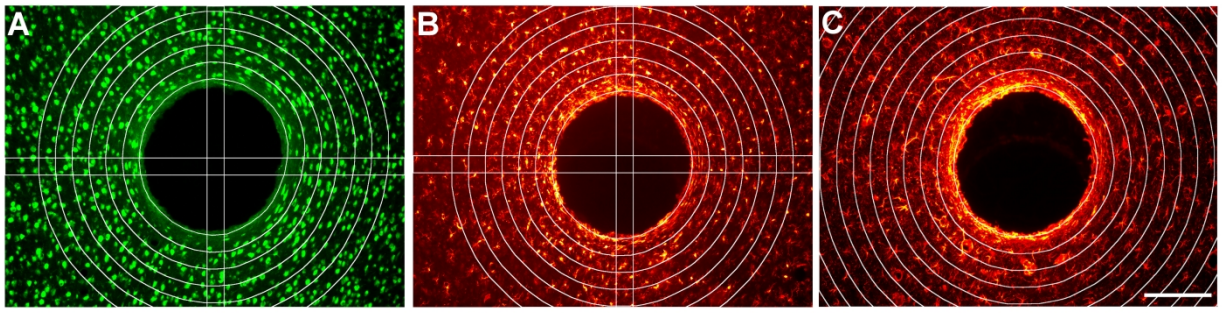

Fig. 5.3. Image analysis. Fluorescent images of tissue sections from layers V of the CFA two weeks after cannula implantation. ROIs were defined in 50 µm concentric circles up to 300 µm from the interface for neurons **(A)** and microglia/macrophages **(B)** and up to 500 µm for astrocytes **(C)**. Horizontal and vertical lines in indicate the bins of 50 µm² for which the average number of cells was calculated. *Scale bar = 200 µm.*

5.3.10 Statistical analysis

Descriptive statistics are based on means and variances indicated as standard error of the mean (+S.E.M.). Statistical analyses were run using the statistical software SigmaStat (version 2.03 for Windows) using a two-way repeated measures analysis of variance (two-way RM ANOVA) for the behavioural tests with the factors treatment and test day, and for the immunohistological investigations with the factors treatment and distance from the

implantation site for each marker and time point. Post-hoc pairwise comparisons using a Tukey's t-test were defined to be significant at $P < 0.05$. Animals that did not reach a stable baseline performance of 75% correct responses in the skilled reaching task or lost the acrylic cap after cannula implantation were excluded from further analysis.

5.4 Results

5.4.1 Behavioural experiments

A total of six animals were excluded from the data analysis either due to a loss of the acrylic cap (n=2) or due to not reaching a stable baseline of at least 75% correct responses in the single-pellet reaching task (n=4). Data of all 54 participating animals (vehicle: n = 18; apyrase: n = 17; minocycline: n = 19) are included in the bar plots and statistics of the first two weeks for all behavioural experiments except for the ladder rung walking task that was exclusively applied to the 2-week animals and contains the data of 28 animals that remained for two weeks in the experiment. Bar plots and statistics of the 6-week group contain the data of 26 animals that remained in the experiment up to the sixth week. Each treatment group accordingly contains eight to ten animals.

5.4.1.1 Single-pellet reaching task

Hit-reach-ratio. Before cannula implantation into the CFA contralateral to the preferred forelimb, rats of all treatment groups had reached a stable baseline in the reaching boxes with a hit-reach-ratio of at least 75%. Local vehicle treatment during cannula implantation decreased the performance at all time points measured. Apyrase and minocycline amended the performance with a stronger effect for minocycline which increased the performance at all time points measured compared to controls. The statistical data analysis revealed for the first two weeks **(Fig. 5.4A)** a significant main effect of drug treatment ($F_{2,102} = 6.148$; $P = 0.004$) and time point of measurement ($F_{2,102} = 50.218$; $P < 0.001$), as well as a significant interaction drug x time point of measurement ($F_{4,102} = 3.634$; $P = 0.008$). Post-hoc comparisons showed that the decrease of the hit-reach-ratio within the first post-surgery week was significant for vehicle and apyrase ($P < 0.001$) as well as for minocycline ($P = 0.001$) compared to pre-surgery. The performance decrease in the second post-surgery week was only significant for vehicle ($P < 0.001$) and apyrase ($P = 0.001$) compared to pre-surgery, but

not for minocycline. After minocycline treatment the performance was significantly improved compared to controls in both post-surgery weeks ($P \leq 0.001$), which was also the case for apyrase in the second post-surgery week ($P = 0.027$). Statistical data analysis of the hit-reach-ratio for the 6-week animals **(Fig. 5.4B)** also revealed a significant main effect of drug treatment ($F_{2,138} = 9.706$; $P < 0.001$) and time point of measurement ($F_{6,138} = 17.997$; $P < 0.001$) with post-hoc comparisons revealing a significantly decreased the hit-reach-ratio after cannula implantation in all six post-surgery weeks compared to pre-surgery for vehicle ($P \leq 0.001$). Performance decrease was also significant for apyrase and minocycline in the first post-surgery week ($P < 0.001$) compared to pre-surgery, but exhibited constant recovery thereafter that reached statistical significance ($P < 0.05$) in the fourth week for apyrase and already in the third week for minocycline. Performance was significantly improved compared to vehicle in the sixth post-surgery week for apyrase ($P = 0.029$) and in all post-surgery weeks for minocycline ($P < 0.05$).

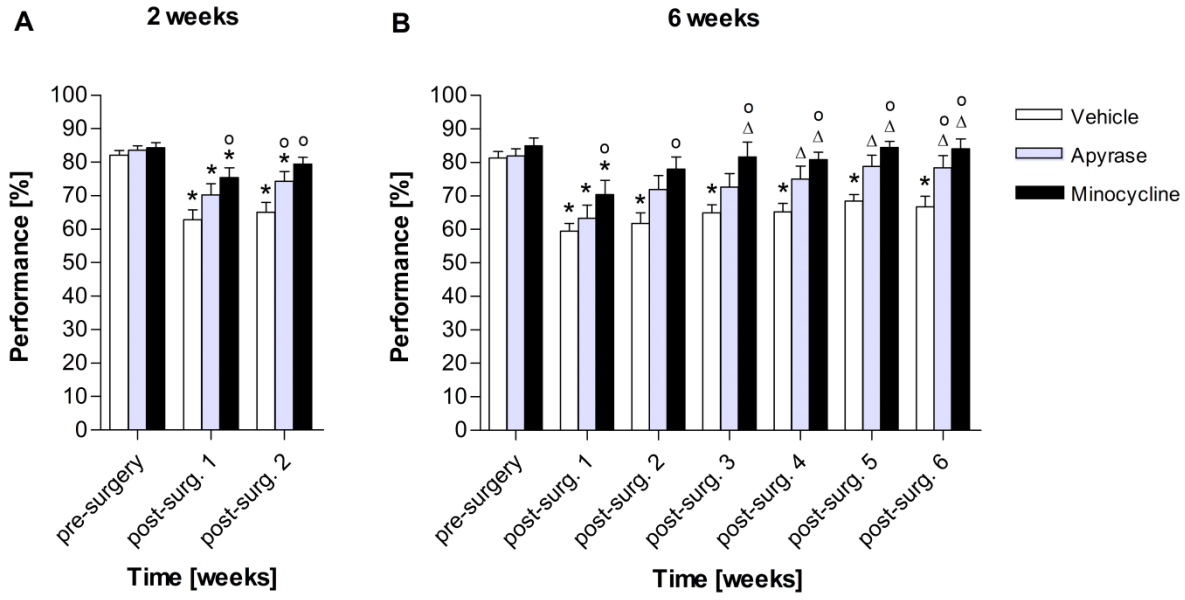

Fig. 5.4. Hit-reach-ratio. Quantitative data analysis of the rats' performance in the skilled reaching task before and once weekly after the implantation of a cannula into the CFA contralateral to the preferred forepaw accompanied by either local vehicle (aCSF), apyrase or minocycline treatment two weeks ($n = 54$) **(A)** and six weeks ($n = 26$) post-surgery **(B).** Data are means +S.E.M. *Asterisks* denote a significant difference (Tukey's t-test; $P < 0.05$) between pre- and post-surgery tests of a certain treatment. Significant treatment differences on a certain test day compared to vehicle are indicated by *circles*. A significant post-surgery effect of a certain treatment is indicated by the *triangle* (here: compared to the first post-surgery week).

Movement pattern analysis. In addition to the quantitative hit-reach-ratio analysis, the qualitative movement pattern analysis of the first five trials on each test day revealed that the subelements most impaired after cannula implantation were *advancing* and *pronation* of the paw. Minor impairments were detected in the subelements *grasp* and *release*. In compliance with the results of the hit-reach-ratio-analysis, vehicle treatment caused the strongest increase in errors within the first post-surgery week with especially minocycline reducing these error scores.

The subelement *advance* revealed the most increased error rates after cannula implantation in all treatment groups with the animals often advancing the paw not far enough through the slot to reach the pellet or sweeping the pellet off the shelf when touching it only with the tips of the digits. The strongest increase in errors occurred with vehicle and apyrase treatment with minocycline amending these motor impairments. The statistical data analysis revealed for the first two weeks **(Fig. 5.5A)** a significant main effect of drug treatment ($F_{2,102} = 5.480$; $P = 0.007$) and time point of measurement ($F_{2,102} = 32.718$; $P < 0.001$) as well as of the interaction drug x time point of measurement ($F_{4,102} = 3.097$; $P = 0.019$). Post-hoc comparisons showed that the increase in the number of errors in this subelement was significant for vehicle treatment ($P < 0.001$) in both post-surgery weeks compared to pre-surgery. For apyrase ($P < 0.001$) and minocycline ($P = 0.013$) the increased error rate only reached statistical significance in the first post-surgery week compared to pre-surgery. Minocycline decreased the error rate in the first ($P < 0.011$) and second ($P < 0.001$) post-surgery week compared to vehicle treatment. For the 6-week animals **(Fig. 5.5B)** there was also a significant main effect of drug treatment ($F_{2,138} = 17.319$; $P < 0.001$) and time point of measurement ($F_{2,138} = 15.044$; $P < 0.001$) with post-hoc comparisons revealing a significant increase in errors for vehicle within the first five post-surgery weeks ($P < 0.05$) with a significant decrease in errors from the first to the fifth and sixth week ($P < 0.05$). For apyrase the increase in errors was significant in the first ($P < 0.001$) and in the third post-surgery week ($P = 0.038$) compared to pre-surgery, with a significant decrease in errors after the first week ($P < 0.05$). Minocycline amended the motor performance and decreased the error rate statistically significant ($P < 0.05$) within the first five post-surgery weeks compared to vehicle and only resulted in a significant increase in errors in the first week ($P = 0.015$) with a significant decrease in post-surgery weeks three to five ($P < 0.05$).

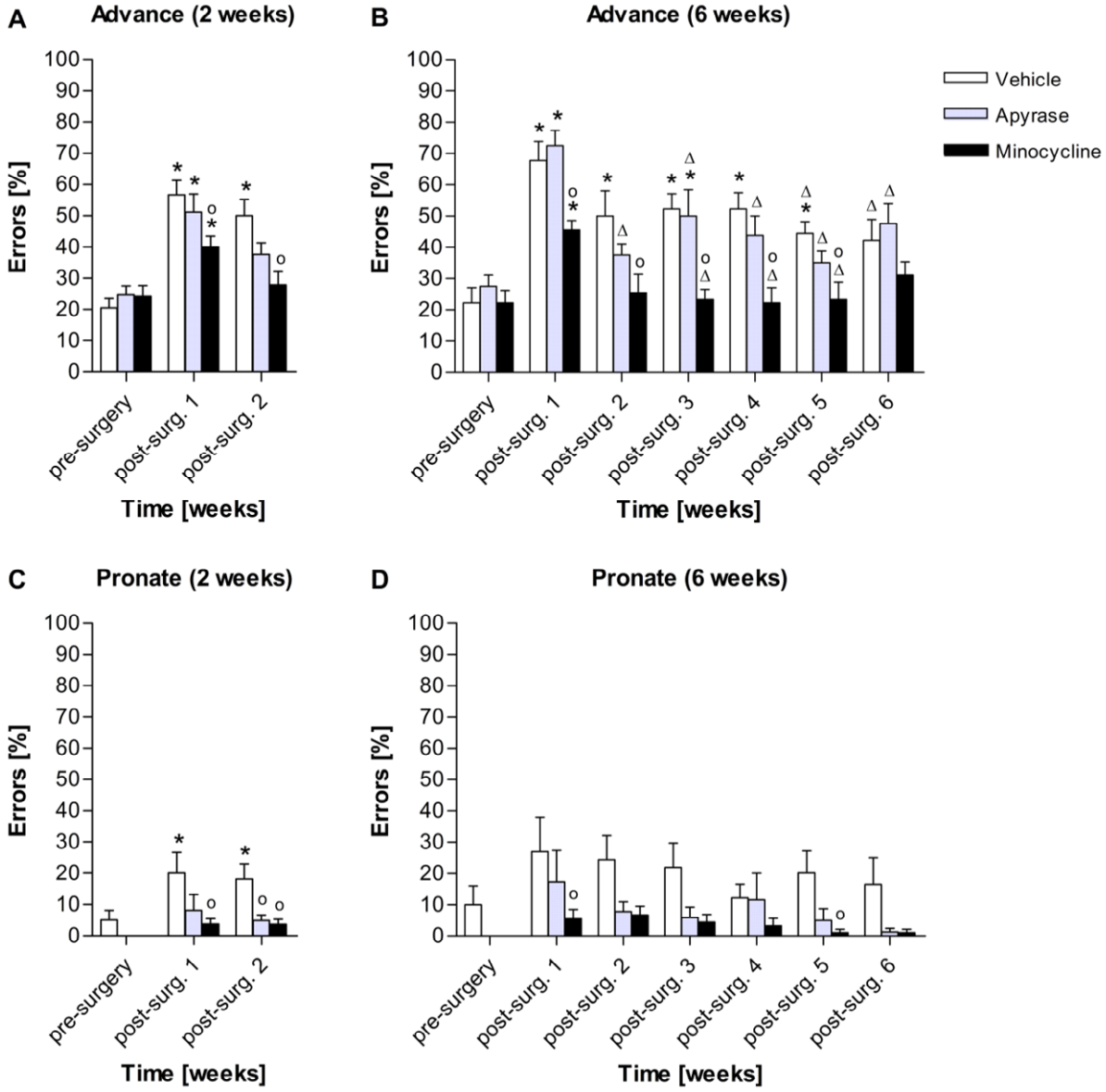

Fig. 5.5. Movement pattern analysis. Qualitative data analysis of the most impaired subelements within the first five trials in the skilled reaching task before and once weekly after cannula implantation accompanied by local vehicle, apyrase or minocycline treatment two (n = 54) **(A,C)** and six weeks (n = 26) post-surgery **(B,D).** Data are means +S.E.M. *Asterisks* denote a significant difference (Tukey's t-test; $P < 0.05$) between pre- and post-surgery tests of a certain treatment. Significant treatment differences on a certain test day compared to vehicle are shown by *circles*. A significant post-surgery effect of a certain treatment is indicated by the *triangle* (here: compared to the first post-surgery week).

The error rate of the subelement *pronate* was not that pronounced, but vehicle-treated rats often not fully extended and opened their digits or omitted the rotation of the wrist, hence missing the pellet or grasping the pellet with a lateral swipe of the paw. This

effect was again most intense within the first two post-surgery weeks and was improved by apyrase and minocycline. Within these first two post-surgery weeks **(Fig. 5.5C)** a significant main effect of drug treatment ($F_{2,102} = 5.524$; $P = 0.007$) and time point of measurement ($F_{2,102} = 9.641$; $P < 0.001$) was revealed. Further post-hoc comparisons showed that the increase of errors in this subelement was significant after vehicle treatment in both post-surgery weeks ($P < 0.01$) compared to pre-surgery. Apyrase as well as minocycline improved the performance within both post-surgery weeks reaching statistical significance in the first post-surgery week for minocycline ($P = 0.004$) and in the second post-surgery week for apyrase as well as minocycline ($P < 0.05$). Within the 6-week group **(Fig. 5.5D)** there was also a significant main effect of drug treatment ($F_{2,138} = 4.816$; $P = 0.018$) and time point of measurement ($F_{2,138} = 2{,}758$; $P = 0.015$). Post-hoc comparisons did not reach statistical significance for the increase in errors after the surgery when treated with vehicle, though, the decrease in errors after minocycline treatment was significant in the first and fifth post-surgery week ($P < 0.01$) compared to vehicle.

The subelements *grasp* and *release* revealed only minor impairments, and are hence, not further illustrated. The error rate of the subelement *grasp* was only slightly enhanced after the surgery with the rats from time to time either pulling the pellet instead of properly grasping and lifting it or grasping the pellet in a deviant way with only one or two digits. Statistical analysis did not reveal a significant main effects for the first two weeks, however for the 6-week group a significant main effect of the drug treatment ($F_{2,138} = 6.087$; $P = 0.008$) was revealed, with the apyrase-treated animals exhibiting a significantly decreased error rate (4.69% ± 3.29) in this subelement compared to vehicle (20.37% ± 7.10) in the third post-surgery week ($P = 0.041$). The subelement *release* also slightly increased after cannula implantation with the animals from time to time showing difficulties to open their paw to release the pellet into the mouth. However, statistical data analysis revealed no significances.

The other subelements were even less or not at all impaired within the first five trials. The subelement *replace* was difficult to examine, since the rats often turned around in the box to walk to the back without replacing the paw pre- as well as post-surgery and hence, often no scores could be given and the subelement had to be excluded.

3.1.2. Open field

The analysis of the rats' locomotor activity measured by the total distance travelled [m] in 30 min served as a control paradigm and revealed no significant main effects of the interaction drug x time point of measurement. Within the first two weeks **(Fig. 5.6A)** only a significant main effect of the time point of measurement ($F_{2,102} = 4.989$; $P = 0.009$) was revealed with post-hoc comparisons indicating a significant increase in the total distance travelled from the first to the second post-surgery week for minocycline ($P = 0.005$), however without any significant differences compared to pre-surgery or compared to vehicle. For the 6-week group **(Fig. 5.6B)** a significant main effect of the drug treatment was revealed ($F_{2,138} = 3.473$; $P = 0.048$), with post-hoc comparisons indicating a significant increase in the distance travelled for the apyrase-treated animals in the fourth ($P < 0.013$) and the sixth post-surgery week ($P < 0.015$) compared to vehicle-treated animals, however, this increase was not significant compared to pre-surgery and a more detailed data analysis indicated that this increase goes back to two outliers.

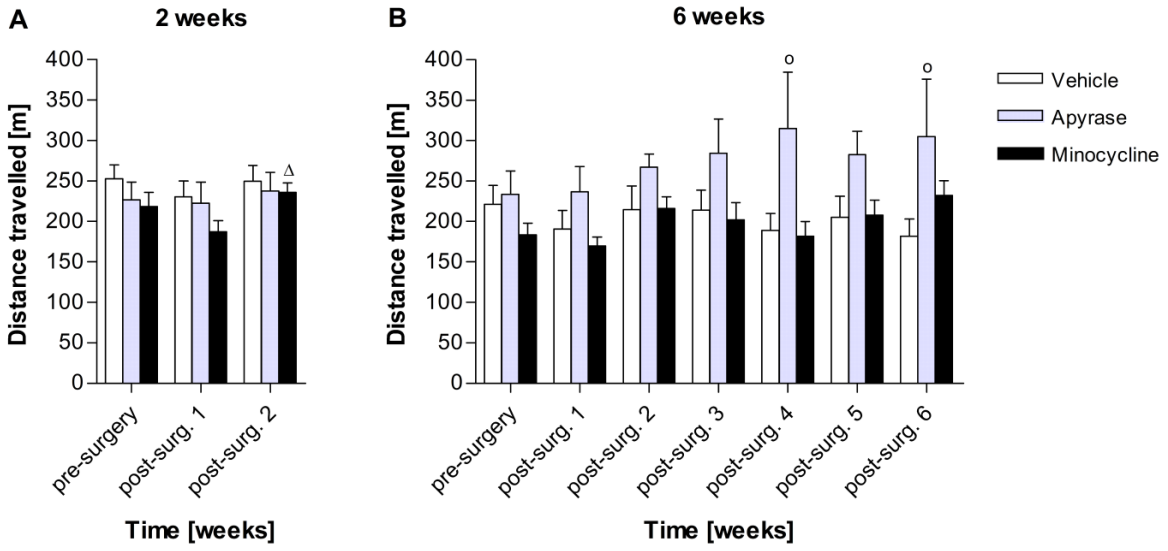

Fig. 5.6. Open field. Analysis of the rats' total distance travelled [m] within 30 min on the day before and once weekly after cannula implantation two ($n = 54$) **(A)** and six weeks ($n = 26$) post-surgery **(B)**. Data are means +S.E.M. Significant treatment differences on a certain test day compared to vehicle are shown by *circles*. The *triangle* denotes a significant post-surgery difference (Tukey's t-test; $P < 0.05$) within a certain treatment (here: compared to the first post-surgery week).

5.4.1.3 Ladder rung walking task

The data analysis of the foot placement scores of the 2-week animals on the rung ladder revealed the ladder's diagonal conditions to be more difficult than the horizontal. Vehicle

treatment during cannula implantation caused a slight decrease of performance in the ladder's horizontal condition **(Fig. 5.7A)** and a more intense decrease in the ladder's upward **(Fig. 5.7B)** and downward conditions **(Fig. 5.7C)** that could be improved by both, apyrase and minocycline. Statistical analysis by means of a two-way RM ANOVA revealed only a significant main effects for the ladders' downward condition ($F_{2,50} = 4.325$; $P = 0.024$) with further post-hoc comparisons indicating that the performance decrease was significant in the first post-surgery week after vehicle treatment compared to pre-surgery ($P = 0.004$) as well as compared to apyrase ($P = 0.002$) and minocycline ($P = 0.013$). The apparent performance decrease in the ladder's upward condition after vehicle treatment compared to apyrase and minocycline in the first post-surgery reached statistical significance when applying a one-way ANOVA. This analysis revealed a significant main effect between the treatment groups ($F_{2,25} = 6.224$; $P = 0.006$) within the first post-surgery week with post-hoc comparisons revealing a significantly improved performance after apyrase ($P = 0.010$) and minocycline treatment ($P = 0.020$) compared to vehicle.

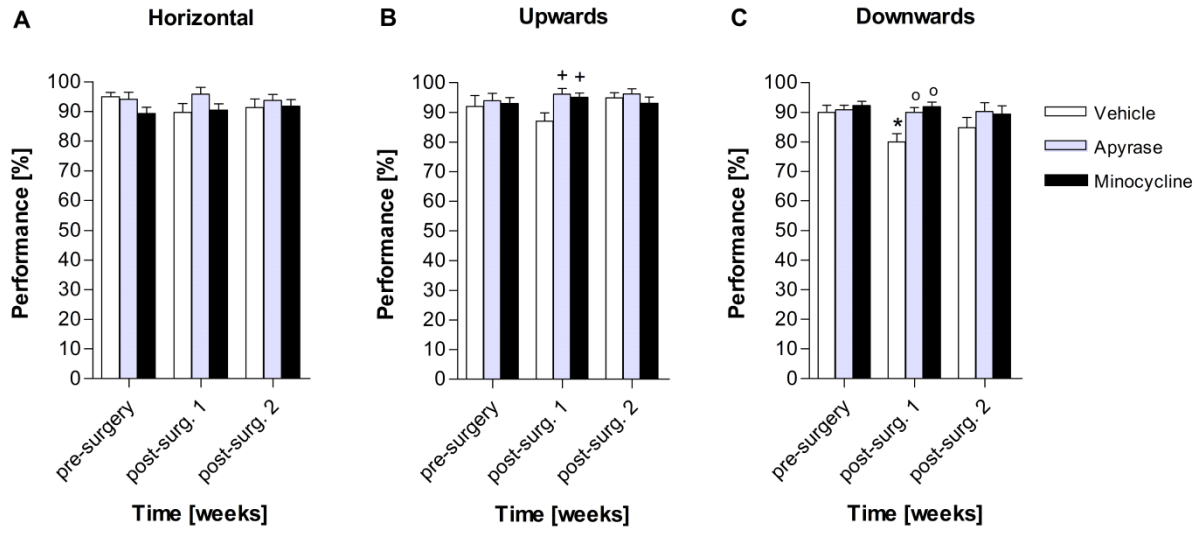

Fig. 5.7. Ladder rung walking task. Analysis of the rats' skilled walking ability on the rung ladder in horizontal **(A)**, upward **(B)** and downward **(C)** conditions on the day before and once weekly for two weeks after the implantation of a cannula (n=28)**.** Data are means +S.E.M. The *asterisk* denotes a significant difference (Tukey's t-test; $P < 0.05$) between pre- and post-surgery tests using a two-way RM ANOVA. *Circles* denote a significant difference on a certain test day compared to vehicle. The *plus* symbolises a significant difference (Tukey's t-test; $P < 0.05$) on a certain test day compared to vehicle using a one-way ANOVA.

5.4.2 Histology

The microscopic examination of the Nissl-stained sections revealed that all implantation sites were located within the CFA. Some of the implantation sites were tattered after cannula removal and hence had to be excluded from further histological analysis. Six weeks post-surgery more brains with well preserved implantation sites and intact glial sheath were obtained compared to two weeks post-surgery obviously due to a stronger and more compact cellular sheath around the cannula that was less easily damaged at this time point. Data analysis for histological examination included 2-3 sections from 4-7 rats per treatment group and per time point.

5.4.2.1 Neuronal distribution

The distribution of neurons in the CFA around the cannula was assessed by immunostaining for NeuN, a nuclear antigen found in neurons. As control tissue served the CFA contralateral to the implantation site of the vehicle-treated animals. Two as well as six weeks after the implantation of the cannula a reduction in neuronal nuclei within a region of 50 µm from the implant was observed after vehicle treatment. Apyrase as well as minocycline was able to increase the number of neurons within this distance. Statistical analysis revealed a significant main effect of distance to the implantation site ($F_{5,80} = 5.569$; $P < 0.001$) and of the interaction drug x distance ($F_{15,80} = 2.964$; $P < 0.001$) for the number of neurons within the 2-week group **(Fig. 5.8A)**. Further post-hoc comparisons indicated a significant reduction in the average number of neurons in the first 50 µm around the implantation site after vehicle treatment compared to all further intervals up to 300 µm ($P < 0.001$) as well as compared to the contralateral control hemisphere ($P < 0.001$). The average number of neurons within the first 50 µm was significantly increased with apyrase ($P = 0.015$) as well as with minocycline ($P = 0.015$) compared to vehicle. For the 6-week animals **(Fig. 5.8B)** no significant main effect was revealed with the two-way RM ANOVA. Since the first interval still implies an enduring loss of neurons in the vehicle group after six weeks a one-way ANOVA was applied that revealed a significant main effect of drug treatment within these first 50 µm ($F_{3,18} = 5.343$; $P = 0.008$). Post-hoc comparisons indicated an enduring significant reduction in the average number of neurons after vehicle treatment compared to the control tissue ($P = 0.021$). Moreover, apyrase was able to significantly increase the number of neurons within this distance ($P = 0.008$), with minocycline also indicating a trend towards an increase ($P = 0.097$).

The average number of neurons contralateral to the implantation site was about the same two and six weeks post-surgery.

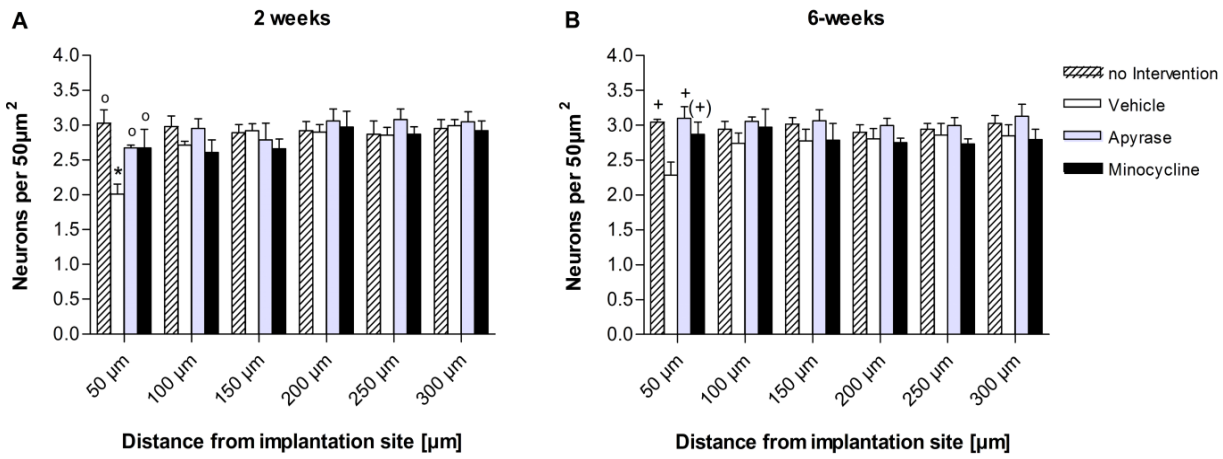

Fig. 5.8. Average number of NeuN$^+$ nuclei. Quantification of the average number of neuronal nuclei, as a function of distance from the implantation site, is shown two (n = 14) **(A)** and six weeks (n = 17) post-surgery **(B)**. Data are means +S.E.M. The *asterisks* denotes a significant difference (Tukey's t-test; $P < 0.05$) between the first interval of 50 µm and an interval further away (up to 300 µm) of a certain treatment. *Circles* denote a significant difference within a certain interval compared to vehicle. The *plus* symbolises a significant difference (Tukey's t-test; $P < 0.05$) on a certain test day compared to vehicle using a one-way ANOVA. *Brackets* () indicate a trend of significance (Tukey's t-test; $P<0.1$).

5.4.2.2 Microglial/Macrophagial distribution

The distribution of microglia/macrophages in the CFA around the cannula was assessed by immunostaining for IBA-1, an antigen that is specifically expressed in resting and activated microglia and macrophages, and is up-regulated upon activation during inflammation. Two as well as six weeks after cannula implantation, a strong increase in microglia/macrophages within the first 50 µm from the implant was observed independent of the treatment. Moreover, an overall increase in the number of microglia/macrophages two weeks compared to six weeks after the implantation was revealed as assessed by means of the control tissue. Apyrase as well as minocycline was able to decrease the total number of microglia/macrophages within the first 50 µm two weeks after the implantation, which remained consistently lower up to six weeks post-surgery for minocycline. Statistical analysis revealed a significant main effect of drug treatment ($F_{3,80} = 7.959$; $P = 0.002$) and distance

($F_{5,80}$ = 39.765; P < 0.001) as well as of their interaction ($F_{15,80}$ = 7.181; P < 0.001) for the microglia/macrophage distribution of the 2-week animals **(Fig. 5.9A)**. Further post-hoc comparisons indicated a significantly increased number of microglia/macrophages in the first 50 µm around the implantation site for all treatments ($P \leq 0.001$) when compared to all further distances as well as when compared to the control tissue. The interval of 50-100 µm comprised a significantly increased number of microglia/macrophages compared to 200-300 µm from the implantation site only after vehicle treatment (P < 0.001). The intervals of 50-100 µm and 150-200 µm also exhibited significantly increased numbers of microglia/macrophages compared to control tissue (P < 0.05) after vehicle treatment. Apyrase as well as minocycline was able to significantly diminish this increase in microglia/macrophages that was present after vehicle treatment within the first 50 µm (P < 0.05).

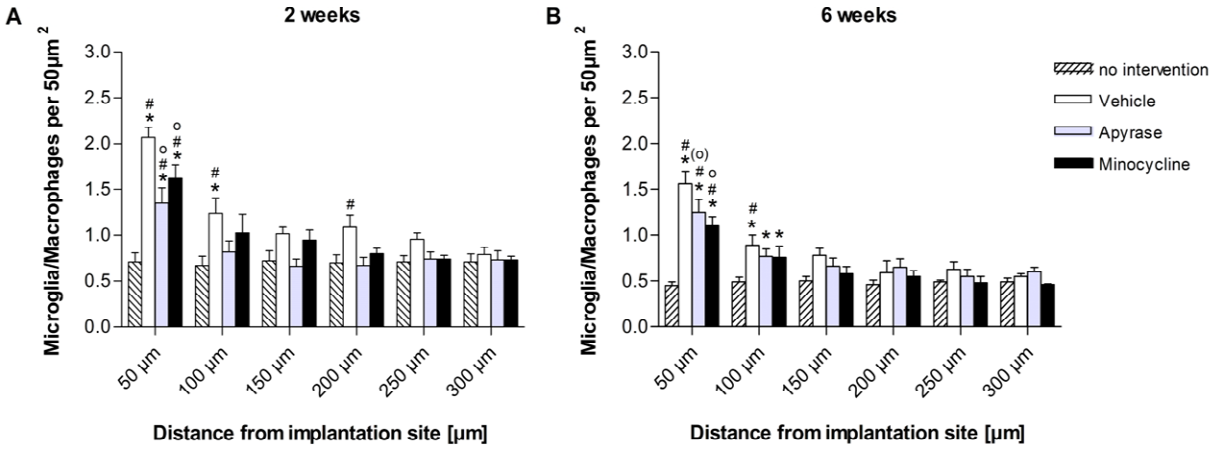

Fig. 5.9. Average number of IBA-1$^+$ cells. Quantification of the average number of microglia/ macrophages, as a function of distance from the implantation site, is shown two (n = 14) **(A)** and six weeks (n = 17) post-surgery **(B)**. Data are means +S.E.M. *Asterisks* denote a significant difference (Tukey's t-test; P < 0.05) between an interval close to the implantation site and any interval further away (up to 300 µm) of a certain treatment. *Circles* denote a significant difference within a certain interval compared to vehicle. A significant difference of any treatment compared to no intervention within a certain interval is indicated by a *rhomb*. *Brackets* () indicate a trend of significance (Tukey's t-test; P<0.1).

Six weeks after cannula implantation **(Fig. 5.9B)** a significant main effect of drug treatment ($F_{3,90}$ = 4.135; P = 0.021) and distance ($F_{5,90}$ = 64.886; P < 0.001) as well as of their interaction ($F_{15,90}$ = 9.112; P < 0.001) was observed. Post-hoc comparisons also revealed for this time

point a significant increase in the number of microglia/macrophages in the first 50 µm for all treatments ($P < 0.001$) when compared to all further distances as well as when compared to the control tissue. Within a distance of 50-100 µm the number of microglia/macrophages was also significantly increased for all treatments ($P < 0.05$) when compared to distances further away than 150 or 200 µm. The number of microglia/macrophages within 50-100 µm from the implantation site was again only significantly increased after vehicle treatment compared to the untreated hemisphere ($P = 0.018$). With minocycline the number of microglia/macrophages within the first 50 µm persisted to be significantly diminished compared to vehicle ($P = 0.006$) with a trend towards a significantly diminished number with apyrase compared to vehicle ($P = 0.061$). Moreover, there was a significant main effect of the time point of measurement evident in the control tissue ($F_{1,45} = 5.512$; $P < 0.043$) with an overall increase of microglia/macrophages two weeks compared to six weeks post-surgery.

5.4.2.3 Astroglial distribution

The distribution of astrocytes in the CFA was assessed by immunostaining for GFAP, an antigen that is expressed in the intermediate filaments of immature and mature resting or activated astrocytes, and is up-regulated upon activation during inflammation. Two as well as six weeks after cannula implantation, an increased astrocytic immunoreactivity around the implant was observed independent of the treatment with a further expansion of the scar tissue in all treatment groups two weeks post-surgery. Moreover, an overall GFAP-upregulation was observed two weeks compared to six weeks after the implantation as assessed by means of the control tissue. Statistical analysis revealed for the 2-week animals **(Fig. 5.10A)** a significant main effect of distance ($F_{9,144} = 490.832$; $P < 0.001$) as well as of the interaction drug treatment x distance ($F_{27144} = 65.870$; $P < 0.001$). Further post-hoc comparisons indicated for the first 100 µm, that cannula implantation increased astrocyte density significantly independent of the treatment when compared to the untreated control hemisphere ($P \leq 0.001$). Astrocyte levels were moreover significantly enhanced ($P < 0.05$) up to 300 µm from implantation site for vehicle, up to 250 µm for apyrase, and up to 200 µm for minocycline compared to distances further away (measured up to 500 µm). At distances further away than 300 µm for apyrase and further away than 350 µm for vehicle and minocycline astrocyte levels were significantly decreased compared to control tissue ($P < 0.05$). Within the first 50 µm minocycline was able to significantly decrease the GFAP up-

regulation around the cannula ($P < 0.001$). Statistical analysis of the 6-week animals **(Fig. 5.10B)** revealed a significant main effect of drug treatment ($F_{3,162} = 3.937$; $P = 0.025$) and distance ($F_{9,162} = 367.472$; $P < 0.001$) as well as of their interaction ($F_{27,162} = 39.187$; $P < 0.001$). Further post-hoc comparisons indicated for the first 50 µm, that cannula implantation increased astrocyte levels significantly independent of the treatment when compared to the control tissue ($P \leq 0.001$) and to distances further away ($P < 0.05$). At distances further away than 150 µm for minocycline and further away than 250 µm for vehicle and apyrase ($P < 0.05$; with a few exceptions for apyrase) astrocyte levels were significantly decreased compared to control tissue. Moreover, a significant main effect of the time point of measurement was evident in the control tissue ($F_{1,81} = 8.095$; $P = 0.019$) with an overall increase of astrocytes two weeks compared to six weeks post-surgery.

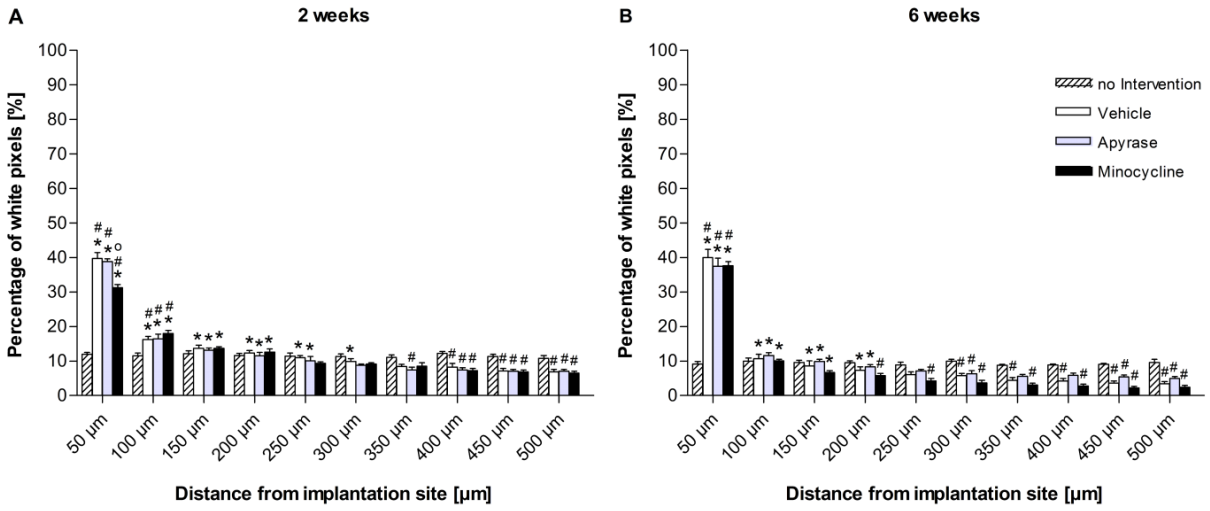

Fig. 5.10. Average distribution of GFAP$^+$ cells. Quantification of the average distribution of astrocytes, as a function of distance from the implantation site, is shown two ($n = 14$) **(A)** and six weeks ($n = 17$) post-surgery **(B).** Data are means +S.E.M. *Asterisks* denote a significant difference (Tukey's t-test; $P < 0.05$) between an interval close to the implantation site and any interval further away (up to 500 µm) of a certain treatment. A significant difference of any treatment compared to no intervention within a certain interval is indicated by a *rhomb*. *Circles* denote a significant difference within a certain interval compared to vehicle.

5.5 Discussion

The results of the present study demonstrate that the chronic implantation of a steel cannula into the CFA of M1 causes a foreign body response that involves glial scar formation and neuronal cell death, accompanied by a deterioration of skilled motor performance. Local apyrase and minocycline administration during cannula implantation improved the skilled motor performance, with minocycline being most effective. Moreover, both substances increased neuronal survival and reduced microglia/macrophage activation within the first 50 µm around the cannula two and six weeks after the implantation, with minocycline also reducing astrogliosis after two weeks.

Neuronal cell death around a chronically indwelling cannula is found frequently (Hayn and Koch, 2015) and is in line with other studies that revealed neuronal “die-back” zones around an implant (Biran et al., 2005;Potter et al., 2012). The decreased neuronal density within the first 50 µm around the implant in controls in this study is accompanied by the formation of a glial scar, which is suggested to occur faster than the re-growth of neuronal processes (Turner et al., 1999). Neuronal cell loss around an implant has not been found to such an extent in stab controls and has been suggested to be to a large degree associated with the foreign body response and the persistent inflammation at the interface(Biran et al., 2005;Winslow and Tresco, 2010;Potter et al., 2012).

The further expanded distribution of microglia/macrophages as well as astrocytes two weeks compared to six weeks post-implantation supports the notion of a more diffuse, loosely organised scar tissue around the implant in the acute phase of the immune response that becomes tighter and more compact in the chronic phase. Previous studies at similar time points (Turner et al., 1999;Szarowski et al., 2003;Potter et al., 2012) underline this assumption which is further buttressed by our finding that more implantation sites were tattered after cannula removal at two weeks compared to six weeks. Turner et al. (1999) also found the cellular structure of the scar tissue better preserved six weeks post-implantation compared to earlier time points at which the scar tissue was often disturbed after probe removal and filled the space that was previously occupied by the probe. The reduction in astrocyte density in distances further away from the implantation site suggests, that astrocyte communication is far-reaching and that even far away cells are activated and migrate towards the implant to help separate the healthy tissue from the inflammatory processes around the implant.

The results of the behavioural tests revealed remarkable impairments in skilled motor performance after cannula implantation in controls. Deficits were most pronounced in the skilled reaching task, which indicates a higher sensitivity of this task to damages of the CFA compared to the rung ladder task. Performance in the skilled reaching boxes was decreased at all time points after vehicle treatment with the subelement *advance* being most sensitive. Since the CFA has been shown to be largely responsible for elbow and shoulder movement and only partly for wrist movement without being involved in digit coordination (Neafsey and Sievert, 1982;Neafsey et al., 1986) our findings are well-founded and further supported by a recent microstimulation study (Brown and Teskey, 2014) and unpublished preliminary inactivation experiments in our lab. The impairment of the subelement *pronate* may indicate changes in cortical movement representation towards an increase in wrist representation in the CFA (Kleim et al., 1998) that goes back to skill acquisition during training (Nudo et al., 1997). An expansion of this area into the coordinates of cannula implantation may be responsible for the impairments in this subelement.

Impairments in the ladder rung walking task were most severe in the ladders' diagonal conditions which appeared more challenging than the horizontal condition. The diagonal condition, introduced by Antonow-Schlorke et al. (2013), increased the demands and the sensitivity of the task. Upward walking was suggested to impose a need for a higher level of motor performance than horizontal walking, due to a higher load on the forelimbs for maintaining balance and grip. Impairments in forelimb use during downward walking even exceeded those discovered for horizontal and upward walking which underlines the demands of downward locomotion. The results of the present study also demonstrates the ladders' downward condition to be most sensitive to impairments of the CFA, followed directly by the upward condition, with only slight impairments in the horizontal condition.

The general locomotor behaviour of the rats as assessed in the open field revealed not to be sensitive to the fine-tuned motor impairments. In contrast to long-term impairments in the skilled reaching or walking tasks following motor system lesions (Metz and Whishaw, 2002;Whishaw and Metz, 2002;Alaverdashvili and Whishaw, 2010), complete movement recovery within one week has been observed when walking on a flat surface even after severe insults (Muir and Whishaw, 1999;Norrie et al., 2005). The difficulties in skilled compared to unskilled motor performance have been suggested to be related to

differences in motor control, with locomotion on a smooth horizontal surface being adequately achieved by subcortical motor systems (Metz and Whishaw, 2002). Spontaneous and functional recovery due to daily exercise and locomotion in their home cages, may additionally cover potential deficits of the rats in the open field test, without rats' majorly benefitting from this general exercise in the skilled motor performance tasks, since specific motor skill training seems to be mandatory for skill recovery (Maldonado et al., 2008;Nudo, 2013).

Apyrase and minocycline have both proven beneficial in amending behavioural deficits after cannula implantation, with minocycline being more effective than apyrase especially in the skilled reaching task. Likewise, immunohistochemistry revealed increased neuronal survival together with reduced microglia/macrophage activation around the cannula with apyrase and minocycline, with the latter one also reducing the astrocytic scar tissue two weeks post-implantation. Davalos et al. (2005) suggested the extracellular ATP released by damaged cells and surrounding astrocytes to be primarily involved in microglial branch dynamics and their migration towards the site of injury. This is in line with the results of the present study that demonstrates a reduction of microglia/macrophages within the first 50 µm around the implant after apyrase treatment. Apyrase has also previously been shown to decrease the level of microglial cytokine secretion (Verderio and Matteoli, 2001;Bianco et al., 2005). The increased number of neurons around the implantation site after lowering extracellular ATP concentrations with apyrase indicates that the inhibition of microglia/macrophage activation that is accompanied by a reduction of released neurotoxic and pro-inflammatory molecules, moreover, supports the neuronal survival. This effect was suggested to be additionally accompanied by an increased release of neurotrophic factors that promote neuronal growth and survival at lower ATP concentrations (Inoue, 2002;Polikov et al., 2005;Hanisch and Kettenmann, 2007). Astrocytic glutamate release has also been shown to further contribute to neuronal death under pathological conditions, but could be antagonised by P2 receptor blockade (Jeremic et al., 2001). Hydrolysing ATP by means of apyrase may have contributed to neuronal survival in a similar way. The ATP metabolites ADP, AMP and adenosine have been reported to be less potent in microglia activation and to require priming with ATP (Chakfe et al., 2002;Farber and Kettenmann, 2006), although some potential has also been demonstrated for ADP itself (Davalos et al.,

2005). Likewise, nitric oxide (NO) has been shown to be insufficient as a chemoattractant to microglia without extracellular ATP (Dibaj et al., 2010). The density of astrocytes around the implantation site was not significantly decreased at any time point after cannula implantation with apyrase compared to vehicle. Although, apyrase was demonstrated to inhibit the ATP-mediated Ca^{2+}-wave propagation (Davalos et al., 2005), a wide range of different types of molecules has been suggested to trigger reactive astrogliosis and also involves astrocyte proliferation (Sofroniew, 2009).

It is to be emphasised that astrogliosis is not primarily harmful, but also exerts numerous beneficial functions that improve the outcome after implantation of a foreign body. Astrocytes are essential in wound closure and BBB repair, in the restriction of CNS inflammation, and hence, in neuronal protection by forming functional barriers to separate the healthy tissue from the enduring inflammation at the interface. Experimental disruption of astrogliosis has been shown to be associated with a spread of neurotoxic inflammation and increased lesion sizes (Sofroniew, 2015). The initial activation and migration of microglial cells is also to some extent partly beneficial by clearing cellular debris and excess fluid. However, their long-term response is largely adverse due to the enduring inflammatory events at the implant interface that result in neuronal damage and “die-back” zones, preventing neurons to be recorded or stimulated (Polikov et al., 2005;McConnell et al., 2009;Marin and Fernandez, 2010). Hence, it is important to only reduce the glial cell activation to a minimum, with the focus on the microglial cells.

Minocycline was even more effective than apyrase and did not only improve the skilled motor performance more efficiently after cannula implantation, but additionally reduced astrogliosis in the acute phase. Although exhibiting similar levels of surviving neurons around the implant as well as of microglia/macrophages, minocycline seems to be more effective than apyrase in preserving neuronal vitality and networks according to the behavioural data, which probably arises from its much broader range of anti-inflammatory, anti-apoptotic and glutamate-antagonist properties (Elewa et al., 2006). In a previous study of Rennaker et al. (2007) minocycline was administered via the drinking water and resulted in reduced astrogliosis around a chronic multi-channel microwire compared to controls especially in the first week post-surgery, with only minor differences between the groups four weeks post-surgery. The reduction in astrogliosis was accompanied by improvements in

quality and longevity of neural recordings from the interfaces at both time points. In the present study, local minocycline application also resulted in a reduction of astrogliosis two weeks post-surgery with only a minor effect being maintained at six weeks. Moreover, the reduced microglia/macrophage activation and the enhanced neuronal distribution in implant vicinity in this study as well as of the improved behavioural outcome underline the neuroprotective and anti-inflammatory characteristics of minocycline. Several previous studies also suggested minocycline to be not only neuroprotective, but also to be neurorestorative, via the inhibition of inducible NO-synthase (Yrjanheikki et al., 1998;Yrjanheikki et al., 1999;Hewlett and Corbett, 2006), the reduction of pro-inflammatory molecules such as TNFα, IL-1β or NO and the increase of anti-inflammatory molecules such as TGF-β or IL-10 (Yang et al., 2015b), as well as via a decrease of glutamatergic neurotoxicity by inhibiting the NMDA-induced activation of p38 MAPK in microglial cells, which subsequently inhibits the microglial activation and provides neuroprotection (Tikka and Koistinaho, 2001;Tikka et al., 2001). Moreover, minocycline ameliorates BBB integrity and reduces edema following hemorrhage (Wasserman and Schlichter, 2007;Yang et al., 2015a;Yang et al., 2015b). Besides being neuroprotective in stroke minocycline has also been suggested to be an effective therapeutic in traumatic brain injury (Sanchez Mejia et al., 2001), spinal cord injury (Wells et al., 2003), amyotrophic lateral sclerosis (Zhu et al., 2002), Huntington disease (Bonelli et al., 2004), Parkinson disease (Du et al., 2001) and Alzheimer's disease (Ryu et al., 2004) and its neuroprotective and anti-inflammatory potentials are further supported by the present study, which suggests it as an effective therapeutic in the suppression of the foreign body response.

In conclusion, our results suggest that reducing the microglial response to a minimum and thereby the degree of pro-inflammatory and neurotoxic molecules seems to be an effective approach to increase the neuronal survival in the vicinity of an implant. Apyrase and minocycline were shown to have neuroprotective and anti-inflammatory potential by improving the neuronal survival and skilled motor performance accompanied by a reduction of the inflammatory response mediated by microglia/macrophages. Minocycline was however considerably more effective than apyrase in improving the behavioural performance after cannula implantation into the CFA and, moreover, reduced the astrogliosis in the acute phase. The local application of minocycline proved sufficiently

beneficial to suggest it as a promising therapeutic candidate in the acute phase of chronic foreign body implantation without any need for systemic applications. Further studies on the efficacy of minocycline-coated electrodes will be however needed to evaluate the biocompatibility and long-term recording quality.

6 General discussion

For the widespread clinical application of BCIs it is of particular interest to understand and control the foreign body response of the brain to chronically indwelling devices. Since a few patients with long-standing tetraplegia have already successfully been implanted with neural interface systems, an initial proof of concept is provided that recording of neuronal spiking activity enables the execution of complex tasks such as controlling a robotic arm. However, the foreign body response that involves glial scar formation and neuronal cell loss continues to represent a major obstacle that disturbs neuronal signal acquisition and causes signal loss over time. A reliable extraction of movement commands needs to be achieved to verify a consistent functional outcome and to obtain the highest possible benefit from these systems. Cannula implantation and local substance application during the implantation procedure of a cannula in this work aimed to mimic the local drug delivery from coated electrodes and served as a proof-of-principle investigation for different pharmacological approaches.

6.1 Implications after foreign body implantation into the CFA

In order to investigate behavioural differences caused by the foreign body response after cannula implantation into the CFA, the skilled reaching task, that has evolved into a model system to analyse the functionality of the motor cortex, has also proven instrumental during this work. Impairments in the skilled reaching movement after cannula implantation could be measured by means of an elaborated movement scoring system (Alaverdashvili et al., 2008) and assigned to specific subelements. A preceding reversible inactivation study allowed for an easier discrimination of behavioural deficits in the follow-up experiments.

6.1.1 Behavioural deficits after reversible inactivation of the CFA by muscimol

The reversible inactivation study by means of the $GABA_A$ agonist muscimol permitted the examination of acute deficits in the skilled reaching task and the precise function of the CFA in rats. Since permanent tissue inactivation possibly entails potential functional compensatory mechanisms by adjacent brain areas or compensatory strategies by the animal itself, this makes it more difficult to evaluate the results in chronic settings. In reversible inactivation no recovery of function can take place since the inactivation only lasts

for limited time, which allows the examination of the true function of the inactivated tissue (Lomber, 1999). Moreover, reversible inactivation has the advantage that the animals' behaviour can be examined immediately after injection and the same animal can be repeatedly tested with and without functional inactivation during multiple experimental sessions. This enables within-subject designs that exclude any possible side-effects of the surgery, since the guide cannula is implanted above the actual area that is examined and animals are trained post-surgically until they re-establish their pre-surgical baseline level (Martin and Ghez, 1999;Majchrzak and Di Scala, 2000;Jarrard, 2002;Arikan et al., 2002). Muscimol is a potent agonist for the $GABA_A$ receptor and also a weak agonist for the $GABA_B$ receptor and a partial agonist at the $GABA_C$ receptor as well as a specific neuronal and glial GABA uptake inhibitor (Martin and Ghez, 1999;Chebib and Johnston, 1999;Krogsgaard-Larsen et al., 2000). In this work, muscimol could be precisely injected into the CFA by means of a chronically implanted guide cannula that was located 2 mm above the intended injection site. Substance administration after recovery and re-training was enabled by means of an injection cannula that was connected to a microliter syringe via an injection tube **(Fig. 3.2)**. Since the $GABA_A$ receptor has a ubiquitous distribution throughout the CNS, muscimol administration causes neuronal hyperpolarisation of the respective area (Beaumont et al., 1978;Goetz et al., 2007;Jacob et al., 2008). In contrast to GABA, the effects of muscimol persist much longer for up to 12-24 h, with a maximal effect within the first hour following injection (Martin and Ghez, 1999;Arikan et al., 2002).

In this work, muscimol was used in a dose of 0.5 µg/0.3 µl and 1.0 µg/0.3 µl to temporarily inactivate this region, with PBS as the control. Deficits in the reaching movements 45 min after local muscimol application were much more pronounced compared to the chronic injection cannula implantation in the follow-up experiments, in which the foreign body response was evaluated. According to a one-way RM ANOVA ($F_{3,39}$=18.239; P<0.001), there was a significant effect in the hit-reach-ratio between the different treatments with post-hoc Tukey's t-test revealing the hit-reach-ratio to be significantly reduced (P<0.001) in both muscimol-treated groups compared to pre-surgery as well as compared to PBS application (pre-surgery: 76.90% ± 1.71%; PBS: 76.25% ± 2.61%; low dose of muscimol: 53.86% ± 4.41%; high dose of muscimol: 53.59% ± 4.02%; *n* = 10). Deficits in the reaching behaviour after muscimol application were strongly exposed, with individual animals even being unable to lift their paws to reach for the pellet during their first trials and

instead turning around in the box to check for the reward pellet in the back that was however omitted after unsuccessful attempts. Some animals also tried instead to reach for the pellet with the unaffected paw without hitting the pellet that was thus located in the ipsilateral indentation or tried to lick the pellet from the shelf without being able to reach it **(Fig. 6.1A, B)**. After several complete fails, rats usually continued to exhibit strong impairments in advancing the paw towards the pellet as well as in paw pronating and accordingly dropped the paw instead in an uncoordinated manner on the shelf **(Fig. 6.1C, D)**. In case they hit the pellet, they showed further difficulties to lift the paw with the pellet from the shelf and the paw dropped from the shelf onto the floor of the box during retraction **(Fig. 6.1E, F)**. Moreover, during pellet release they often used the second paw to support paw lifting and to direct the paw towards the mouth with the head turning towards the paw with the pellet in order to release it into the mouth **(Fig. 6.1G, H)**.

This reversible inactivation study in the initial phase of this work confirmed the appropriateness of the coordinates chosen according to more previous stimulation and tracer studies (Neafsey and Sievert, 1982;Neafsey et al., 1986;Hyland, 1998;Colechio and Alloway, 2009) that either differentiate only between the RFA and CFA without further assigning concrete functions to these areas or only roughly assign functions to both areas without a clear functional and topographical dissociation of the RFA as a grasping area and the CFA as a reaching area (Brown and Teskey, 2014). Acute deficits in the reaching movement after reversible inactivation were revealed in a much more exposed manner than in the chronic settings of the follow-up experiments. On the one hand this was due to the unmasking characteristics of this reversible inactivation technique, but on the other hand muscimol diffusion was certainly more widespread compared to the tissue loss caused by chronic implantation of the injection cannula. Nevertheless, due to the preceding inactivation study, deficits in the follow-up experiments were yet easier to identify.

Acute deficits in forelimb movement also resulted in locomotor impairments in the open field with a significant effect on the distance travelled [m] between the treatment groups according to a one-way RM ANOVA ($F_{3,39}$=18.239; P<0.001). Post-hoc Tukey's t-test revealed a significant decrease of the total distance travelled (P<0.001) for both muscimol-treated groups compared to pre-surgery as well as compared to PBS application (pre-surgery: 218.66 m ± 16.44 m; PBS: 215.44 m ± 12.48 m; low dose of muscimol: 130.32 m ± 13.14 m; high dose of muscimol: 127.27 m ± 18.13 m).

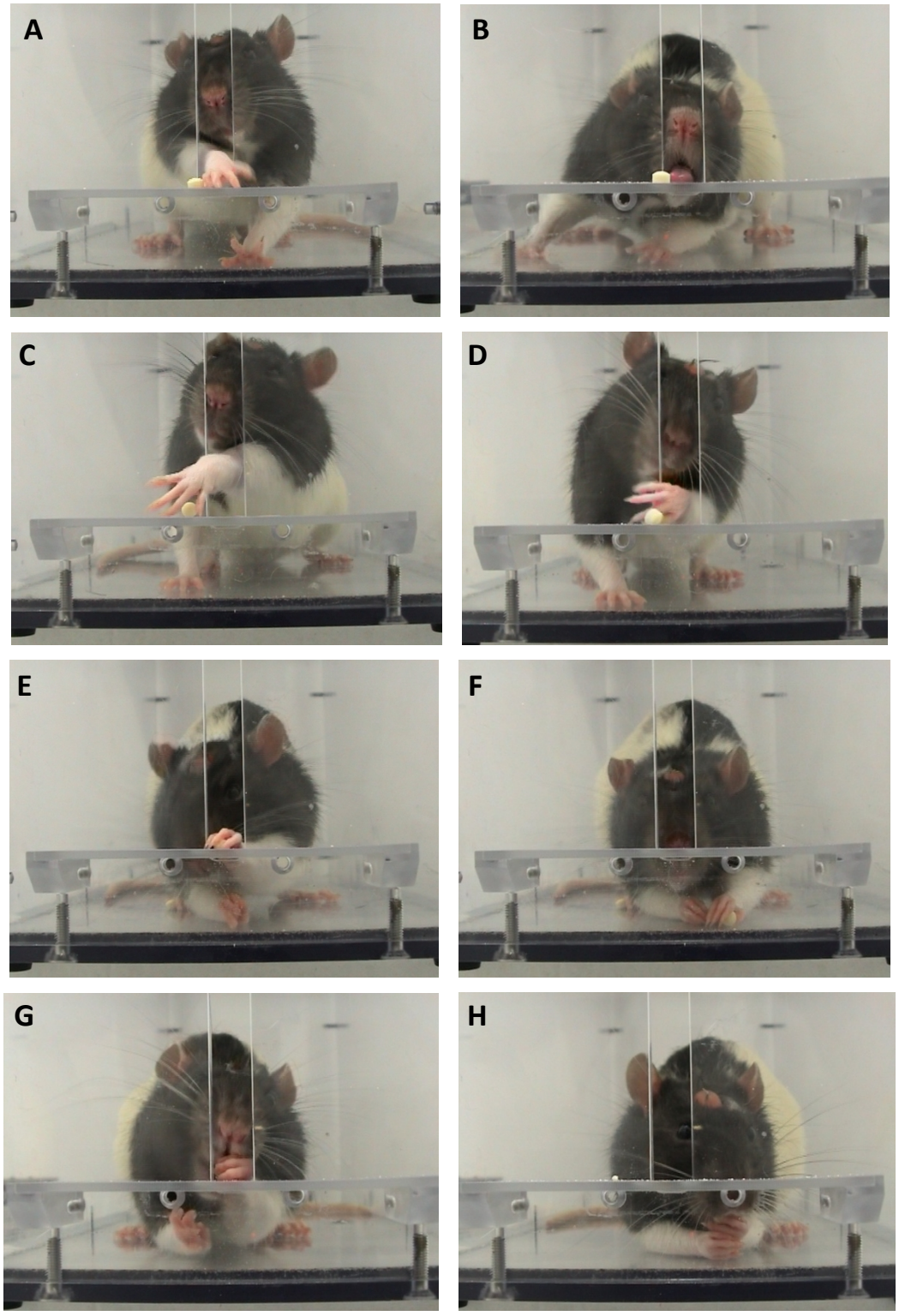

Fig. 6.1. Behavioural deficits in the skilled reaching task after reversible inactivation of the CFA. Reversible inactivation of the CFA caused deficits such as: the change of the preferred paw and the use of the unaffected paw instead, or rats trying to lick the pellet from the shelf **(A, B)**; strong impairments in advancing the paw towards the pellet as well as in paw pronation **(C, D)**; difficulties to lift the paw with the pellet from the shelf with the paw dropping from the shelf during retraction **(E, F)**; support by the second paw during pellet release with the head turning towards the paw in order to release the pellet into the mouth **(G, H)**.

Since animals demonstrated strong impairments in the use of the forepaw contralateral to the inactivated CFA in the reaching box, deficits in the total distance travelled were accordingly, expected, because the animals had no opportunity to cope with their deficits or to rely on secondary circuits or on compensatory strategies. It has been suggested that many cortical or subcortical lesions result only in minor or transitory deficits in forelimb or hindlimb locomotor performance with total recovery within a few days after surgery (Muir and Whishaw, 1999;Metz and Whishaw, 2002). Since rats were tested with muscimol within the first hour after inactivation, a reduction in locomotion is in line with this assumption. Moreover, it has been suggested that forebrain motor circuits are not necessarily required for locomotion on a horizontal surface, which can be adequately achieved by subcortical motor systems. Only more complex tasks that are sufficiently challenging and require forebrain control reveal subtle chronic impairments in forelimb and hindlimb use (Metz and Whishaw, 2002). Likewise, corticospinal-lesioned animals show only transient locomotor deficits 24-48 h after lesioning and exhibit complete recovery after this time suggesting that the corticospinal tract does not play an essential role in normal overground locomotion in the open field. Transient changes in gait and locomotion were suggested to be the result of temporary general locomotor compensations after unilateral CNS injury in quadrupeds that quickly recover thereafter (Muir and Whishaw, 1999).

The ladder rung walking task had not been introduced before the follow-up experiments started and the animals were accordingly not tested in this paradigm after muscimol administration.

6.1.2 Behavioural deficits after foreign body implantation

Behavioural deficits after guide cannula implantation in order to examine the foreign body response were less exposed than after muscimol application. However, the hit-reach-ratio continued to be significantly reduced during the course of the 6-week test period with no significant recovery. The most impaired subelement was the advancing of the paw through the slot towards the pellet with the animals often advancing not far enough to reach the pellet or sweeping the pellet off the shelf when touching it only with the tips of the digits. The recent inactivation study of Brown and Teskey (2014) confirmed that the coordinates used during this work are primarily involved in paw advancing. They assigned grasping and digit flexion representations to the RFA and forelimb elevation, advance and retraction to

the CFA. They were first assigning a clear functional and topographical dissociation of the RFA as the grasping area and the CFA as the reaching area. Deficits in paw pronation and pellet release were less exposed than advancing of the paw. The more previous microstimulation mapping study of Neafsey and Sievert (1986) specifically assigned pronation and supination movements also to the CFA, with the associated regions being slightly more caudally located within the CFA and the region for supination also more laterally. Deficits in paw pronation were also more exposed than in paw supination in the preceding inactivation study. This suggests a closer association of the area responsible for paw pronation to the area responsible for advancing compared to the area responsible for paw supination. According to Brown and Teskey (2014), the area topographically bordering laterally and caudally on the area responsible for advancing within the CFA is responsible for elbow flexion. The coordinates used in this work for cannula implantation slightly overlap with this area, since the injection cannula had a diameter of 0.4 mm that was additionally surrounded by an area of neuronal cell loss and glial scar formation that extended even further into the surrounding tissue. The slight impairments in pellet release may go back to the deficits in elbow flexion. Disrupted interconnections and dissection of the projections of surrounding neuronal networks bordering on the area responsible for paw advancing probably also contribute to the impairments in additional subelements. Paw elevation was however only impaired after muscimol application and not during injection cannula implantation, which further supports the assumption of a more widespread diffusion of muscimol. According to Brown and Teskey (2014), movement representation for paw elevation is also located within a small area located medially/caudally to the representation of elbow flexion. It is difficult to compare the impairments in reaching in this work with those of other inactivation studies, since motor cortical lesions in other studies generally extend much further into the surrounding tissue and include most parts of the motor cortex with both forelimb areas as well as the hindlimb area. For example, in the study of Alaverdashvili and Whishaw (2010) the skull was removed from 1 mm posterior to 4 mm anterior to bregma and 1-4 mm lateral to the midline to induce motor cortical stroke by means of devascularisation. Also, Whishaw et al. (2004) impacted the brain with a 3 mm and a 5 mm diameter piston to produce cortical contusion injuries. Hence, impairments in their work are usually more pronounced and include a much broader spectrum of impaired

subelements, additionally involving e.g. the subelements supination I/II, which could not be identified as significantly impaired in this work.

The skilled reaching task proved to be more sensitive to cannula implantation in the CFA than the ladder rung walking task. The results of the ladder rung walking task demonstrated that the skilled walking performance strongly depended on the walking direction along the ladder. Walking along an inclined rung ladder turned out to be more difficult for the rats and to be more sensitive to motor cortical disturbances than walking along a horizontal ladder. Motor impairments in forelimb use after cannula implantation were reflected by a reduction in the average score in the walking performance. After cannula implantation, rats more often placed the impaired paw on the rung with only the wrist or the digits, repositioned the paw or replaced it, slipped off the rung or also totally missed it. Average scores, however, revealed only a decline in the first post-surgery week and had recovered by the second post-surgery week, which is why this test was only applied to the 2-week groups. In the skilled reaching task, rats had particularly impairments in advancing the paw, which involves forward displacement of the elbow and shoulder as well as wrist extension and hand opening. Since upward and downward walking was more demanding and accordingly more impaired than horizontal walking, the impairments in advancing may also account for the increase in errors in the performance in the first post-surgery week. Since step sizes still varied in a normal range without demanding the rat to especially stretch its legs to reach the subsequent rung performance had already recovered by the second week. In a motor cortical lesion study of Antonow-Schlorke et al. (2013), deficits are more exposed than in this work which is obviously again a result of the much broader cortical photothrombotic lesion size. They applied light transmission within a rectangular area limited by the coordinates −2.5 mm to +4.52 mm anteroposterior and +0.5 mm to +4.5 mm mediolateral from bregma which hence included again both forelimb areas as well as the hindlimb area. Although deficits are more exposed in their study and include forelimb as well as hindlimb use, only the contralateral side is impaired without any significant effect on the ipsilateral side. In line with this are the results of a study of Whishaw and Metz (2002) that suggested the ipsilateral portion of the corticospinal tract to make no contribution to skilled movements of the kind made by the contralateral portion of the corticospinal tract, which further supports the assumption that deficits are particularly present in the contralateral side, since only 5% of corticospinal projections do not cross and descend on the ipsilateral

side into the spinal cord. Moreover, the results from the lesion study of Antonow-Schlorke et al. (2013) further demonstrated that contralateral forepaw use is more impaired during upward and downward walking than during horizontal walking, with downward walking exhibiting most errors. Interestingly, despite the larger lesion size in their study deficits are also only present at post-ischemic day 7 and recover at day 28, which was the second test day in their study. This is in agreement with the smaller lesion size in this work and performance recovery within two weeks post-surgery.

Performance in the open field did not reveal any significant differences between pre- and post-surgical test days. The total distance travelled was often slightly reduced in the first post-surgery week, but increased again in the following weeks. Individual animals that did not like to be kept in the open field boxes showed an intense increase in the total distance travelled in later post-surgery weeks which increased the average as well as the error bars, but also seemed to be treatment-independent and to be caused by only a few outliers. As already suggested above, impairments in walking on a horizontal surface are only transient in nature with forebrain motor circuits not being required for locomotion on a horizontal surface. Accordingly, no significant reduction in the total distance travelled [m] could be revealed after one week of recovery or during the subsequent weekly test sessions.

Complete movement recovery within one week after motor cortical injury in unskilled motor tasks has not only been observed in this work, but also in other studies (Muir and Whishaw, 1999;Norrie et al., 2005). In contrast to this short-term recovery in unskilled motor tasks, long-term impairments have been demonstrated in skilled motor tasks, including skilled reaching as well as skilled walking (Metz and Whishaw, 2002;Whishaw and Metz, 2002;Alaverdashvili and Whishaw, 2010). The ability of skilled walking on the rung ladder had already recovered two weeks after cannula implantation. However, skilled reaching deficits persisted up to six weeks and had not recovered by the end of the test period. Hence, the time span of recovery apparently correlates with the complexity and the skill demands of the task. Spontaneous and functional recovery due to daily locomotion in the home cages only contributes to cover deficits of the rats' locomotion in the open field, without rats majorly benefitting from this general exercise in the skilled motor tasks. For skill recovery especially during skilled reaching, specific motor skill training seems to be mandatory.

The transfer of functional responsibility has been suggested to take about 4-8 weeks, with animals still comprising significant deficits when not undergoing daily rehabilitative training. The redistribution of cortical representation occurs by neuroanatomical changes such as local axonal sprouting, dendritic spine expansion and synaptogenesis in the regions surrounding the lesion. Neurite outgrowth occurs into intact motor areas surrounding the lesion. Moreover, remote cortical neurons that project to the lesion site contribute to a reassembly of cortical networks and functional recovery (Maldonado et al., 2008;Nudo, 2013). Since animals in this work did not undergo daily training, deficits in skilled reaching were still obvious six weeks after cannula implantation.

In contrast to true functional recovery, movement compensation is mediated by spontaneous recovery that also occurs without rehabilitative training. Young as well as aged rats have been demonstrated to preserve a remarkable ability to compensate for motor impairments due to the plastic properties of the brain. Although aged rats display a decline in motor ability and are more affected by brain injuries, plastic properties are preserved and aged rats display a similar recovery rate as young rats. Compensatory motor behaviour following injury to the motor cortical forelimb region is suggested to be mediated especially by the peri-lesional regions of the cortex (Alaverdashvili and Whishaw, 2010).

Movement compensation after cannula implantation into the CFA has particularly been observed in the first test session after cannula implantation in the skilled reaching task, during which the animals had to cope with their deficits for the first time. After several misses usually due to impairments in paw advancing, which became obvious from the high error scores within the first five trials of each session, they learned to cope with these deficits and compensated for them. This compensation is reflected by the hit-reach-ratio performance that was not as badly decreased as would have been expected after these first trials. Especially within the 6-week group, the error score within the first 5 trials in the subelement advance increased from 22.22% ± 4.94% pre-surgery to 66.67% ± 6.24% in post-surgery week one. However, the hit-reach-ratio only decreased from 81.35% ± 1.90% pre-surgery to 59.49% ± 2.29% in post-surgery week one, which indicates that rats quickly compensated their deficits to a large extent within the first test session. Six weeks post-surgery rats only exhibited an error rate in advancing of 42.22% ± 6.62% and a slight non-significant increase in the hit-reach-ratio performance to 66.82% ± 3.09%, which indicates that some functional recovery most probably occurred due to the weekly training sessions.

Although rehabilitative training seems to be essential for true functional recovery after an injury especially in skill requiring tasks, it has to be mentioned that early training may exacerbate brain damage and functional outcome after brain injury. Activity-induced increases in brain temperature and excitatory neurotransmitter release is suggested to further contribute to the loss of vulnerable tissue surrounding the site of injury (Humm et al., 1999;Risedal et al., 1999). This finding is in line with the assumption in this work that excessive glutamate release after cortical brain injury induces a cascade of glutamate-mediated excitotoxicity, which causes neuronal cell death of apoptotic and necrotic nature that accordingly exacerbates behavioural outcome. Accordingly, Humm et al. (1999) suggested neuronal tissue to be susceptible to the effects of intensive rehabilitation targeted at the impaired limb within a post-surgical time interval of two weeks.

6.1.3 Brain tissue response to foreign body implantation

The immunohistological investigation of the foreign body response suggests that deficits in the rats' behavioural performance after injection cannula implantation particularly correlate to the amount of neuronal cell loss around the implantation site. Neuronal cell loss around the implanted cannula was most significant after two weeks with about one third less neurons within the first 50 µm around the implant (data for control tissue response after cannula implantation are derived from the second study, since this group has been complemented by additional animals compared to the first study). By six weeks, cell loss within the first 50 µm was also significant, but was not exacerbated. Neuronal cell loss around chronic implants has been suggested to not solely result from the mechanical trauma of insertion, but rather from the chronic inflammation at the interface, since in stab controls no such loss was demonstrated (Biran et al., 2005;Winslow and Tresco, 2010;Potter et al., 2012). Although reductions in neurofilament were also observed in stab wounds in the study of Biran et al. (2005) at two weeks, the extent of reduction was much smaller compared to chronically indwelling devices. Since, in their study, the microglial activity inversely correlates to the neuronal cell loss, they concluded that the large amount of secondary cell death is microglial-induced. However, in this work, neuronal cell loss has not been observed to be exacerbated after six weeks compared to two weeks, which suggests that microglial cell activation particularly contributes to neuronal cell loss within the vulnerable phase within the first one to two weeks after implantation.

Since cannula implantation into the brain is accompanied by damage and loss of neurons in the implantation tract and by the disruption of blood vessels, the oxygen and energy supply of surrounding neurons gets impaired, which results in an ionic imbalance that is followed by sustained release of glutamate due to uncontrolled membrane depolarisation (Iadecola and Anrather, 2011;Bretón and Rodríguez, 2012). Glutamate is suggested to be released via numerous mechanisms after an injury and to induce a cascade of glutamate-mediated excitotoxicity that exacerbates neuronal cell loss and tissue damage (Lipton and Rosenberg, 1994;Lynch and Guttmann, 2002). The degree to which extent neurons die by apoptosis or necrosis depends on the severity of the insult and the amount of glutamate released (Bretón and Rodríguez, 2012), but presumably also on the number of microglial cells activated during this vulnerable phase. The increased vulnerability of neurons after cannula implantation presumably makes them unable to cope with the additional amount of neurotoxic substances released by the microglial cells, which accordingly further contributes to an exacerbation of the cascade of glutamate-mediated excitotoxicity.

In electrode implantation, it has been suggested that the survival of neurons within the first 50 µm surrounding the electrode is imperative for optimal device functioning (Buzsaki, 2004). The loss in signal strength has been suggested to be either a result of the formation of a neuronal kill zone around the implant or to be a result from slow neuronal regression from the electrode due to glial scar formation that pushes cell bodies away from the electrode site. The number of neurons within this work has been shown to be significantly reduced by about one third within the first 50 µm. This cell loss is most probably accountable for the inconsistent performance of electrode arrays in chronic applications that report a drop in the number of functional electrodes and recorded signals over time as summarised by Polikov et al. (2005). Recorded signals were reported to either grow in stability and to remain stable after a few weeks or to degenerate from high stability to nearly no signals with day-to-day changes over the first 1-2 weeks and week-to-week changes for 1-2 months (Liu et al., 1999;Nicolelis et al., 2003). This inconsistency in electrode performance has also been characterised at the cellular level with strong variability in gliosis and neuronal kill zones around electrodes with identical characteristics (Stensaas and Stensaas, 1976;Edell et al., 1992). During this work variances in neuronal kill zones and gliosis around the implantation site have also been observed. However, it has to be mentioned, that it is of particular importance to minimise disturbances during implant

removal since lateral movements of the implant or an inclination during removal causes most devastating variances and pushes neurons not only further away from the implantation site, but also causes enormous tattering of the scar tissue **(Fig. 6.2.A, B)**. Whether cannula removal was successful could be derived from the shape of the implantation site with oval or tattered sites being excluded from further analysis. Since more implantation sites were tattered two weeks compared to six weeks after implantation, this buttresses the assumption that the scar tissue is tighter and more compact after six weeks. A further point that most probably affects a homogenous tissue analysis and contributes to considerable variances in neuronal kill zones and gliosis around the implant is the dependence on blood vessels **(Fig. 6.2.C, D)**. Rupture of large blood vessels during the implantation procedure has been observed to cause a stronger neuronal loss and more pronounced gliosis compared to no haemorrhage during implantation. Brains, in which haemorrhage was evident during cannula implantation, were notated and were also excluded from histological analysis.

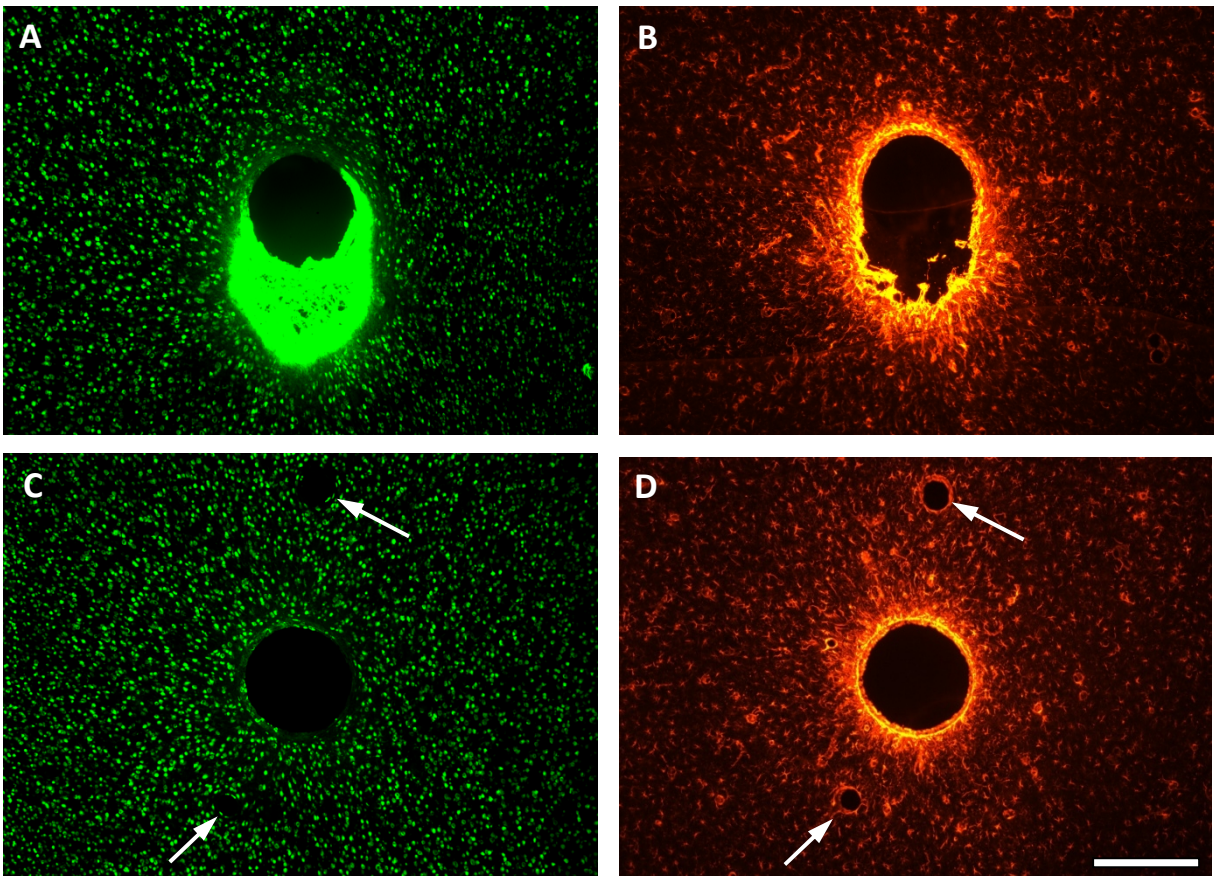

Fig. 6.2. Cannula implantation sites with factors affecting a homogeneous tissue analysis. Tattered implantation site due to lateral cannula movement or cannula inclination during removal **(A, B)**. Approved implantation site with two medium-sized blood vessels in the vicinity of the implantation tract as indicated by the arrows **(C, D)**. Neuronal nuclei are depicted in **(A, C)** and astrocytes in **(B, D).** Scale bar = 400 µm.

In the initial wound healing response reactive microglial cells and infiltrated macrophages exhibit a scattered distribution, followed by clustering in a reactive sheath around the implant after two weeks (Polikov et al., 2005). In this work, microglia/macrophage clustering was also observed after two weeks with an increased number of microglial cells up to 200 µm around the implantation site compared to control tissue. Six weeks after cannula implantation, microglial cells formed a tight cellular sheath around the implant and exhibited an increased number only within the first 100 µm. Additionally, microglia/macrophages were not only increased in the vicinity of the implant two as well as six weeks after cannula implantation, but also two weeks after implantation in the hemisphere contralateral to the implantation site. Glial cell up-regulation in the contralateral hemisphere was not only the case for the microglia/macrophages, but also for the astrocytes and has already been described previously (Marks et al., 2001) as well as in this work. The increase in glial cells was suggested to either result from far ranging signals of the glial cells (Marks et al., 2001), from functional changes due to interhemispheric connectivity (Lindenberg et al., 2012) or from enduring brain swelling (Loddick et al., 1998). Since the formation of the glial scar resulted in a tight cellular sheath around the cannula at six weeks, it became difficult to distinguish between the four different morphological phenotypes of microglial cells that have been introduced by Torres-Platas et al. (2014) and were suggested to be classified into ramified, primed, reactive and amoeboid cells according to their degree of activation. Cell bodies close to the implantation site were too closely packed and merged with the processes, which made it impossible to distinguish the different types. Nevertheless, it can be assumed that the largest degree of cells close to the implantation site had transformed into the amoeboid type that is fully “activated” and devoid of any processes, and that cells further away from the implantation site constitute the ramified morphology which are highly branched and correspond to the “resting” microglia. Cells in between can also transform into an intermediate phenotype that is either primed or reactive and can return to ramified or further transform to amoeboid. Persistent microglial activity at the interface between the implant and the brain tissue has also been described previously and is founded in the inability of microglial cells and infiltrated macrophages to phagocytose the insoluble foreign body (Polikov et al., 2005;Biran et al., 2005).

Cannula removal during this work revealed especially microglia/macrophages to adhere to the implant, but rarely astrocytes, which could be demonstrated by cannula immunostaining and subsequent microscopic investigations **(Fig. 6.3.A, B)**. Persistent microglia/macrophage activation at the implant surface of explanted microelectrodes has also been found by Biran et al. (2005). The rare amounts of $GFAP^+$ material found on the surface of retrieved electrodes by them were attached to the layer of microglia/macrophages rather than directly to the electrode surface. They also suggested the persistent up-regulation of microglia/macrophages around the implant to be associated with the chronic implantation of the foreign body, since in stab wounds only a temporary up-regulation was observed that had significantly declined by four weeks.

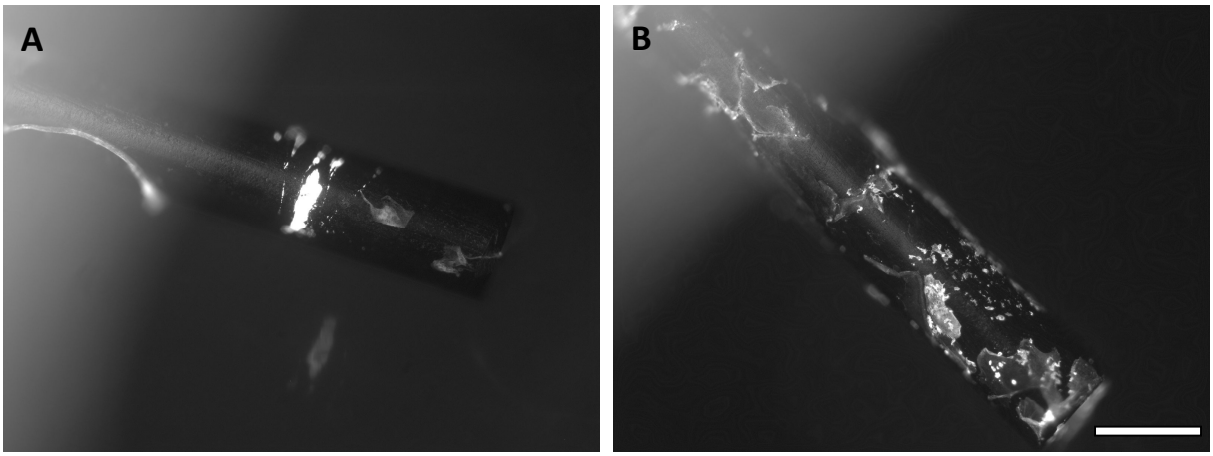

Fig. 6.3. Cannula immunostaining two weeks after implantation. Immunostaining revealed almost no GFAP reactivity (astrocytes) **(A)**, but persistent IBA1 reactivity (microglia/macrophages) at the implant surface of explanted cannulas **(B)**. Scale bar = 400 µm.

Since cannula implantation causes significant tissue injury and persistent microglia up-regulation, these cells are most probably transformed into the “classically activated” pro-inflammatory (type-1) microglia that release pro-inflammatory and neurotoxic molecules including excitatory amino acids, reactive oxygen and nitrogen intermediates, and diverse cytokines, including IL-1, IL-6 or TNFα (Kigerl et al., 2009). Due to their inability to phagocytose the insoluble foreign body they remain in this state of “frustrated phagocytosis” (Polikov et al., 2005;Biran et al., 2005). The enduring release of neurotoxic substances causes a self-perpetuating cycle of cell death due to further activation of microglial cells that release even more pro-inflammatory and neurotoxic substances (Block et al., 2007;Schwartz and Shechter, 2010). Hence, as a consequence, neuronal cell loss

around a chronically implanted foreign body is likely an interplay of the initial acute damage triggering a cascade of glutamate-mediated excitotoxicity and the persistently enhanced microglial activation around the implant.

The persistent release of pro-inflammatory substances by the microglial cells also induces astrocyte activation that separate the healthy neuronal tissue from the enduring inflammatory processes at the implant (Schwartz et al., 2006). In this work, astrocyte activation also extended furthest around the implantation site at two weeks after cannula implantation, with a significant increase within the first 100 µm compared to control tissue and within the first 300 µm compared to distances further away from the implantation site. After six weeks, this increase had reduced to the first 50 µm around the implantation site compared to control tissue and to the first 200 µm compared to distances further away from the implantation site. This supports the assumption that the glial scar gets more compact and forms a tight cellular sheath around the implant after six weeks. A reduction in astrocyte levels at distances further away than 350 µm at two weeks and further away than 250 µm at six weeks compared to control tissue suggests that astrocytes migrate to the site of injury. Since astrocyte levels are reduced up to 500 µm at two as well as six weeks compared to control levels and most probably even further away, the assumption of far reaching communication and activation of astrocytes can be herewith supported. This far reaching astrocyte communication has been suggested to be mediated via Ca^{2+}-wave propagation that largely depends on the extracellular release of ATP (Guthrie et al., 1999). Previous studies of Turner et al. (1999) and Szarowski et al. (2003) revealed reactive astrocyte regions that even extend 500-600 µm around the implant at two weeks and become also more compact thereafter, extending only 50-100 µm around the insertion site at six weeks and remaining constant at later time points.

The dense, organised sheath around the implant formed by the astrocytes, in order to separate the healthy tissue from the ongoing inflammatory processes around the implant, protects the surrounding neurons from the neurotoxic substances released by the microglia/macrophages, but also prevents re-growth of neuronal processes into the implantation site. Since the process of neuronal re-growth is suggested to be slower than sheath formation, surviving neurons are prevented to re-approach and contact the implant with the glial scar forming a high resistance barrier between the probe and the implant (Turner et al., 1999). However, the astroglial response, in contrast to the persistent

microglial response, has been suggested to exhibit primarily beneficial, protective function after ischemia-related injuries expressing high levels of neurotrophic factors and cytokines that help to repair and rebuild lost synapses, as well as the blood-brain barrier and to limit immune cell influx and neuronal death (Zamanian et al., 2012). Although shielding surrounding neurons from the implant, they are essential to remodel the extracellular space and to restrict the spread of inflammation into surrounding tissue serving as anti-inflammatory barrier (Sofroniew, 2015). Accordingly, it seems important that the glial scar is reduced to a minimum in a way that neurons are still protected from the ongoing inflammation at the implant. Preventing neuronal cell death and excitotoxic cascades around the implant in the acute phase after foreign body implantation was presumed in this work to also reduce the amount of glial cells activated.

6.2 Pharmacological influence on the foreign body response

In order to block the initial steps of the foreign body response and to promote neuronal survival in the vicinity of the implant, the excitotoxic and inflammatory cascades after device implantation were aimed to be suppressed at a very early stage. For this purpose, in a first approach the uncompetitive NMDA receptor antagonist memantine with a preference for extrasynaptically located NR2BRs was locally applied during cannula implantation in order to reduce the glutamate-induced excitotoxic cascade induced by the initial trauma. The second approach aimed to counteract the extent of glial cell activation by means of the ATP/ADP-hydrolysing enzyme apyrase in order to decrease the self-perpetuating cycle of microglial-induced secondary cell death. The third approach with minocycline combined both strategies due to its broad range of anti-inflammatory and anti-apoptotic properties. The local substance application during cannula implantation aimed to mimic the local drug delivery from coated electrodes, since the experiments in this thesis served as a proof-of-principle investigation mimicking the implantation of a device such as an electrode array into the cortex.

6.2.1 Memantine

In order to reduce the glutamate-induced excitotoxic cascade caused by the initial trauma of cannula implantation, the uncompetitive NMDA receptor antagonist memantine was locally applied during cannula implantation. Since extrasynaptically located NR2BRs are suggested

to be key in mediating excitotoxic cell death (Bonfoco et al., 1995), the preference of memantine for extrasynaptic over synaptic NMDA receptors together with its fast off-rate kinetics, sparing physiological functions at the synapse (Lipton et al., 2004;Lipton et al., 2006;Xia et al., 2010), makes it an ideal candidate for neuroprotection in the acute phase of brain injury as caused by device implantation.

The excessively increased glutamate concentrations for hours or even days in the acute phase after an injury to the CNS (Lipton, 2004), allow memantine to gain its full potential in this work. Both applied doses were able to increase the number of neurons in the vicinity of the implant even above baseline, indicating that neurons in the implantation tract must not only have survived the original trauma, but that moreover neurons in the implantation tract must have been pushed aside during the implantation procedure without getting implicated in and exacerbating the neurotoxic cascade of progressive cell death. As an uncompetitive antagonist, memantine binds to a separate allosteric binding site within the channel pore of the NMDA receptor and hence requires prior activation of the receptor by its agonist. NMDA receptors have a complex structure with a binding site for its agonist NMDA or glutamate at the NR2-subunit, a binding site for its co-agonist glycine or D-serine at the NR1-subunit and a central ion channel that is blocked by Mg^{2+}. When agonist and co-agonist bind to the receptor and the cell is depolarised by cation influx through α-amino-3-hydroxy-5-methyl-4-isoxazolepropionic acid (AMPA) receptors, the Mg^{2+}-block is removed and the channel opens and allows influx of Ca^{2+} and Na^{+}. The allosteric binding site of memantine is the same as the Mg^{2+}-binding site within the channel and requires receptor activation and the relief of the Mg^{2+}-block. The dwell-time of memantine within the channel is much shorter compared to conventional channel blocker, such as MK-801 or phencyclidine (Angel Dust), which is why it does not cause psychotropic side-effects. However, memantine still has a slower off-rate than the Mg^{2+}-block and preferentially blocks NMDA receptors when excessively open. The higher the concentration of an agonist the better works the channel block with memantine, while relatively sparing normal neurotransmission (Parsons et al., 1999;Lipton, 2004;Lipton, 2006;Parsons et al., 2007;Chen and Lipton, 2006). Since NR2BR activation by excessive amounts of glutamate promotes ERK dephosphorylation and inhibits the transcription factor CREB, which results in the inhibition of pro-survival pathways and excitotoxic cell death of apoptotic or necrotic nature, memantine's preference for

extrasynaptic NR2BRs counteracts these cell death promoting effects and promotes neuronal survival (Ehrnhoefer et al., 2011).

In addition to memantine's neuroprotective effects, a further neurotrophic effect has been suggested, with memantine inducing astrocytes to produce neurotrophic factors such as GDNF and most likely also BDNF and TGF-β, which further promote neuronal survival (Wu et al., 2009). Glial scar formation around the cannula in this work was only slightly reduced and affected only the astrocyte levels. The slight decrease of astrocytic scar tissue in the vicinity of the implant was coupled to a reduction of the hypotrophic regions surrounding the glial scar that was observed in controls. Since memantine primarily inhibited the progressive cell death in the acute phase, the presumption that preventing neuronal cell death reduces the amount of glial cells activated was herewith supported. Due to the shielding and neuroprotective function of astrocytes, only a slight reduction in astrocytic scar tissue was desired as it was the case for memantine. A reduction of microglial activation after memantine treatment accompanied by a reduction of released pro-inflammatory molecules, such as NO, TNFα or ROS, has also been suggested previously (Wu et al., 2009), however could not be revealed in this work. In conflict to this is a further study of Liu et al. (2009) that demonstrated the chemotactic response of microglial cells to glutamate to be especially mediated by AMPA, kainate and metabotropic glutamate receptors, but not by NMDA receptors, which buttresses the finding in this work. Moreover, the microglial response has been suggested to primarily result from the persistent presence of the foreign body and to be to a lesser extent caused by the initial trauma of device implantation. Hence, the mere prevention of cell death in the acute phase does not reduce the persistent microglial activation in chronic settings.

The increased number of neurons within the vicinity of the implant also improved the behavioural performance, except for a slight performance decrease within the first two post-surgery weeks in the skilled reaching task. This suggests that, although neurons in the vicinity of the implant had survived, originally existing neuronal networks were most probably nonetheless disturbed and many of the neurons originally located in the implantation tract were lost. These neuronal networks, that most probably needed to be re-established, nevertheless appeared beneficial in amending behavioural performance. Since both applied doses of memantine resulted in comparable behavioural and immunhistological outcomes, tissue saturation may be assumed. It has been suggested, that too high doses of

memantine also target synaptic NMDARs (Ehrnhoefer et al., 2011). This however is not expected to result in severe side-effects, due to memantine's fast off-rate kinetics sparing physiological functions anyway. Since there is only poor evidence of local memantine application and previous studies only examined systemic administration, it is difficult to exactly classify the doses used in this study. However, since the dilution of the high dose was almost saturated, it can be assumed that it was rather high.

With a half-life time of memantine of approximately 12 h in rat brain (Rao et al., 2001), this time span seems to be particular important to interrupt the cascade of glutamate-induced progressive cell death. Glutamate uptake from the extracellular space is achieved by different glutamate transporters present in the plasma membranes of neurons and glial cells, especially astrocytes, and represents the only effective mechanism for glutamate removal (Danbolt, 2001). Due to memantine's lipophilic nature, it can also easily cross the BBB, which is why it is also administered orally in patients suffering from Alzheimer's disease (Robinson and Kreating, 2006). Memantine, that is generally well tolerated when administered systemically with a favourable side-effect profile, has only occasionally been reported to cause dizziness or restlessness at high doses (Lipton 2004; Parsons et al., 1999). This made it the first clinically successful NMDA receptor antagonist that is approved for the treatment of moderate-to-severe Alzheimer's disease (Scarpini et al., 2003;Lipton, 2006;Wenk et al., 2006), with also some potential therapeutic benefit in patients with Huntington's disease (Fan and Raymond, 2007). Further therapeutic potential has also been suggested for a broad spectrum of CNS disorders ranging from acute disorder like stroke and trauma, over further chronic neurodegenerative disorders like Parkinson's disease and amyotrophic lateral sclerosis, to the symptomatic treatment of epilepsy, depression, multiple sclerosis and further diseases (Parsons et al., 1999;Lipton, 2006). Beyond this, according to the results of this work, memantine also seems to be a promising candidate in the acute phase of chronic foreign body implantation to enhance the vicinity of neurons to the implant.

6.2.2 Apyrase

In order to counteract the extent of glial cell activation and thereby decrease the self-perpetuating cycle of microglial-induced secondary cell death, the ATP/ADP-hydrolysing enzyme apyrase was locally applied during the implantation procedure. Since ATP is

suggested to be key in mediating the microglial response towards the site of injury and also in astrocyte communication, apyrase was assumed to reduce the glial cell activation in the acute phase of brain injury as well as the microglial-induced secondary cell death.

After an insult, high levels of ATP have been shown to persist in the peritraumatic zone for many hours, triggering irreversible increases of cytosolic Ca^{2+} via the activation of purinergic receptors, and causing cell death of even healthy neurons (Wang et al., 2004). Since ATP and also to a lesser extent its metabolite ADP are important activators of glial cells (Davalos et al., 2005) by binding to purinergic P2 receptors (Fields and Burnstock, 2006;Burnstock, 2008), the ATPase apyrase, that hydrolyses ATP as well as ADP, was chosen in this work. Here, apyrase was able to reduce the extent of microglial activation by about one third particularly after two weeks, accompanied by a reduction of neuronal cell death particularly after six weeks with the neuronal population having recovered to a large extent at this later time point. Since microglial activation is accompanied by the release of pro-inflammatory cytokines that further amplify the immune response and cause a self-perpetuating cycle of cell death (Bianco et al., 2005;Schwartz and Shechter, 2010), the assumption that a decrease in microglial cell activation causes an increase in surviving neurons can be further supported by this work. Interestingly, although sheath formation was suggested to occur faster than the re-growth of neuronal processes (Turner et al., 1999), our findings indicate that some degree of neuronal re-approach towards the implantation site seems to be possible, most probably as a result from glial scar contraction.

While apyrase was able to increase the neuronal density in the vicinity of the implant back to baseline levels after six weeks, performance in the skilled reaching task was only slightly increased compared to controls, without re-establishing baseline levels within this time. Especially in the first week after cannula implantation, performance was almost as reduced as that of the vehicle-treated animals. Since apyrase does not interfere with the excitotoxic cascade of glutamate-induced progressive cell death, but instead aims at interfering with the subsequent cascade of microglial-induced cell death, this may account for a larger acute cell loss that may be more harming than the subsequent events. Inhibition of the self-perpetuating cycle of microglial-induced cell death proved also to be beneficial in promoting neuronal survival, however to a later time point and accordingly less effectively. Moreover, due to the performance decrease, it is debatable in which condition surviving neurons are, and it can be assumed that at least neuronal networks are majorly affected and

need to be rebuilt as derived from the initial decrease in neuronal population around the implant.

In contrast to the reduction in the number of microglial cells, the astrocytic scar revealed no obvious reduction at either time point. Since astrocytes respond to changes in tissue homeostasis with the release of Ca^{2+} from the endoplasmatic reticulum (Goodenough and Paul, 2003;Fischer et al., 2009), which results in the release of regenerative ATP from internal pools (Anderson et al., 2004), they seem to be independent in their communication from the initially released ATP by injured cells. ATP-induced ATP release from astrocytes has been suggested to be not only responsible for the far reaching communication via Ca^{2+}-wave propagation between astrocytes with ATP as an intercellular messenger (Guthrie et al., 1999), but to be also required for the activation and migration of microglial cells to the site of injury (Davalos et al., 2005). Hence, the astrocytic ATP release may be responsible for a delayed activation of microglial cells in this work. Since Dibaj et al. (2010) suggested other messenger molecules, such as NO, to be only effective chemoattractants for microglial cells in the presence of ambient ATP, and initial amounts of ATP are most probably hydrolysed by apyrase, this further supports the assumption that microglial cells depend in their activation to a large extent on ATP released by astrocytes (Davalos et al., 2005). In addition to ATP release, astrocytes moreover release glutamate in response to ATP binding, which exacerbates the glutamate-mediated excitotoxicity (Lynch and Guttmann, 2002;Lipton, 2004) and may further account for existing performance deficits in this work.

Due to the rather transient nature of nucleotides with short half-life times of about 5-10 min for ATP and about 45-60 min for ADP, they are under normal conditions quickly metabolised by ectonucleases from ATP to ADP and AMP that is subsequently transformed to adenosine. The large amounts of ATP and ADP that are released after severe injuries, however induce microglial cell activation that constitutes the first line in defence (Buvinic et al., 2007). Since the plasma half-life time of apyrase has been suggested to be about 1 h (Moeckel et al., 2014), this time span is most probably only sufficient to inhibit the first surge of ATP and ADP released by the injured cells, however not to inhibit the massive amounts of ATP that are subsequently released by the astrocytes. The metabolite adenosine has been suggested to be beneficial after an injury by exhibiting anti-inflammatory, anti-thrombotic and cardioprotective properties, which makes apyrase also a target candidate to treat arterial thrombosis (Moeckel et al., 2014). An optimised version of apyrase has recently been

engineered by Moeckel et al. (2015) with a 50 times longer plasma half-life time compared to native apyrase. This optimised form completely prevents thrombotic re-occlusion and significantly decreases infarction sizes after thrombotic occlusion of a coronary artery and induced fibrinolysis in a canine model and also decreases infarct size in a murine model of myocardial reperfusion injury when injected intravenously (Moeckel et al., 2014). It would be interesting, how the tissue and behavioural response would turn out when ATP gets effectively hydrolysed for a much longer period of time, as suggested for this optimised version of apyrase.

6.2.3 Minocycline

In order to combine both strategies to reduce neuronal cell death as well as microglial activation in the acute phase after foreign body implantation the antibiotic minocycline with anti-apoptotic and anti-inflammatory properties was locally applied during the implantation procedure in the third approach. Since the cascades of enduring cell death induced by the initial trauma are accompanied by persistent microglial cell activation that further contributes to the self-perpetuating cycle of cell death, minocycline seems to be an ideal candidate to antagonise both these concerns.

Secondary cell death of neurons, induced by the initial release of cellular contents from injured and dying cells such as glutamate and ATP, causes neuronal “die-back” zones around implants, that are further exacerbated by subsequent persistent microglial activation (Biran et al., 2005;Potter et al., 2012). The release of pro-inflammatory and neurotoxic substances by injured neurons and glial cells causes secondary damage to originally uninjured cells and the release of further cellular contents (Polikov et al., 2005). The broad-spectrum antibiotic minocycline was intended to interrupt the neurotoxic as well as the inflammatory cascade at a very early stage. Minocycline not only enhanced the number of neurons in the vicinity of the implant at both time points in this work, but also decreased the number of microglial cells, which was moreover accompanied by a decrease in astrocyte density around the implant at two weeks. This inhibition of the foreign body response was accompanied by an increase in performance that was only significantly reduced in the first post-surgery week in the skilled reaching box and had recovered by post-surgery week three, with rats having regained their baseline performance level. Although acting through a broad range of mechanisms, minocycline’s neuroprotective effects result to a large extent from the

inhibition of the p38 MAPK pathway in neurons and microglia, that is an important regulator of immune cell function and cell death (Stirling et al., 2005). The activation of p38 MAPK pathways in neurons due to NMDA receptor activation by glutamate is involved in apoptosis and is directly inhibited by minocycline. The PI3-K/Akt (phosphatidylinositol 3-kinase/protein kinase B) pathway that inhibits apoptosis and promotes cell survival is however maintained by minocycline (Pi et al., 2004). Additionally, minocycline also inhibits p38 MAPK in microglial cells, in which the p38 MAPK pathway induces the activation and proliferation of these cells and the release of NO and IL-1β (Tikka and Koistinaho, 2001).

Minocycline's neuroprotective and neurorestorative effects have also been demonstrated in ischemic stroke accompanied by a prevention of microglia activation (Yrjanheikki et al., 1998;Yrjanheikki et al., 1999;Hewlett and Corbett, 2006). Moreover, a reduction of neurotoxic and pro-inflammatory molecules including NO, TNFα and IL-1β, as well as an increase of anti-inflammatory molecules such as TGF-β or IL-10 was revealed (Yang et al., 2015b). Both effects are beneficial for neuronal survival after foreign body implantation and are further supported by this work. Furthermore, minocycline has been demonstrated to effectively decrease neurotoxicity of glutamate by inhibiting the NMDA-induced activation of p38 MAPK in microglial cells, thereby inhibiting microglial activation and providing neuroprotection (Tikka and Koistinaho, 2001;Tikka et al., 2001). Due to minocycline's further attribute to ameliorate BBB integrity and edema following haemorrhage (Wasserman and Schlichter, 2007;Yang et al., 2015a;Yang et al., 2015b), surrounding neurons are protected from oxygen and glucose deprivation and ionic imbalances that is accompanied by a loss in energy supply. A study by Rennaker et al. (2007), in which minocycline is administered via the drinking water, also demonstrated reduced astrogliosis and improvements in quality and longevity of neural recordings from the interfaces. The local application of minocycline in the present study further supports their approach and demonstrates that local minocycline administration mimicking electrode coating is also effective in enhancing neuronal vicinity to the implant and in reducing glial scar formation.

Compared to first-generation tetracyclines, minocycline has a longer half-life time that is approximately 17 h in humans, but only about 3 h in rats. It is highly lipophilic and can easily pass the BBB when administered orally. Being rapidly and completely absorbed, CSF concentrations of 11-56% of plasma concentrations are achieved (Elewa et al., 2006).

Although minocycline is well-tolerated in humans with a good safety record when used chronically, most common side-effects when administered systemically include nausea, vertigo and mild dizziness (Garrido-Mesa et al., 2013). Besides being neuroprotective in stroke minocycline has also been suggested to be an effective therapeutic in traumatic brain injury (Sanchez Mejia et al., 2001), spinal cord injury (Wells et al., 2003), amyotrophic lateral sclerosis (Zhu et al., 2002), Huntington's disease (Bonelli et al., 2004), Parkinson's disease (Du et al., 2001) as well as Alzheimer's disease (Ryu et al., 2004). In the context of this work, minocycline's neuroprotective and anti-inflammatory potential is further supported, suggesting it as an effective local therapeutic in the suppression of the foreign body response.

6.3 Conclusion and further direction

Taken together, trying to reduce the foreign body response by interfering with the very early events after device implantation seems to be a good approach to inhibit the induced cascades of enduring cell death and persistent microglial activation. The uncompetitive NMDA receptor antagonist memantine, with a preference for extrasynaptically located NR2BRs, seems to be most effective in reducing the glutamate-induced excitotoxic cascade induced by the initial trauma, by increasing the number of neurons in the vicinity of the implant as well as the behavioural performance. The ATP/ADP-hydrolysing enzyme apyrase, that aimed to reduce the self-perpetuating cycle of microglial-induced cell death, was least effective in terms of maintaining the behavioural performance. Despite a rather temporary decrease of microglial cells in the vicinity of the implant, neuronal populations had quickly recovered, which however did not automatically result in an equivalent recovery of behavioural performance. The broad-spectrum antibiotic minocycline, with anti-inflammatory and anti-apoptotic properties, had the broadest spectrum of effects, ranging from a permanent increase in neurons and behavioural performance to a permanent decrease in microglial cells accompanied by a temporary decrease in astrocyte density. Nevertheless, compared to memantine, neuron levels after minocycline treatment were lower and performance in the skilled reaching box exhibited an obvious initial performance drop.

This suggests that interfering with the very initial events after device implantation targeting the cascades of secondary cell death due to glutamate excitotoxicity seems to be

an efficient approach to maintain neuronal networks in the vicinity of an implant. Although reducing the microglial response and thereby the degree of pro-inflammatory and neurotoxic molecules increases the neuronal survival in the vicinity of an implant, targeting these delayed cascades does not maintain neuronal networks to the same extent. Moreover, regarding the long-term results, glial scar formation is apparently rather less influenced by the acute administration of substances during cannula implantation, but instead seems to be primarily a consequence of the chronic setting.

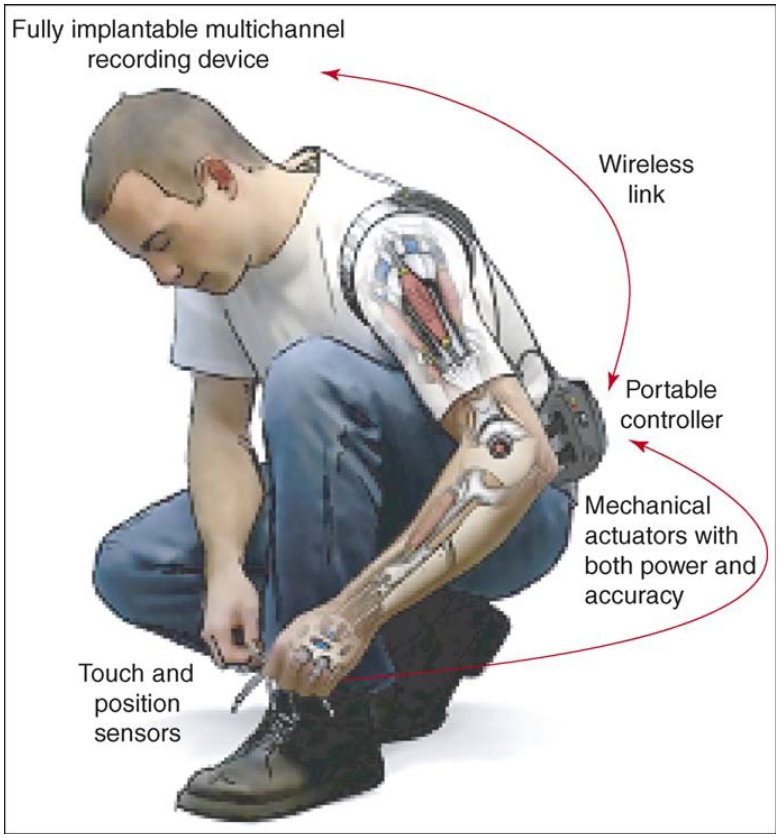

Fig. 6.4. Vision of a fully-implantable wireless brain-computer interface. Deriving signals from thousand of neurons by means of a fully-implantable electrode array, could restore limb mobility in paralysed subjects or amputees via wireless telemetry, being equipped with touch and position sensors and the functionality of a human limb in terms of accuracy and power (Lebedev and Nicolelis, 2006).

The local substance application during cannula implantation in this work, that aimed to mimic the local drug delivery from coated electrodes, served as a proof-of-principle investigation mimicking the implantation of a device such as an electrode array into the cortex. The next stage to further consolidate the findings of this work would be coating of

electrodes with the substances regarded as most efficient, that is memantine, closely followed in efficiency by minocycline. Coating of electrodes with bioactive molecules in order to manipulate the biological response is a promising direction in research, since previous approaches that dealt with different electrode designs, material science strategies or implantation techniques failed to provide a satisfactory control of the foreign body response (Polikov et al., 2005). Limiting or eliminating the foreign body response and reliably enhancing the vicinity of viable neurons to a chronic implant that remain electrically active, is an obstacle that needs to be overcome to introduce CNS implants into clinical application. Cortical neuronal ensemble signals, derived from local populations of M1 neurons, might be used by paralysed patients to reanimate paralysed muscles using functional electrical stimulation of the neuro-motor system or by people with limb loss to control prosthetic limbs (Chadwick et al., 2011;Hochberg et al., 2012). The vision of fully-implantable wireless electrode arrays **(Fig. 6.4)**, deriving signals from thousands of neurons to a BCI via wireless telemetry, enabling the restoration of limb mobility in paralysed subjects or amputees by being equipped with touch and position sensors and the functionality of a human limb in terms of accuracy and power (Lebedev and Nicolelis, 2006), remains an incentive to keep on improving current electrode designs in terms of biocompatibility.

7 References

Alaverdashvili M, Leblond H, Rossignol S, Whishaw IQ (2008) Cineradiographic (video X-ray) analysis of skilled reaching in a single pellet reaching task provides insight into relative contribution of body, head, oral, and forelimb movement in rats. Behav Brain Res 192: 232-247.

Alaverdashvili M, Whishaw IQ (2010) Compensation aids skilled reaching in aging and in recovery from forelimb motor cortex stroke in the rat. Neuroscience 167: 21-30.

Alderton WK, Cooper CE, Knowles RG (2001) Nitric oxide synthases: structure, function and inhibition. Biochem J 357: 593-615.

Allen NJ, Barres BA (2009) Neuroscience: Glia - more than just brain glue. Nature 457: 675-677.

Anderson CM, Bergher JP, Swanson RA (2004) ATP-induced ATP release from astrocytes. J Neurochem 88: 246-256.

Antonow-Schlorke I, Ehrhardt J, Knieling M (2013) Modification of the ladder rung walking task-new options for analysis of skilled movements. Stroke Res Treat 2013: 418627.

Arikan R, Blake NM, Erinjeri JP, Woolsey TA, Giraud L, Highstein SM (2002) A method to measure the effective spread of focally injected muscimol into the central nervous system with electrophysiology and light microscopy. J Neurosci Methods 118: 51-57.

Badan I, Buchhold B, Hamm A, Gratz M, Walker LC, Platt D, Kessler C, Popa-Wagner A (2003) Accelerated glial reactivity to stroke in aged rats correlates with reduced functional recovery. J Cereb Blood Flow Metab 23: 845-854.

Ballerini P, Rathbone MP, Di Iorio P, Renzetti A, Giuliani P, D'Alimonte I, Trubiani O, Caciagli F, Ciccarelli R (1996) Rat astroglial P2Z (P2X7) receptors regulate intracellular calcium and purine release. Neuroreport 7: 2533-2537.

Barretto RP, Ko TH, Jung JC, Wang TJ, Capps G, Waters AC, Ziv Y, Attardo A, Recht L, Schnitzer MJ (2011) Time-lapse imaging of disease progression in deep brain areas using fluorescence microendoscopy. Nat Med 17: 223-228.

Beaumont K, Chilton WS, Yamamura HI, Enna SJ (1978) Muscimol binding in rat brain: association with synaptic GABA receptors. Brain Res 148: 153-162.

Bianco F, Pravettoni E, Colombo A, Schenk U, Moller T, Matteoli M, Verderio C (2005) Astrocyte-derived ATP induces vesicle shedding and IL-1 beta release from microglia. J Immunol 174: 7268-7277.

Biran R, Martin DC, Tresco PA (2005) Neuronal cell loss accompanies the brain tissue response to chronically implanted silicon microelectrode arrays. Exp Neurol 195: 115-126.

Block ML, Zecca L, Hong JS (2007) Microglia-mediated neurotoxicity: uncovering the molecular mechanisms. Nat Rev Neurosci 8: 57-69.

Bonelli RM, Hodl AK, Hofmann P, Kapfhammer HP (2004) Neuroprotection in Huntington's disease: a 2-year study on minocycline. Int Clin Psychopharmacol 19: 337-342.

Bonfoco E, Krainc D, Ankarcrona M, Nicotera P, Lipton SA (1995) Apoptosis and necrosis: two distinct events induced, respectively, by mild and intense insults with N-methyl-D-aspartate or nitric oxide/superoxide in cortical cell cultures. Proc Natl Acad Sci U S A 92: 7162-7166.

Bretón RR, Rodríguez JCG (2012) Excitotoxicity and oxidative stress in acute ischemic stroke. stroke 8: 9.

Brown AR, Teskey GC (2014) Motor cortex is functionally organized as a set of spatially distinct representations for complex movements. J Neurosci 34: 13574-13585.

Brown GC (2010) Nitric oxide and neuronal death. Nitric Oxide 23: 153-165.

Burgner D, Rockett K, Kwiatkowski D (1999) Nitric oxide and infectious diseases. Arch Dis Child 81: 185-188.

Burnstock G (2008) Purinergic signalling and disorders of the central nervous system. Nat Rev Drug Discov 7: 575-590.

Buvinic S, Bravo-Zehnder M, Boyer JL, Huidobro-Toro JP, Gonzalez A (2007) Nucleotide P2Y1 receptor regulates EGF receptor mitogenic signaling and expression in epithelial cells. J Cell Sci 120: 4289-4301.

Buzsaki G (2004) Large-scale recording of neuronal ensembles. Nat Neurosci 7: 446-451.

Carmel JB, Martin JH (2014) Motor cortex electrical stimulation augments sprouting of the corticospinal tract and promotes recovery of motor function. Front Integr Neurosci 8: 51.

Chadwick EK, Blana D, Simeral JD, Lambrecht J, Kim SP, Cornwell AS, Taylor DM, Hochberg LR, Donoghue JP, Kirsch RF (2011) Continuous neuronal ensemble control of simulated arm reaching by a human with tetraplegia. J Neural Eng 8: 034003.

Chakfe Y, Seguin R, Antel JP, Morissette C, Malo D, Henderson D, Seguela P (2002) ADP and AMP induce interleukin-1beta release from microglial cells through activation of ATP-primed P2X7 receptor channels. J Neurosci 22: 3061-3069.

Chebib M, Johnston GA (1999) The 'ABC' of GABA receptors: a brief review. Clin Exp Pharmacol Physiol 26: 937-940.

Colechio EM, Alloway KD (2009) Differential topography of the bilateral cortical projections to the whisker and forepaw regions in rat motor cortex. Brain Struct Funct 213: 423-439.

Conti A, Miscusi M, Cardali S, Germano A, Suzuki H, Cuzzocrea S, Tomasello F (2007) Nitric oxide in the injured spinal cord: synthases cross-talk, oxidative stress and inflammation. Brain Res Rev 54: 205-218.

Danbolt NC (2001) Glutamate uptake. Prog Neurobiol 65: 1-105.

Davalos D, Grutzendler J, Yang G, Kim JV, Zuo Y, Jung S, Littman DR, Dustin ML, Gan WB (2005) ATP mediates rapid microglial response to local brain injury in vivo. Nature Neuroscience 8: 752-758.

Dawson VL, Dawson TM (1996) Nitric oxide neurotoxicity. J Chem Neuroanat 10: 179-190.

Deffeyes JE, Touvykine B, Quessy S, Dancause N (2015) Interactions between rostral and caudal cortical motor areas in the rat. J Neurophysiol 113: 3893-3904.

Dibaj P, Nadrigny F, Steffens H, Scheller A, Hirrlinger J, Schomburg ED, Neusch C, Kirchhoff F (2010) NO mediates microglial response to acute spinal cord injury under ATP control in vivo. Glia 58: 1133-1144.

Du Y, Ma Z, Lin S, Dodel RC, Gao F, Bales KR, Triarhou LC, Chernet E, Perry KW, Nelson DL, Luecke S, Phebus LA, Bymaster FP, Paul SM (2001) Minocycline prevents nigrostriatal dopaminergic neurodegeneration in the MPTP model of Parkinson's disease. Proc Natl Acad Sci U S A 98: 14669-14674.

Duan S, Anderson CM, Keung EC, Chen Y, Chen Y, Swanson RA (2003) P2X7 receptor-mediated release of excitatory amino acids from astrocytes. J Neurosci 23: 1320-1328.

Eddleston M, Mucke L (1993) Molecular profile of reactive astrocytes--implications for their role in neurologic disease. Neuroscience 54: 15-36.

Edell DJ, Toi VV, McNeil VM, Clark LD (1992) Factors influencing the biocompatibility of insertable silicon microshafts in cerebral cortex. IEEE Trans Biomed Eng 39: 635-643.

Ehrnhoefer DE, Wong BK, Hayden MR (2011) Convergent pathogenic pathways in Alzheimer's and Huntington's diseases: shared targets for drug development. Nat Rev Drug Discov 10: 853-867.

Elewa HF, Hilali H, Hess DC, Machado LS, Fagan SC (2006) Minocycline for short-term neuroprotection. Pharmacotherapy 26: 515-521.

Fan MM, Raymond LA (2007) N-methyl-D-aspartate (NMDA) receptor function and excitotoxicity in Huntington's disease. Prog Neurobiol 81: 272-293.

Farber K, Kettenmann H (2006) Purinergic signaling and microglia. Pflugers Arch 452: 615-621.

Feja M, Hayn L, Koch M (2014) Nucleus accumbens core and shell inactivation differentially affects impulsive behaviours in rats. Prog Neuropsychopharmacol Biol Psychiatry 54: 31-42.

Fendt M, Koch M, Schnitzler HU (1994) Sensorimotor gating deficit after lesions of the superior colliculus. Neuroreport 5: 1725-1728.

Fields RD, Burnstock G (2006) Purinergic signalling in neuron-glia interactions. Nat Rev Neurosci 7: 423-436.

Fischer W, Appelt K, Grohmann M, Franke H, Norenberg W, Illes P (2009) Increase of intracellular Ca2+ by P2X and P2Y receptor-subtypes in cultured cortical astroglia of the rat. Neuroscience 160: 767-783.

Garrido-Mesa N, Zarzuelo A, Galvez J (2013) Minocycline: far beyond an antibiotic. Br J Pharmacol 169: 337-352.

Gewaltig MT, Kojda G (2002) Vasoprotection by nitric oxide: mechanisms and therapeutic potential. Cardiovasc Res 55: 250-260.

Goetz T, Arslan A, Wisden W, Wulff P (2007) GABA(A) receptors: structure and function in the basal ganglia. Prog Brain Res 160: 21-41.

Gong CS, Lai HY, Huang SH, Lo YC, Lee N, Chen PY, Tu PH, Yang CY, Lin JC, Chen YY (2015) A programmable high-voltage compliance neural stimulator for deep brain stimulation in vivo. Sensors (Basel) 15: 12700-12719.

Goodenough DA, Paul DL (2003) Beyond the gap: functions of unpaired connexon channels. Nat Rev Mol Cell Biol 4: 285-294.

Griffith RW, Humphrey DR (2006) Long-term gliosis around chronically implanted platinum electrodes in the Rhesus macaque motor cortex. Neurosci Lett 406: 81-86.

Guthrie PB, Knappenberger J, Segal M, Bennett MV, Charles AC, Kater SB (1999) ATP released from astrocytes mediates glial calcium waves. J Neurosci 19: 520-528.

Habib S, Ali A (2011) Biochemistry of nitric oxide. Indian J Clin Biochem 26: 3-17.

Hanisch UK (2002) Microglia as a source and target of cytokines. Glia 40: 140-155.

Hanisch UK, Kettenmann H (2007) Microglia: active sensor and versatile effector cells in the normal and pathologic brain. Nat Neurosci 10: 1387-1394.

Hardingham GE, Bading H (2010) Synaptic versus extrasynaptic NMDA receptor signalling: implications for neurodegenerative disorders. Nat Rev Neurosci 11: 682-696.

Hardingham GE, Fukunaga Y, Bading H (2002) Extrasynaptic NMDARs oppose synaptic NMDARs by triggering CREB shut-off and cell death pathways. Nat Neurosci 5: 405-414.

Hayn L, Koch M (2015) Suppression of excitotoxicity and foreign body response by memantine in chronic cannula implantation into the rat brain. Brain Res Bull 117: 54-68.

Haynes SE, Hollopeter G, Yang G, Kurpius D, Dailey ME, Gan WB, Julius D (2006) The P2Y12 receptor regulates microglial activation by extracellular nucleotides. Nat Neurosci 9: 1512-1519.

He W, McConnell GC, Bellamkonda RV (2006) Nanoscale laminin coating modulates cortical scarring response around implanted silicon microelectrode arrays. J Neural Eng 3: 316-326.

He W, McConnell GC, Schneider TM, Bellamkonda RV (2007) A novel anti-inflammatory surface for neural electrodes. Advanced Materials 19: 3529-+.

Hewlett KA, Corbett D (2006) Delayed minocycline treatment reduces long-term functional deficits and histological injury in a rodent model of focal ischemia. Neuroscience 141: 27-33.

Hochberg LR, Bacher D, Jarosiewicz B, Masse NY, Simeral JD, Vogel J, Haddadin S, Liu J, Cash SS, van der SP, Donoghue JP (2012) Reach and grasp by people with tetraplegia using a neurally controlled robotic arm. Nature 485: 372-375.

Hochberg LR, Serruya MD, Friehs GM, Mukand JA, Saleh M, Caplan AH, Branner A, Chen D, Penn RD, Donoghue JP (2006) Neuronal ensemble control of prosthetic devices by a human with tetraplegia. Nature 442: 164-171.

Humm JL, Kozlowski DA, Bland ST, James DC, Schallert T (1999) Use-dependent exaggeration of brain injury: is glutamate involved? Exp Neurol 157: 349-358.

Hyland B (1998) Neural activity related to reaching and grasping in rostral and caudal regions of rat motor cortex. Behav Brain Res 94: 255-269.

Iadecola C, Anrather J (2011) The immunology of stroke: from mechanisms to translation. Nat Med 17: 796-808.

Ignatius MJ, Sawhney N, Gupta A, Thibadeau BM, Monteiro OR, Brown IG (1998) Bioactive surface coatings for nanoscale instruments: effects on CNS neurons. J Biomed Mater Res 40: 264-274.

Inoue K (2002) Microglial activation by purines and pyrimidines. Glia 40: 156-163.

Iwaniuk AN, Whishaw IQ (2000) On the origin of skilled forelimb movements. Trends Neurosci 23: 372-376.

Jackson A (2012) Neuroscience: Brain-controlled robot grabs attention. Nature 485: 317-318.

Jacob TC, Moss SJ, Jurd R (2008) GABA(A) receptor trafficking and its role in the dynamic modulation of neuronal inhibition. Nat Rev Neurosci 9: 331-343.

Jara JH, Genc B, Klessner JL, Ozdinler PH (2014) Retrograde labeling, transduction, and genetic targeting allow cellular analysis of corticospinal motor neurons: implications in health and disease. Front Neuroanat 8: 16.

Jarrard LE (2002) Use of excitotoxins to lesion the hippocampus: update. Hippocampus 12: 405-414.

Jeremic A, Jeftinija K, Stevanovic J, Glavaski A, Jeftinija S (2001) ATP stimulates calcium-dependent glutamate release from cultured astrocytes. J Neurochem 77: 664-675.

Kam L, Shain W, Turner JN, Bizios R (2002) Selective adhesion of astrocytes to surfaces modified with immobilized peptides. Biomaterials 23: 511-515.

Kigerl KA, Gensel JC, Ankeny DP, Alexander JK, Donnelly DJ, Popovich PG (2009) Identification of two distinct macrophage subsets with divergent effects causing either neurotoxicity or regeneration in the injured mouse spinal cord. J Neurosci 29: 13435-13444.

Kim DH, Martin DC (2006) Sustained release of dexamethasone from hydrophilic matrices using PLGA nanoparticles for neural drug delivery. Biomaterials 27: 3031-3037.

Kim YT, Hitchcock RW, Bridge MJ, Tresco PA (2004) Chronic response of adult rat brain tissue to implants anchored to the skull. Biomaterials 25: 2229-2237.

Kleim JA, Barbay S, Nudo RJ (1998) Functional reorganization of the rat motor cortex following motor skill learning. J Neurophysiol 80: 3321-3325.

Kleim JA, Hogg TM, VandenBerg PM, Cooper NR, Bruneau R, Remple M (2004) Cortical synaptogenesis and motor map reorganization occur during late, but not early, phase of motor skill learning. J Neurosci 24: 628-633.

Koch M, Schmid A, Schnitzler HU (1996) Pleasure-attenuation of startle is disrupted by lesions of the nucleus accumbens. Neuroreport 7: 1442-1446.

Koch M, Schmid A, Schnitzler HU (2000) Role of nucleus accumbens dopamine D1 and D2 receptors in instrumental and Pavlovian paradigms of conditioned reward. Psychopharmacology (Berl) 152: 67-73.

Kono H, Rock KL (2008) How dying cells alert the immune system to danger. Nat Rev Immunol 8: 279-289.

Krase W, Koch M, Schnitzler HU (1993) Glutamate antagonists in the reticular formation reduce the acoustic startle response. Neuroreport 4: 13-16.

Kringelbach ML, Jenkinson N, Owen SL, Aziz TZ (2007) Translational principles of deep brain stimulation. Nat Rev Neurosci 8: 623-635.

Krogsgaard-Larsen P, Frolund B, Frydenvang K (2000) GABA uptake inhibitors. Design, molecular pharmacology and therapeutic aspects. Curr Pharm Des 6: 1193-1209.

Lai TW, Shyu WC, Wang YT (2011) Stroke intervention pathways: NMDA receptors and beyond. Trends Mol Med 17: 266-275.

Leach JB, Achyuta AK, Murthy SK (2010) Bridging the Divide between Neuroprosthetic Design, Tissue Engineering and Neurobiology. Front Neuroeng 2: 18.

Lebedev MA, Nicolelis MA (2006) Brain-machine interfaces: past, present and future. Trends Neurosci 29: 536-546.

Lenarz T, Lim HH, Reuter G, Patrick JF, Lenarz M (2006) The auditory midbrain implant: a new auditory prosthesis for neural deafness-concept and device description. Otol Neurotol 27: 838-843.

Leuthardt EC, Schalk G, Moran D, Ojemann JG (2006) The emerging world of motor neuroprosthetics: a neurosurgical perspective. Neurosurgery 59: 1-14.

Leveille F, El Gaamouch F, Gouix E, Lecocq M, Lobner D, Nicole O, Buisson A (2008) Neuronal viability is controlled by a functional relation between synaptic and extrasynaptic NMDA receptors. FASEB J 22: 4258-4271.

Lindenberg R, Zhu LL, Ruber T, Schlaug G (2012) Predicting functional motor potential in chronic stroke patients using diffusion tensor imaging. Hum Brain Mapp 33: 1040-1051.

Lipton SA (2004) Failures and successes of NMDA receptor antagonists: molecular basis for the use of open-channel blockers like memantine in the treatment of acute and chronic neurologic insults. NeuroRx 1: 101-110.

Lipton SA (2006) Paradigm shift in neuroprotection by NMDA receptor blockade: memantine and beyond. Nat Rev Drug Discov 5: 160-170.

Lipton SA, Rosenberg PA (1994) Excitatory amino acids as a final common pathway for neurologic disorders. N Engl J Med 330: 613-622.

Liu GJ, Nagarajah R, Banati RB, Bennett MR (2009) Glutamate induces directed chemotaxis of microglia. Eur J Neurosci 29: 1108-1118.

Liu X, McCreery DB, Carter RR, Bullara LA, Yuen TG, Agnew WF (1999) Stability of the interface between neural tissue and chronically implanted intracortical microelectrodes. IEEE Trans Rehabil Eng 7: 315-326.

Loddick SA, Turnbull AV, Rothwell NJ (1998) Cerebral interleukin-6 is neuroprotective during permanent focal cerebral ischemia in the rat. J Cereb Blood Flow Metab 18: 176-179.

Loeb GE (1990) Cochlear prosthetics. Annu Rev Neurosci 13: 357-371.

Loftis JM, Janowsky A (2003) The N-methyl-D-aspartate receptor subunit NR2B: localization, functional properties, regulation, and clinical implications. Pharmacol Ther 97: 55-85.

Lomber SG (1999) The advantages and limitations of permanent or reversible deactivation techniques in the assessment of neural function. J Neurosci Methods 86: 109-117.

Lopes JP, Tarozzo G, Reggiani A, Piomelli D, Cavalli A (2013) Galantamine potentiates the neuroprotective effect of memantine against NMDA-induced excitotoxicity. Brain Behav 3: 67-74.

Lynch DR, Guttmann RP (2002) Excitotoxicity: perspectives based on N-methyl-D-aspartate receptor subtypes. J Pharmacol Exp Ther 300: 717-723.

Maher A, El Sayed NS, Breitinger HG, Gad MZ (2014) Overexpression of NMDAR2B in an inflammatory model of Alzheimer's disease: modulation by NOS inhibitors. Brain Res Bull 109: 109-116.

Majchrzak M, Di Scala G (2000) GABA and muscimol as reversible inactivation tools in learning and memory. Neural Plast 7: 19-29.

Mak JN, Wolpaw JR (2009) Clinical Applications of Brain-Computer Interfaces: Current State and Future Prospects. IEEE Rev Biomed Eng 2: 187-199.

Malarkey EB, Parpura V (2008) Mechanisms of glutamate release from astrocytes. Neurochem Int 52: 142-154.

Maldonado MA, Allred RP, Felthauser EL, Jones TA (2008) Motor skill training, but not voluntary exercise, improves skilled reaching after unilateral ischemic lesions of the sensorimotor cortex in rats. Neurorehabil Neural Repair 22: 250-261.

Marin C, Fernandez E (2010) Biocompatibility of intracortical microelectrodes: current status and future prospects. Front Neuroeng 3: 8.

Markram H, Toledo-Rodriguez M, Wang Y, Gupta A, Silberberg G, Wu C (2004) Interneurons of the neocortical inhibitory system. Nat Rev Neurosci 5: 793-807.

Marks L, Carswell HV, Peters EE, Graham DI, Patterson J, Dominiczak AF, Macrae IM (2001) Characterization of the microglial response to cerebral ischemia in the stroke-prone spontaneously hypertensive rat. Hypertension 38: 116-122.

Martin JH (2005) The corticospinal system: from development to motor control. Neuroscientist 11: 161-173.

Martin JH, Ghez C (1999) Pharmacological inactivation in the analysis of the central control of movement. J Neurosci Methods 86: 145-159.

Matthies C, Brill S, Varallyay C, Solymosi L, Gelbrich G, Roosen K, Ernestus RI, Helms J, Hagen R, Mlynski R, Shehata-Dieler W, Muller J (2014) Auditory brainstem implants in neurofibromatosis Type 2: is open speech perception feasible? J Neurosurg 120: 546-558.

Maynard EM, Fernandez E, Normann RA (2000) A technique to prevent dural adhesions to chronically implanted microelectrode arrays. J Neurosci Methods 97: 93-101.

McConnell GC, Rees HD, Levey AI, Gutekunst CA, Gross RE, Bellamkonda RV (2009) Implanted neural electrodes cause chronic, local inflammation that is correlated with local neurodegeneration. J Neural Eng 6: 056003.

Metz GA, Whishaw IQ (2002) Cortical and subcortical lesions impair skilled walking in the ladder rung walking test: a new task to evaluate fore- and hindlimb stepping, placing, and co-ordination. J Neurosci Methods 115: 169-179.

Metz GA, Whishaw IQ (2009) The ladder rung walking task: a scoring system and its practical application. J Vis Exp.

Moeckel D, Jeong SS, Sun X, Broekman MJ, Nguyen A, Drosopoulos JH, Marcus AJ, Robson SC, Chen R, Abendschein D (2014) Optimizing human apyrase to treat arterial thrombosis and limit reperfusion injury without increasing bleeding risk. Sci Transl Med 6: 248ra105.

Montero TD, Orellana JA (2015) Hemichannels: new pathways for gliotransmitter release. Neuroscience 286: 45-59.

Muir GD, Whishaw IQ (1999) Complete locomotor recovery following corticospinal tract lesions: measurement of ground reaction forces during overground locomotion in rats. Behav Brain Res 103: 45-53.

Neafsey EJ, Bold EL, Haas G, Hurley-Gius KM, Quirk G, Sievert CF, Terreberry RR (1986) The organization of the rat motor cortex: a microstimulation mapping study. Brain Res 396: 77-96.

Neafsey EJ, Sievert C (1982) A second forelimb motor area exists in rat frontal cortex. Brain Res 232: 151-156.

Nguyen QT, Schroeder LF, Mank M, Muller A, Taylor P, Griesbeck O, Kleinfeld D (2010) An in vivo biosensor for neurotransmitter release and in situ receptor activity. Nat Neurosci 13: 127-132.

Nicolelis MA (2001) Actions from thoughts. Nature 409: 403-407.

Nicolelis MA, Dimitrov D, Carmena JM, Crist R, Lehew G, Kralik JD, Wise SP (2003) Chronic, multisite, multielectrode recordings in macaque monkeys. Proc Natl Acad Sci U S A 100: 11041-11046.

Nicolelis MA, Lebedev MA (2009) Principles of neural ensemble physiology underlying the operation of brain-machine interfaces. Nat Rev Neurosci 10: 530-540.

Nimmerjahn A, Kirchhoff F, Helmchen F (2005) Resting microglial cells are highly dynamic surveillants of brain parenchyma in vivo. Science 308: 1314-1318.

Norrie BA, Nevett-Duchcherer JM, Gorassini MA (2005) Reduced functional recovery by delaying motor training after spinal cord injury. J Neurophysiol 94: 255-264.

Nudo RJ (2013) Recovery after brain injury: mechanisms and principles. Front Hum Neurosci 7: 887.

Nudo RJ, Plautz EJ, Milliken GW (1997) Adaptive plasticity in primate motor cortex as a consequence of behavioral experience and neuronal injury. Seminars in Neuroscience 9: 13-23.

O'Driscoll M, El Deredy W, Atas A, Sennaroglu G, Sennaroglu L, Ramsden RT (2011) Brain stem responses evoked by stimulation with an auditory brain stem implant in children with cochlear nerve aplasia or hypoplasia. Ear Hear 32: 300-312.

Parsons CG, Danysz W, Quack G (1999) Memantine is a clinically well tolerated N-methyl-D-aspartate (NMDA) receptor antagonist--a review of preclinical data. Neuropharmacology 38: 735-767.

Parsons CG, Stoffler A, Danysz W (2007) Memantine: a NMDA receptor antagonist that improves memory by restoration of homeostasis in the glutamatergic system--too little activation is bad, too much is even worse. Neuropharmacology 53: 699-723.

Paxinos G, Watson C (1998) The rat brain in stereotaxic coordinates. Academic Press, San Diego.

Pelvig DP, Pakkenberg H, Stark AK, Pakkenberg B (2008) Neocortical glial cell numbers in human brains. Neurobiol Aging 29: 1754-1762.

Pezaris JS, Eskandar EN (2009) Getting signals into the brain: visual prosthetics through thalamic microstimulation. Neurosurg Focus 27: E6.

Pi R, Li W, Lee NT, Chan HH, Pu Y, Chan LN, Sucher NJ, Chang DC, Li M, Han Y (2004) Minocycline prevents glutamate-induced apoptosis of cerebellar granule neurons by differential regulation of p38 and Akt pathways. J Neurochem 91: 1219-1230.

Polikov VS, Block ML, Fellous JM, Hong JS, Reichert WM (2006) In vitro model of glial scarring around neuroelectrodes chronically implanted in the CNS. Biomaterials 27: 5368-5376.

Polikov VS, Tresco PA, Reichert WM (2005) Response of brain tissue to chronically implanted neural electrodes. J Neurosci Methods 148: 1-18.

Potter KA, Buck AC, Self WK, Capadona JR (2012) Stab injury and device implantation within the brain results in inversely multiphasic neuroinflammatory and neurodegenerative responses. J Neural Eng 9: 046020.

Queiroz G, Gebicke-Haerter PJ, Schobert A, Starke K, von K, I (1997) Release of ATP from cultured rat astrocytes elicited by glutamate receptor activation. Neuroscience 78: 1203-1208.

Rao VL, Dogan A, Todd KG, Bowen KK, Dempsey RJ (2001) Neuroprotection by memantine, a non-competitive NMDA receptor antagonist after traumatic brain injury in rats. Brain Res 911: 96-100.

Rennaker RL, Miller J, Tang H, Wilson DA (2007) Minocycline increases quality and longevity of chronic neural recordings. J Neural Eng 4: L1-L5.

Risedal A, Zeng J, Johansson BB (1999) Early training may exacerbate brain damage after focal brain ischemia in the rat. J Cereb Blood Flow Metab 19: 997-1003.

Robinson DM, Keating GM (2006) Memantine: a review of its use in Alzheimer's disease. Drugs 66: 1515-1534.

Roland PE, Larsen B, Lassen NA, Skinhoj E (1980) Supplementary motor area and other cortical areas in organization of voluntary movements in man. J Neurophysiol 43: 118-136.

Rossi DJ, Oshima T, Attwell D (2000) Glutamate release in severe brain ischaemia is mainly by reversed uptake. Nature 403: 316-321.

Rouiller EM, Moret V, Liang F (1993) Comparison of the connectional properties of the two forelimb areas of the rat sensorimotor cortex: support for the presence of a premotor or supplementary motor cortical area. Somatosens Mot Res 10: 269-289.

Ryu JK, Franciosi S, Sattayaprasert P, Kim SU, McLarnon JG (2004) Minocycline inhibits neuronal death and glial activation induced by beta-amyloid peptide in rat hippocampus. Glia 48: 85-90.

Sacrey LA, Alaverdashvili M, Whishaw IQ (2009) Similar hand shaping in reaching-for-food (skilled reaching) in rats and humans provides evidence of homology in release, collection, and manipulation movements. Behav Brain Res 204: 153-161.

Sadato N, Yonekura Y, Waki A, Yamada H, Ishii Y (1997) Role of the supplementary motor area and the right premotor cortex in the coordination of bimanual finger movements. J Neurosci 17: 9667-9674.

Sanchez Mejia RO, Ona VO, Li M, Friedlander RM (2001) Minocycline reduces traumatic brain injury-mediated caspase-1 activation, tissue damage, and neurological dysfunction. Neurosurgery 48: 1393-1399.

Scarpini E, Scheltens P, Feldman H (2003) Treatment of Alzheimer's disease: current status and new perspectives. Lancet Neurol 2: 539-547.

Schwartz AB, Cui XT, Weber DJ, Moran DW (2006) Brain-controlled interfaces: movement restoration with neural prosthetics. Neuron 52: 205-220.

Schwartz M, Shechter R (2010) Systemic inflammatory cells fight off neurodegenerative disease. Nat Rev Neurol 6: 405-410.

Seitz RJ, Azari NP, Knorr U, Binkofski F, Herzog H, Freund HJ (1999) The role of diaschisis in stroke recovery. stroke 30: 1844-1850.

Shain W, Spataro L, Dilgen J, Haverstick K, Retterer S, Isaacson M, Saltzman M, Turner JN (2003) Controlling cellular reactive responses around neural prosthetic devices using peripheral and local intervention strategies. IEEE Trans Neural Syst Rehabil Eng 11: 186-188.

Simons M, Nave KA (2015) Oligodendrocytes: Myelination and Axonal Support. Cold Spring Harb Perspect Biol.

Skoglund TS, Pascher R, Berthold CH (1997) The existence of a layer IV in the rat motor cortex. Cereb Cortex 7: 178-180.

Sofroniew MV (2009) Molecular dissection of reactive astrogliosis and glial scar formation. Trends Neurosci 32: 638-647.

Sofroniew MV (2015) Astrocyte barriers to neurotoxic inflammation. Nat Rev Neurosci 16: 249-263.

Stensaas SS, Stensaas LJ (1976) The reaction of the cerebral cortex to chronically implanted plastic needles. Acta Neuropathol 35: 187-203.

Stirling DP, Koochesfahani KM, Steeves JD, Tetzlaff W (2005) Minocycline as a neuroprotective agent. Neuroscientist 11: 308-322.

Suadicani SO, Brosnan CF, Scemes E (2006) P2X7 receptors mediate ATP release and amplification of astrocytic intercellular Ca2+ signaling. J Neurosci 26: 1378-1385.

Szarowski DH, Andersen MD, Retterer S, Spence AJ, Isaacson M, Craighead HG, Turner JN, Shain W (2003) Brain responses to micro-machined silicon devices. Brain Res 983: 23-35.

Terashima T (1995) Anatomy, development and lesion-induced plasticity of rodent corticospinal tract. Neurosci Res 22: 139-161.

Tikka T, Fiebich BL, Goldsteins G, Keinanen R, Koistinaho J (2001) Minocycline, a tetracycline derivative, is neuroprotective against excitotoxicity by inhibiting activation and proliferation of microglia. J Neurosci 21: 2580-2588.

Tikka TM, Koistinaho JE (2001) Minocycline provides neuroprotection against N-methyl-D-aspartate neurotoxicity by inhibiting microglia. J Immunol 166: 7527-7533.

Torres-Platas SG, Comeau S, Rachalski A, Bo GD, Cruceanu C, Turecki G, Giros B, Mechawar N (2014) Morphometric characterization of microglial phenotypes in human cerebral cortex. J Neuroinflammation 11: 12.

Turner JN, Shain W, Szarowski DH, Andersen M, Martins S, Isaacson M, Craighead H (1999) Cerebral astrocyte response to micromachined silicon implants. Exp Neurol 156: 33-49.

VandenBerg PM, Hogg TM, Kleim JA, Whishaw IQ (2002) Long-Evans rats have a larger cortical topographic representation of movement than Fischer-344 rats: a microstimulation study of motor cortex in naive and skilled reaching-trained rats. Brain Res Bull 59: 197-203.

Verderio C, Matteoli M (2001) ATP mediates calcium signaling between astrocytes and microglial cells: modulation by IFN-gamma. J Immunol 166: 6383-6391.

Vizi ES, Kisfali M, Lorincz T (2013) Role of nonsynaptic GluN2B-containing NMDA receptors in excitotoxicity: evidence that fluoxetine selectively inhibits these receptors and may have neuroprotective effects. Brain Res Bull 93: 32-38.

Wang X, Arcuino G, Takano T, Lin J, Peng WG, Wan P, Li P, Xu Q, Liu QS, Goldman SA, Nedergaard M (2004) P2X7 receptor inhibition improves recovery after spinal cord injury. Nat Med 10: 821-827.

Wang Z, Haydon PG, Yeung ES (2000) Direct observation of calcium-independent intercellular ATP signaling in astrocytes. Anal Chem 72: 2001-2007.

Wasserman JK, Schlichter LC (2007) Minocycline protects the blood-brain barrier and reduces edema following intracerebral hemorrhage in the rat. Exp Neurol 207: 227-237.

Waxman EA, Lynch DR (2005) N-methyl-D-aspartate receptor subtypes: multiple roles in excitotoxicity and neurological disease. Neuroscientist 11: 37-49.

Wei G, Dawson VL, Zweier JL (1999) Role of neuronal and endothelial nitric oxide synthase in nitric oxide generation in the brain following cerebral ischemia. Biochim Biophys Acta 1455: 23-34.

Weiler N, Wood L, Yu J, Solla SA, Shepherd GM (2008) Top-down laminar organization of the excitatory network in motor cortex. Nat Neurosci 11: 360-366.

Wells JE, Hurlbert RJ, Fehlings MG, Yong VW (2003) Neuroprotection by minocycline facilitates significant recovery from spinal cord injury in mice. Brain 126: 1628-1637.

Wenk GL, Parsons CG, Danysz W (2006) Potential role of N-methyl-D-aspartate receptors as executors of neurodegeneration resulting from diverse insults: focus on memantine. Behav Pharmacol 17: 411-424.

Whishaw IQ, Gorny B, Foroud A, Kleim JA (2003) Long-Evans and Sprague-Dawley rats have similar skilled reaching success and limb representations in motor cortex but different movements: some cautionary insights into the selection of rat strains for neurobiological motor research. Behav Brain Res 145: 221-232.

Whishaw IQ, Metz GA (2002) Absence of impairments or recovery mediated by the uncrossed pyramidal tract in the rat versus enduring deficits produced by the crossed pyramidal tract. Behav Brain Res 134: 323-336.

Whishaw IQ, O'Connor WT, Dunnett SB (1986) The contributions of motor cortex, nigrostriatal dopamine and caudate-putamen to skilled forelimb use in the rat. Brain 109 (Pt 5): 805-843.

Whishaw IQ, Pellis SM (1990) The structure of skilled forelimb reaching in the rat: a proximally driven movement with a single distal rotatory component. Behav Brain Res 41: 49-59.

Whishaw IQ, Pellis SM, Gorny B, Kolb B, Tetzlaff W (1993) Proximal and distal impairments in rat forelimb use in reaching follow unilateral pyramidal tract lesions. Behav Brain Res 56: 59-76.

Wilson BS, Finley CC, Lawson DT, Wolford RD, Eddington DK, Rabinowitz WM (1991) Better speech recognition with cochlear implants. Nature 352: 236-238.

Winslow BD, Christensen MB, Yang WK, Solzbacher F, Tresco PA (2010) A comparison of the tissue response to chronically implanted Parylene-C-coated and uncoated planar silicon microelectrode arrays in rat cortex. Biomaterials 31: 9163-9172.

Winslow BD, Tresco PA (2010) Quantitative analysis of the tissue response to chronically implanted microwire electrodes in rat cortex. Biomaterials 31: 1558-1567.

Wolpaw JR, Birbaumer N, Heetderks WJ, McFarland DJ, Peckham PH, Schalk G, Donchin E, Quatrano LA, Robinson CJ, Vaughan TM (2000) Brain-computer interface technology: a review of the first international meeting. IEEE Trans Rehabil Eng 8: 164-173.

Wolpaw JR, Birbaumer N, McFarland DJ, Pfurtscheller G, Vaughan TM (2002) Brain-computer interfaces for communication and control. Clin Neurophysiol 113: 767-791.

Wolpaw JR, McFarland DJ (2004) Control of a two-dimensional movement signal by a noninvasive brain-computer interface in humans. Proc Natl Acad Sci U S A 101: 17849-17854.

Wu HM, Tzeng NS, Qian L, Wei SJ, Hu X, Chen SH, Rawls SM, Flood P, Hong JS, Lu RB (2009) Novel neuroprotective mechanisms of memantine: increase in neurotrophic factor release from astroglia and anti-inflammation by preventing microglial activation. Neuropsychopharmacology 34: 2344-2357.

Xia P, Chen HS, Zhang D, Lipton SA (2010) Memantine preferentially blocks extrasynaptic over synaptic NMDA receptor currents in hippocampal autapses. J Neurosci 30: 11246-11250.

Yang F, Zhou L, Wang D, Wang Z, Huang QY (2015a) Minocycline ameliorates hypoxia-induced blood-brain barrier damage by inhibition of HIF-1alpha through SIRT-3/PHD-2 degradation pathway. Neuroscience 304: 250-259.

Yang Y, Salayandia VM, Thompson JF, Yang LY, Estrada EY, Yang Y (2015b) Attenuation of acute stroke injury in rat brain by minocycline promotes blood-brain barrier remodeling and alternative microglia/macrophage activation during recovery. J Neuroinflammation 12: 26.

Yrjanheikki J, Keinanen R, Pellikka M, Hokfelt T, Koistinaho J (1998) Tetracyclines inhibit microglial activation and are neuroprotective in global brain ischemia. Proc Natl Acad Sci USA 95: 15769-15774.

Yrjanheikki J, Tikka T, Keinanen R, Goldsteins G, Chan PH, Koistinaho J (1999) A tetracycline derivative, minocycline, reduces inflammation and protects against focal cerebral ischemia with a wide therapeutic window. Proc Natl Acad Sci U S A 96: 13496-13500.

Zamanian JL, Xu L, Foo LC, Nouri N, Zhou L, Giffard RG, Barres BA (2012) Genomic analysis of reactive astrogliosis. J Neurosci 32: 6391-6410.

Zhou L, Li F, Xu HB, Luo CX, Wu HY, Zhu MM, Lu W, Ji X, Zhou QG, Zhu DY (2010) Treatment of cerebral ischemia by disrupting ischemia-induced interaction of nNOS with PSD-95. Nat Med 16: 1439-1443.

Zhou L, Zhu DY (2009) Neuronal nitric oxide synthase: structure, subcellular localization, regulation, and clinical implications. Nitric Oxide 20: 223-230.

Zhu S, Stavrovskaya IG, Drozda M, Kim BY, Ona V, Li M, Sarang S, Liu AS, Hartley DM, Wu DC, Gullans S, Ferrante RJ, Przedborski S, Kristal BS, Friedlander RM (2002) Minocycline inhibits cytochrome c release and delays progression of amyotrophic lateral sclerosis in mice. Nature 417: 74-78.

Zhu X, Dong J, Shen K, Bai Y, Zhang Y, Lv X, Chao J, Yao H (2015) NMDA receptor NR2B subunits contribute to PTZ-kindling-induced hippocampal astrocytosis and oxidative stress. Brain Res Bull 114: 70-78

9 Danksagung

Mein besonderer Dank gilt…

…Prof. Dr. Michael Koch, für die Möglichkeit, meine Dissertation und die dazugehörigen Verhaltensexperimente in dieser wunderbaren Arbeitsgruppe durchführen zu können. Vielen Dank für dieses spannende Projekt, das es mir ermöglichte, einen tiefen Einblick in die zellulären und immunologischen Aspekte der neuropharmakologischen Grundlagenforschung zu erhalten. Ich werde die eigenständige Arbeit, bei dennoch hervorragender Betreuung, in deiner Arbeitsgruppe vermissen. Es war eine wunderbare, wenn auch zugleich sehr arbeitsintensive Zeit, an die ich mich auf jeden Fall gerne zurück erinnern werde.

…Prof. Dr. Ursula Dicke für die Zusage zur Erstellung des Zweitgutachtens und den hierfür benötigten Zeit- und Arbeitsaufwand, sowie Prof. Fahle, dass auch er meinem Dissertationskolloquium als Prüfer beiwohnt.

…Malte Feja für die mentale Unterstützung in stressigen Phasen, den fachlichen Rat als ehemaliger Betreuer, und die zahlreichen Ablenkungen zwischendurch, sei es in der AG zum Kickern oder über die Landesgrenzen hinaus.

…der AG Koch für die wunderbare Zeit, aber auch tatkräftige Unterstützung, wenn man mal in Arbeit unterging. Speziell danke ich Ellen für die tollen Bürozeiten und Unternehmungen zwischendurch, Jannis für seine tatkräftige Unterstützung bei Computerproblemen und den Crashkursen in diversen Programmen, Simone für die Unterstützung beim wochenlangen Training vor dem Beginn der Testphasen und Maja für ihre Unterstützung in der Histologie.

…und ganz besonders danke ich meinen Eltern für die liebevolle und konstante Unterstützung in allen Lebenslagen.